A possible role for Salicylic Acid-induced genes in *Fusarium graminearum* infection

By
Reem Alharthi

Thesis submitted to the Faculty of Graduate and Postdoctoral Studies in partial fulfillment of the requirements for the degree of

Master of Science in Biology

Under the auspices of the Ottawa-Carleton Institute for Biological Science

University of Ottawa
Ottawa, Ontario, Canada
February, 2015

Abstract

The ability of *Fusarium graminearum* to metabolize the plant hormone salicylic acid (SA) and use it as a carbon source was investigated in previous studies in our laboratory. The expression of some *F. graminearum* genes was upregulated in presence of SA. However, the role of those induced genes in SA degradation was not investigated. This study aimed at characterizing six candidate genes predicted to encode enzymes with ability to catalyze one of the first two-enzymatic steps in SA degradation by *F. graminearum*. Those genes are FGSG_09063, FGSG03657, FGSG_09061, FGSG_03667, FGSG08358 and FGSG_08037. In order to investigate the function of those genes, genes were individually inactivated by gene replacement and the deletion mutant strains were tested for their ability to grow in solid and liquid medium supplemented with SA as the sole carbon source. Results indicated that FGSG_03667 is an essential gene in the SA degradation pathway. This gene is predicted to encode a hydroxyquinol 1,2 dioxygenase, an enzyme that catalyzes the conversion of hydroxyquinol to 3-hydroxy-cis,cis-munocate. In addition, results indicated that two other genes, FGSG_03657 and FGSG_09061, contribute to the initial degradation of SA in culture. Those genes are predicted to encode a salicylate 1-monooxygenase and a 2,3 dihydroxybenzoic acid decarboxylase, respectively. Those two enzymes can catalyze the conversion of SA to catechol. Taken all together, the results of this study suggest that catechol is the first catabolic intermediate in the degradation of SA in *F. graminearum,* and that FGSG_03667 is a gene encoding a wide range substrate enzyme that can use catechol. Further studies need to be done to support this interpretation from the biochemistry perspective.

Résumé

La capacité de métaboliser la phytohormone acide salicylique (AS) et de l'utiliser comme une source de carbone fut examinée chez *Fusarium graminearum* dans des études précédentes de notre laboratoire. L'expression de certains gènes de *F. graminearum* était augmentée en présence d'AS. Cependant, le rôle de ces gènes induits dans la dégradation de l'AS ne fut pas examiné. Cette étude vise à caractériser six gènes candidats qui sont prédits coder pour des enzymes avec la capacité de catalyser une des deux premières étapes dans la dégradation de l'AS par *F. graminearum*. Ces gènes sont FGSG_09063, FGSG03657, FGSG_09061, FGSG_03667, FGSG08358 et FGSG_0803. Dans le but d'examiner la fonction de ces gènes, ceux-ci furent inactivés individuellement par remplacement de gène, et les souches mutantes de délétion furent testées pour leur capacité à pousser en milieux solide et liquide contenant l'AS comme seule source de carbone. Les résultats ont indiqué que FGSG_03667 est un gène essentiel dans la voie de dégradation de l'AS. Ce gène est prédit coder pour une hydroxyquinol 1,2 dioxygénase, une enzyme qui catalyse la conversion du hydroxyquinol en 3-hydroxy-cis,cis-munocate. De plus, les résultats ont indiqué que deux autres gènes, FGSG_03657 et FGSG_09061, participent dans la dégradation initiale de l'AS en culture. Ces gènes sont prédits coder pour une salicylate 1-monooxygénase et une 2,3 dihydroxybenzoique acide décarboxylase. Ces deux enzymes peuvent catalyser la conversion de l'AS en catéchol. Pris ensemble, les résultats de cette étude suggèrent que le catéchol est le premier intermédiaire catabolique dans la dégradation de l'AS par *F. graminearum*, et que FGSG_03667 est une enzyme avec une variété de substrats qui peut utiliser le catéchol.

D’autres études seront nécessaires pour supporter cette interprétation du point de vue biochimique.

Acknowledgments

First of all, I would like to express my gratitude to God, for giving me the health, strength and patience to go through all the ups and downs during my study.

A special thanks goes to my family for their confidence in me, their motivation and their support during my studies. They have sacrificed so many things in their lives to allow me to be as ambitious as I dreamed. They are the main reason for what I have done so far in my life.

I owe my deepest gratitude to my supervisor Dr. Thérèse Ouellet for giving me the opportunity to work in her lab and for her constant advising, encouragement and supporting during this study. This thesis would not have been possible without her help and advice. Thanks for your patience, motivation and inspiration.

I would also like to thank the technicians in my lab, Hélène Rocheleau and Margaret Balcerzak. Thank you all for your support, advises, friendship and sharing your wide knowledge with me. Thank you all for your encouragement not only in my study but also in many other aspects of my life.

I would also like to thank my committee members: Dr. Doug Johnson, Dr. Keith Seifert and Dr. Steve Gleddie for their time, advices and invaluable feedback.

I would also like to thank Dr. Rajagopal Subramaniam for letting me run the HPLC experiments in his lab.

Table of Contents

List of Figures

List of Tables

List of Abbreviations

A. thaliana	*Arabidopsis thaliana*
ATMT	*Agrobacterium tumefaciens*-mediated transformation
A. tumefaciens	*Agrobacterium tumefaciens*
BLAST	Basic local alignment search tool
BTH	Benzothiadiazole
CMC	Carboxymethyl cellulose
DAOM	Department of Agriculture, Ottawa, mycology
DNA	Deoxyribonucleic acid
DON	Mycotoxin deoxynivalenol
DFM	Defined *fusarium* medium
F. graminearum	*Fusarium graminearum*
FHB	Fusarium head blight
gDNA	Genomic DNA
GOI	Genes of interest
HPLC	High performance liquid chromatography
hph	Hygromycin phosphotransferase
HRSs	Homologous recombinant segments
LB	LB-Miller broth
MB	Mega bases
MIPS	Munich Information Center for Protein Sequences
MMTL	Molecular microbiology technology lab
ORF	Open reading frame
PCR	Polymerase chain reaction
PDA	Potato Dextrose Agar
PR	pathogen related proteins
pRF-HU2	pRF-HU2 gene replacement vector
RPM	Revolutions per minute
SA	Salicylic Acid
SAR	Systemic acquired resistance
SNA	Synthetic Nutrient Deficient Agar
T. cutaneum	*Trichosporon cutaneum*
TFA	Trifluoroacetic acid
TMV	Tobacco mosaic virus
U	Uracil nucleic acid
USER	Uracil-specific excision reagent
WT	Wild-type
1,2-HQD	Hydroxyquinol 1,2-dioxygenase

Chapter 1- Introduction

1.1 Fusarium Head Blight of Cereals

Fusarium species are responsible for several plant diseases, including diseases that affect cereal crops. *Fusarium graminearum* Schwabe (teleomorph *Gibberella zeae* (Schwein.) Petch) predominantly causes a major disease of cereal crops that is known as fusarium head blight (FHB) or scab (Saharan and Kumar, 2004). FHB is a destructive disease that affects cereal crops such as wheat (*Triticum aestivum L.*), barley (*Hordeum vulgare L.*), wild rice (*Zizania palustris L.*), oats (*Avena sativa L.*) and maize (*Zea mays L.*). FHB was firstly identified in 1884 in England and termed wheat scab. Thereafter, outbreaks of this disease were observed in US, Canada, Asia and Europe (Stack, 2000). FHB occurs in certain conditions, warm and moist, when *F. graminearum* is able to infect the spikelets during the flowering period. The infection results in an accumulation of tombstone kernels, which are shriveled, light in weight, with white or pink color, and produced by bleached and blighted heads (Goswami and Kistler, 2004; Trail 2009).

Consequently, the infection causes low grain yield, with losses that can reach 50-60% of the yield, and low grain quality, reduction of milling and malting quality, that lead to significant economic losses. In the 1990's, United States lost approximated 3$ billion due to FHB-infected wheat crops, while Manitoba lost approximated 300$ million between 1993 and 1998 (Windels, 2000). Beside the economic losses, FHB is considered to be a health concern for animals and humans due to production of the mycotoxin deoxynivalenol (DON), which is also known as vomitoxin, by *F. graminearum*. Wheat grain that is contaminated with DON is unsuitable for agricultural uses and human and animal consumption. The maximum allowed level of DON is regulated by many countries; in Canada for example, 2.0 ppm DON in grain is the maximum contamination level for non-stable food uses, and 1.0 ppm for baby food uses (Saharan and Kumar, 2004; Government of Canada, 2005). The large economical and biological impact of *F. graminearum* on wheat makes it a priority to reduce its pathological effects, including via molecular and genetic studies.

1.2 The Pathogen *F. graminearum*

1.2.1 Overview of *F. graminearum*

F. graminearum, the most important causal agent of FHB, belongs to the Phylum Ascomycota, and has a teleomorph called *Gibberella zeae*. It is homothallic, meaning that it has the ability to reproduce sexually and asexually by itself with no need of a distinct partner. The sexual spores, or ascospores, are produced in fruiting bodies called perithecia. It produces macroconidia that elongate to 5-6 septate and ascospores that elongate to 1-3 septate (Leslie and Summerell, 2006; Trail, 2009). Unlike the ascospores, the conidia or asexual spores are produced directly by hyphal endings in the mycelium. *F. graminearum* gets much attention from biologists and researchers to better understand its life cycle, pathogenicity, as well as its genome.

1.2.2 *F. graminearum* genome sequence

The *F. graminearum* genome was sequenced in 2003 by the Broad Institute (http://www.broadinstitute.org/), and released to public at the Munich Information Center For Protein Sequence (MIPS) (http://mips.helmholtz-muenchen.de/genre/proj/fusarium Munich Information Center for Protein Sequence, 2003). *Fusarium graminearum* has a typical filamentous fungi genome size of 36 MB (mega bases) spread over four chromosomes (Cuomo et al. 2007). Bioinformatic analyses of the genome sequence predicted 13,937 genes and only a few duplicated sequences. Sequence comparison with different fungal species indicated that 2001 genes of *F. graminearum* were different from those species and 5812 genes were homologous to proteins of 'unknown functions' (Cuomo et al. 2007). Knowing the whole genome sequence has opened the door to a better understanding of the biology and pathogenicity of *F. graminearum* using molecular, transcriptomic, and proteomic approaches. Combining different gene predictions from the genomic sequence, the Broad Institute and MIPS designed an Affymetix gene chip to detect and analyze gene expression in *F. graminearum* (Güldener et al. 2006; Trail, 2009). The availability of genome sequence and the ability to produce mutagenic strains using *Agrobacterium*-mediated transformation makes *F. graminearum* an ideal model organism to study pathogenicity; this approach will be used in this work.

1.2.3 *F. graminearum* life cycle

The life cycle of *F. graminearum* is clear and simple (Figure 1). It can be completed in culture in two weeks as well as on its host in several weeks. *Fusarium graminearum* ascospores are considered to be the main inoculum in natural conditions (Trail, 2009). Even though *F. graminearum* is homothallic, it spends most of its life as a haploid. Interestingly, *F. graminearum* is able to survive over the winter on crop residues as perithecia, mycelia, and spores (Trail, 2009).

At the cellular level, the development of *F. graminearum* starts with binucleate cells, each containing two genetically identical nuclei. To form hyphae, the binucleate cells elongate and divide to produce identical binucleate cells attached to each other in a linear, filament-like fashion (Trail, 2009). Binucleate cells also develop into small-coiled cells that are responsible to form perithecia, which contain asci that hold ascospores generated through meiotic division (Trail and Common, 2000). Once the asci are fully filled with ascospores, they forcibly discharge them into the air. At this point, the airborne ascospores constitute the principal inoculum for FHB and they spread through rain, wind, insects and animals (Trail et al., 2002; Trail, 2009). On the other hand, the asexual stage starts with the formation of the conidia from cushion-shaped structures called sporodochia, through mitotic division. Conidia produced in a slimy mass during a moist period, and they spread through rain splash to infect plants within short distances (Deacon, 2006; Bushnell et al., 2003; Trail, 2009). Both sexual and asexual stages can be observed on the surface of infected plants and on crop residues.

In the spring and early summer, when the weather is warm and moist, and when wheat is at the anthesis phase, *F. graminearum* ascospores and/or conidia land on flowering spikelets, germinate and initiate the infection process by entering into the plant tissues. Spores can penetrate directly via natural openings such as the base of the lemma and palea or indirectly via breaking anther tissues (Bushnelln et al., 2003; Trail et al. 2002; Trail, 2009). At the beginning, *F. graminearum* grows intercellularly through the xylem and pith. Then it switches to grow intracellularly through the apoplast and cortex. At this stage of infection, the fungus produces mycotoxins, including DON, that lead to necrosis and infection of the tissues, and spread to the rachis and distant spikelets, colonizing the developing seeds of the whole spike (Trail, 2009).

Many scientists consider that *F. graminearum* grows in a biotrophic mode at first, without showing any symptoms, then switches to necrotrophic mode once it produces DON, to colonize the tissues; this is when the typical symptoms of the disease appear. This has led some scientists to consider *F. graminearum* as a hemibiotrophic fungus. The principal symptoms observed during *F. graminearum* infection of wheat are water soaking, browning and tissue bleaching. Infected seeds are shriveled and undersized (Bushnell et al., 2003; Trail, 2009).

Finally, the disease cycle can start again in a new plant after overwintering of the fungus on infected crop residue or soil, and/or through airborne ascospores traveling from infected wheat spikelets within a field (Trail, 2009).

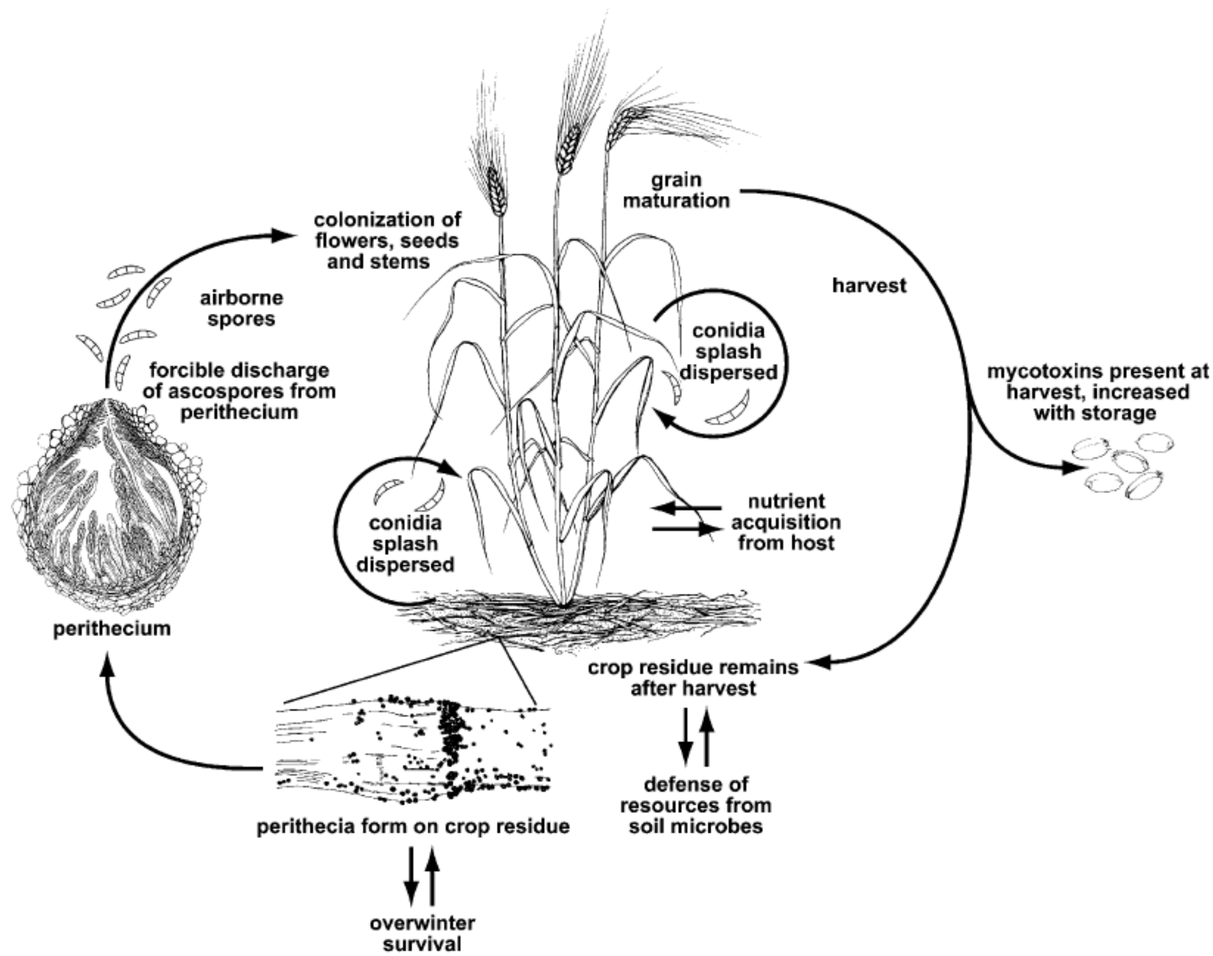

Figure 1: ***F. graminearum*** **lifecycle in FHB in wheat (Trail, 2009).**

1.3 Plant Hormone in Defense, Salicylic Acid

1.3.1 Overview of the role of salicylic acid in plant defense

Plants are organisms under constant threat of attack by numerous pathogenic microorganisms, including bacteria, viruses and fungi. One of the ways that plants naturally put up a defense against those is by producing phytohormones. Phytohormones are a set of small molecules that arise in low concentrations, including in response to biotrophic, necrotrophic and hemibiotropic pathogens (Pieterse and Leon-Reyes, 2009). They play important roles in plant growth and development, photosynthesis, transpiration, as well as in defense signaling (Hayat et al., 2007). One of the key phytohormones involved in defense is salicylic acid (SA).

In 1979, SA was first demonstrated to be an endogenous signaling molecule mediating plant defense against pathogens by White and his colleagues. They injected exogenous SA into tobacco plants and infected those with tobacco mosaic virus (TMV); the plants showed enhanced resistance as well as induction of pathogenesis-related (PR) proteins (White, 1979; Antoniw and White, 1980). This study brought some light into the role of SA in plant defense. In 1990, the role of SA in the defense response was confirmed in both tobacco and cucumber plants (Malamy et al., 1990).

In addition, SA was shown to be required to induce systemic acquired resistance (SAR) in both dicot and monocot plants (Malamy et al., 1990; Métraux et al., 1990). SAR was activated in non-infected areas, initiating defense in distal areas and protecting healthy leaves from infection, conferring long-lasting protection. The activation of SAR was correlated with the expression of pathogenesis-related (PR) genes (Antoniw and White, 1980; Ward and Uknes, 1991; Uknes et al., 1992).

To demonstrate the role of SA as a signal molecule, especially as an endogenous signal to activate the SAR system, transgenic *A. thaliana* and tobacco were generated by introducing a bacterial *NahG* gene, which encodes for the SA-degrading enzyme salicylate hydroxylase. After inoculation of the transgenic plants with different pathogens, it was found that those plants were extremely susceptible to disease, due to a significant reduction of SA accumulation. Thus, the activation of SAR was impaired, and the expression of PR genes was inhibited. Since most of the studies were done in dicot plants, the role of SA in monocot species, including wheat, is still poorly understood (Durrant and Dong, 2004; Gaffney et al., 1993; Delaney et al., 1994).

1.3.2 SA degradation by microorganisms

Plant pathogens develop different strategies to interact with the host plant, in order to initiate and spread the diseases, especially biotropic and hemibiotropic pathogens that need live cells. To overcome the plant defense response, several microbial pathogens, such as bacteria, yeast, and fungi, degrade the plant hormone SA, and use it as a carbon source. The metabolic degradation of SA has been investigated previously for other fungal genera, including *Aspergillus, Trichosporon, Trichoderma, Glomerella* and *Rhodotorula* (Wright, 1993). Interestingly, Qi et al., (2012) showed that *F. graminearum* has the ability to degrade SA and use it as a carbon source. However, the SA degradation pathway has not been determined yet in *Fusarium* species.

The pathways of aromatic compound degradation, including SA and its closely related metabolites, were intensively studied in bacteria; in contrast, little is known in fungi. Bacterial studies have contributed to predicting and understanding the aromatic compound degradation pathways by fungi, and the variations among microorganisms (Wright, 1993). A review of knowledge on aromatic compounds degradation pathways in fungi was provided by Wright (Wright, 1993). Combining that work with more recent findings, Qi and his colleagues (2012) proposed possible degradation pathways for SA, and related aromatic compound in *F. graminearum* (Figure 2). These pathways will be briefly described below. The initial pathway, known as the upper pathway, is the conversion of SA and closely related compounds to an intermediate product, either catechol or gentisate. Subsequently, those intermediate substrates are processed through an *ortho* ring cleavage, where the cleavage takes place between the two-hydroxyl groups, to eventually produce 3-oxoadipate that can then be used by the TCA cycle.

In the upper pathway, SA is converted to either one of the intermediate substrates, catechol or gentisate, by the involvement of one of two enzymatic activities: monooxygenase and hydroxylase (Figure 2). A monooxygenase activity is responsible for the conversion of SA to catechol by incorporating one atom of oxygen under the following reaction:

$$\text{salicylate} + \text{NADH} + 2\ H^+ + \text{oxygen} <=> \text{catechol} + CO_2 + NAD^+ + H_2O$$

However, a hydroxylase activity is responsible for the conversion of SA to gentisate, by introducing one hydroxyl group to the benzene ring at the carbon 5 position. The conversion of SA to gentisate follows the reaction:

$$\text{salicylate} + \text{NADH} + \text{oxygen} + H^+ \rightarrow \text{gentisate} + NAD^+ + H_2O.$$

Recently, studies in yeast have shown that SA could be decarboxylated to phenol, oxidated to catechol and then enter the *ortho* ring-cleavage (Iwasaki et al., 2009). In this case, SA is converted to phenol by the following reaction:

$$\text{salicylate} + H^+ = \text{phenol} + CO_2$$

However, there is no report of this action in other fungi yet.

In microorganisms in general, in the lower pathway, the intermediate substrates catechol, gentisate and protocatechuate are further degraded through either the intradiol or the extradiol ring cleavage pathways. The difference between those pathways is in the position of the cleavage activity. In the intradiol (ortho) pathway, the cleavage occurs between the two carbon-bearing hydroxyl groups. However, in the extradiol (meta) pathway, the cleavage occurs between two carbons, with only one bearing a hydroxyl group. Wright (1993) indicated that in fungi studied, the *ortho* pathway is used, as demonstrated by the presence of enzymes involved in the *ortho* pathway. In brief, the first step of the *ortho* ring-cleavage is via a dioxygenase activity on one of the 3 intermediate substrates, which are analogous to each other. Catechol is dioxygenated to form cic,cis muconate, while protocatechuate and gentisate are converted to 3-carboxy-cis,cis muconate and 3-hydroxy-cis,cis muconate, respectively. Following that step, the three forms of cic,cis muconate are converted to either (+)-muconolactone, 3-carboxy-muconolactone, or 2-maleylacetate, depending on the starting intermediate substrate. Each of those compounds is then converted to 3-oxoadipate.

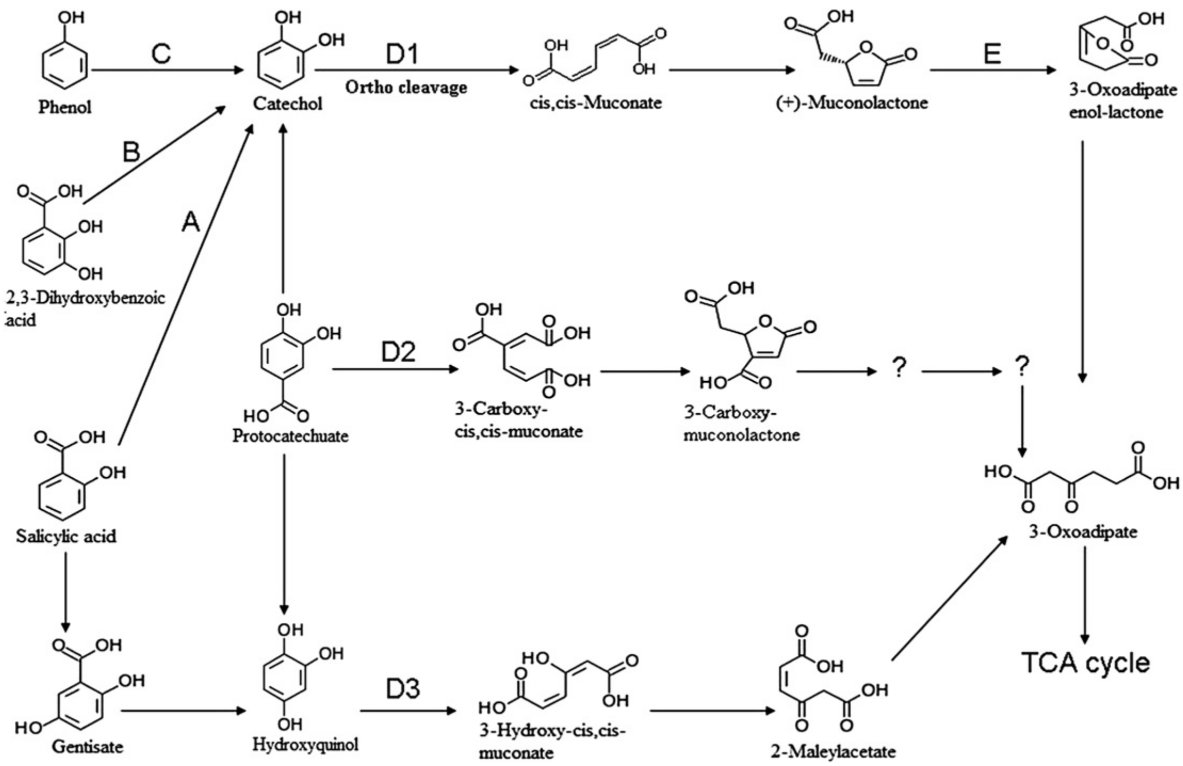

Figure 2: Postulated pathway for aromatic compound catabolism, including SA, in fungal species. Reproduced from Qi et al. (2012). Based on sequence homology, *F. graminearum* genes predicted to catalyze different steps in SA metabolism were identified. Step A represents the predicted salicylate 1-monooxygenase enzyme encoded by the genes FGSG_09063 and FGSG_03657, to convert SA directly to catechol. Step B represents a possible 2 3-dihydroxybenzoic acid decarboxylase (FGSG_09061) that could catalyze the conversion of 2,3- dihydroxybenzoic acid to catechol and may also convert SA to catechol. Steps D1, D2 and D3 represent intradiol dioxygenase, hydroxyquinol 1,2-dioxygenase and homogentisate 1,2-dioxygenase that could catalyse one or many of the D steps. Step E represents a predicted 3-oxoadipate enol-lactone hydrolase that could convert muconolactone to 3-oxidipate enol-lactone.

1.4 The Role of SA in Wheat-*F. graminearum* Interaction

1.4.1 The role of SA in wheat defense response to FHB

Understanding how wheat and *F. graminearum* recognize and interact with each other is a key step in developing novel strategies to enhance wheat resistance to FHB. many aspects of the interaction between wheat and *F. graminearum* are still unclear, in part due to limitations in wheat molecular and genetic tools (Makandar et al., 2010). Nonetheless, many groups have investigated some aspects of that interaction. In 2001, Yu and Muehlbauer studied the effect of the SA analogue benzothiadiazole (BTH) on wheat defense response against FHB by measuring the expression of PR genes, defense response genes, in BTH-treated spikes. The results suggested that SA and BTH do not contribute to FHB resistance in wheat.

However, Anand et al. (2003) generated a transgenic wheat line overexpressing a combination of two PR genes. Transgenic wheat expressing high level of PR genes showed high level of type II FHB resistance in greenhouse experiments compared with other transgenic wheat lines expressing moderate to non-detectable levels of those genes. In field experiment, transgenic wheat expressing high level of PR genes showed a delay in the disease symptoms at 3 days after inoculation compared with the parental, non-transgenic line; however it displayed similar disease levels in later rating time points. Because high expression of those PR genes was associated with a high level of endogenous SA, this result suggested that endogenous SA played an important role in signaling for defense against FHB (Anand, 2003). In order to understand the contribution of SA in wheat defense against FHB, Makandar et al. (2006) generated a transgenic wheat line overexpressing AtNPR1, which is the *Arabidopsis thaliana* NPR1 gene.

In *A. thaliana*, overexpression of the NPR1 gene led to a fast response of the plant to SA, and induction of the PR1 gene. Likewise, overexpression of AtNPR1 gene in wheat enhanced the activation of the PR1 gene and led to a faster and stronger SAR than in wild type plants. Overexpression of AtNPR1 also enhanced type II wheat resistance to FHB, which limits the spread of the disease to non-inoculated spikelets. So, it was suggested that, in addition to the production of SA contributing to FHB resistance, the rapid response of the plant to elevated levels of SA and activation of the NPR1 gene were important contributing factors. They also indicated that BTH acts similarly to SA toward the FHB resistance in AtNPR1 transgenic wheat (Makandar et al., 2006).

More recently, it was found that the way SA and BTH were introduced in the *F. graminearum*-infected wheat heads had an impact on the results obtained (Makandar et al., 2012) In brief, spraying wheat spikes with SA and BTH resulted in no accumulation of SA in infected spikes, and no expression of the PR1 gene (Li and Yen 2008; Makandar et al., 2012). On the other hand, drenching soil with SA or BTH raised the accumulation of SA in the spikes and enhanced the expression of the PR1 and WCI1 genes, which have been associated with FHB resistance in wheat (Makandar et al., 2012). The differences in results between the two methods, associated with the ability of the wheat spike to soak up a high amount of SA to induce the PR1 gene, may explain contradictory results obtained by different groups in studying the effect of SA on FHB resistance (Makandar et al., 2012).

To complement the observations that exogenous applications of SA and BTH into wheat spikes by drenching enhanced FHB resistance, Makandar et al. (2012) generated a transgenic plant that overexpressed the bacterial gene *NahG* in order to confirm the role of SA in FHB resistance. *NahG* is a bacterial gene encoding a salicylate hydroxylase enzyme that converts SA to catechol. Inoculation of *NahG* transgenic wheat with *F. graminearum* enhanced wheat susceptibility to FHB. Treatment of *NahG* transgenic wheat and wild type plants with catechol showed no effect on the resistance or susceptibility of the plant to FHB. However, treatment of *NahG* transgenic wheat and wild type plants with BTH resulted in a reduction of disease severity and enhancement of resistance to FHB, respectively. These results strongly suggested a significant role for SA signaling in basal resistance against FHB (Makandar et al., 2012). Nonetheless, these authors suggested that a molecular-genetic study should be done to better understand the specific role of SA in the wheat-*F. graminearum* interaction.

1.4.2 The effect of SA on *F. graminearum*

To complement the studies that focused on the effect of SA in wheat defense against FHB, Qi and his colleagues (2012) investigated the direct effect of SA on *F. graminearum* fitness and pathogenicity. Three different responses were examined: germination of the conidia, growth of the mycelia, and the production of the mycotoxin DON. Increasing amounts of SA led to a progressive inhibition then halt of mycelium growth and conidia germination. In addition, a decrease in the production of DON was noted. Although addition of SA to media generated more acidic conditions, it was shown that a simple acidification of the media could not reproduce the inhibitory effects, suggesting that those were specific to SA. In contrast, it was found that in slightly alkaline conditions, pH 8, the addition of SA promoted mycelium growth. Growth of *F. graminearum* in the absence of sugars showed that it was able to utilize SA as a carbon source. To confirm the ability of *F. graminearum* to catabolize SA, supernatants from liquid cultures were analyses by HPLC; the results showed that SA was completely consumed by the fungus in 24 hours.

To identify the pathway used by *F. graminearum* to degrade SA, a transcription profiling experiment was performed to compare cultures of *F. graminearum* in presence and absence of SA. It was found that SA significantly affected 258 *F. graminearum* genes, including 187 genes that were up regulated and 71 genes that were down regulated. Among the up-regulated genes, a group of 15 genes were highly induced at 8 and 24 hrs after addition of SA (Table #1). Many of those genes have a predicted function suggesting that they play a role in aromatic compound degradation. Moreover, six of those genes encoded enzymatic functions associated with predicted pathways for SA degradation in fungi. Those genes can be divided into two groups of three genes representing the best *F. graminearum* candidate genes for the catalysis of the first two-enzymatic steps in SA degradation. The first group contains FGSG_09063, FGSG_03657 and FGSG_09061, respectively predicted to encode two salicylate 1-monooxygenases and a 2,3 dihydroxybenzoic acid decarboxylase, enzymes that could catalyze the conversion of SA to catechol. The second group contains the best candidate genes for the catalysis of the second step of the SA degradation, which is the first step of the *ortho* ring fission pathway. Those genes, FGSG_03667, FGSG_08037 and FGSG_08358, are predicted to encode a hydroxyquinol-1,2-dioxygenase, an intradiol dioxygenase, and a homogentisate 1,2-dioxygenase, respectively. Additional experiments will be needed to characterize those genes, confirm their role in SA degradation by *F. graminearum* and determine if the ability to degrade SA is important for *F. graminearum* pathogenicity on wheat.

Table 1: SA-induced genes in *F. graminearum* that are predicted to be involved in aromatic compound degradation (Qi et al. 2012). *F. graminearum* genes marked with * were chosen for this study. The information under Catabolism target refers to steps in Figure 2**.** Log_2 ratios were calculated as Log_2 of [expression level in SA-treated culture divided by expression level in control culture] for the given gene.

Fusarium graminearum gene	Average log_2 ratio		Predicted gene function	Catabolism target
	8 h	24 h		
**FGSG_09063*	5.1	4.1	salicylate 1-monooxygenase	SA, step A
**FGSG_03657*	0.8	2.3	salicylate 1-monooxygenase	SA, step A
**FGSG_08037*	-3.0	-1.9	Intradiol dioxygenase	SA, step D1 or D2
**FGSG_03667*	2.2	2.4	hydroxyquinol-1,2-dioxygenase	SA, step D_3
FGSG_03604	5.2	4.8	gentisate 1,2 dioxygenase	SA, step D?
FGSG_12397	3.8	4.2	3-oxoadipate enol-lactone hydrolase	SA, step E
**FGSG_09061*	5.4	4.3	2,3 dihydroxybenzoic acid decarboxylase	benzoate, step B
FGSG_13983	4.3	4.5	phenol hydroxylase	phenol, step C
FGSG_15846	1.1	0.8	1,4-benzoquinone reductase	trichlorophenol
FGSG_03422	4.6	4.3	phenolic acid decarboxylase	phenolic acids
**FGSG_08358*	2.6	2.2	homogentisate 1,2-dioxygenase	tyrosine, step D?
FGSG_03605	4.6	4.2	fumarylacetoacetate hydrolase	tyrosine
FGSG_09522	0.6	1.2	tyrosinase precursor	tyrosine
FGSG_04829	-1.6	-0.4	kynureninase	tryptophan
FGSG_09040	1.9	-0.5	indoleamine 2,3 dioxygenase	tryptophan

1.5 Objective

A previous study in our lab has identified six genes potentially involved in the degradation of SA, based on BLAST alignments and expression profiles (Qi et al. 2012). The aim of the present study is to determine the importance of these genes, FGSG_09063, FGSG_03657, FGSG_09061, FGSG_08037, FGSG_03667, and FGSG_08358, in *F. graminearum*'s ability to use SA as a sole carbon source and for its general fitness. We hypothesized that, by disrupting the function of those genes, *F. graminearum*'s ability to degrade SA will be reduced; this reduction would depend on the importance of the contribution of those genes to the degradation pathway.

To test that hypothesis, gene disruption of the candidate genes was done using a homologue recombinant approach. Then, the deletion mutant strains were tested for their ability to utilize SA as a carbon source in solid and liquid media.

Because little is known about the aromatic compound degradation, including SA, in *F. graminearum,* it is expected that this study will contribute to our understanding of the degradation of SA in *F. graminearum*, and eventually to the relationship between that ability and the pathogenicity of *F. graminearum* toward wheat.

Chapter 2 - Materials and Methods

2.1. Fusarium strains, propagation and storage

F. graminearum DAOM 233423 was used as the wild-type (WT) strain. All transgenic strains were derived from this parental strain. Strain DAOM 180378 was also used as a control to measure the ability of *F. graminearum* to use SA as a carbon source in solid medium. Both strains were obtained from the Canadian Collection of Fungal Cultures, Agriculture and Agri-Food Canada, Ottawa, Canada. For storage purposes, mycelium plugs of each mutant strain were taken from cultures on Potato Dextrose Agar (PDA) plate as well as Synthetic Nutrient Deficient Agar (SNA) plate, deposited in tubes containing 15% glycerol (sterile) and stored at -80 ^{o}C. This stock was used as inoculum for testing the ability of the deletion mutant and ectopic insertion strains to grow in solid and liquid medium under SA stress. Spores of WT and mutant strains were produced by inoculating 50 mL of carboxymethyl cellulose (CMC) liquid media with one plug and incubating at 28^{o}C in a shaking incubator at 170 RPM in the dark for 3 days (Cappelli and Peterson, 1965). Spores were counted using a hemocytometer and stored at 4^{o}C for up to 4 days or at -80^{o}C as glycerol stock.

2.2. Generation of *F. graminearum* transgenic (mutant) strains

The disruption of genes of interest (GOI) was performed via homologous recombination between the genomic DNA and gene-specific replacement cassettes, as described in Frandsen et al. (2012). The procedure for the gene replacement is described in Figure 3. Briefly, two DNA fragments, upstream and downstream of the coding sequence of the target gene, plus two DNA fragments of the backbone vector pRF-HU2 (Appendix,

Figure A1) were annealed and combined in only one step. The gene-replacement cassette was then successively transformed into *E. coli* (for recovery of the designed construct) and *A. tumefaciens* (to allow transfer to *F. graminearum*). Each step of the procedure is described in detail in the subsections below.

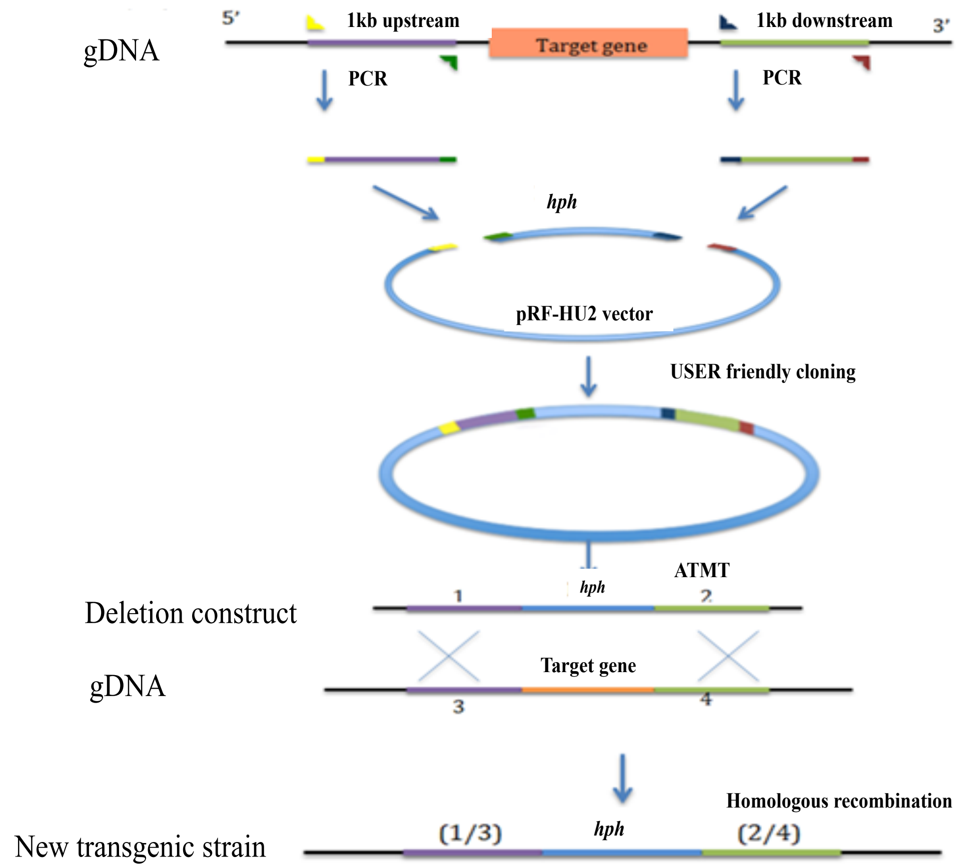

Figure 3: Schematic of Uracil-specific excision reagent (USER) friendly cloning strategy and ATMT strategy for target gene replacement with *hph* resistance gene. USER friendly cloning is a one-step directional cloning by annealing of two PCR products each containing 3' single stranded overhangs with two pRF-HU2 vector fragments containing hygromycin phosphotransferase resistance gene *(hph*). *Agrobacterium tumefaciens*-mediated transformation (ATMT) is a process of transferring the gene-replacement cassette from *Agrobacterium* to *F. graminearum*. Target gene replacement with *hph* is the result of homologous recombination between the deletion construct and *F. graminearum* genomic DNA (gDNA).

2.2.1. Oligonucleotide primers and Polymerase Chain Reaction

The open reading frame sequence (ORF) of each GOI, including their 5' and 3' non-coding regions were obtained from the *F. graminearum* genome database at the Munich Information Center for Protein Sequences (MIPS). The two homologous recombination segments (HRS) for each GOI were selected based on that sequence information. Oligonucleotide primers used in this study were designed using the Primer Select program (DNASTAR software, Canada) and synthetized by Sigma-Aldrich (Canada). Two sets of primers that target the same DNA sequence were used. One of them was typical primers that consisted of the desired DNA nucleotides. It was used for HRS amplification and for further screening for mutants. The other was a special pair of primers that consisted of the same DNA nucleotides as in the first primer set with the addition of specific 9 bp-long 2-deoxyuridine overhangs at their 5' ends containing uracil instead of thymine as nucleic acid base (U). There are four types of overhangs in the USER-friendly protocol and they are sites specific. Those overhangs sequences are; GGGTTTAAU, GGACTTAAU, GGCATTAAU and GGTCTTAAU, and they are specific for upstream forward, upstream reverse, downstream forward and downstream reverse, respectively (Table 2). Those specific U-containing primers used to amplify fragments for cloning purpose.

Polymerase Chain Reaction (PCR) was used to amplify upstream, downstream and target gene fragments for cloning and screening purposes. The standard PCR reaction consisted of 0.2 mM forward primer, 0.2 mM reverse primer, 0.2 mM dNTP mix, 1.5 mM Mgcl2, 2.5µl 10x DNA polymerase reaction buffer, 0.125 µl of DNA polymerase, 1µl (≈15-20ng/µl) of DNA template and DNA-free water to bring the volume to 25µl per reaction.

Two types of DNA polymerase were used; 'non-proofreading' Fermentas Taq polymerase (Thermo scientific, Canada) was used with typical primers, and 'proofreading' PfuTurbo® C_x Hotstart DNA Polymerase (Agilent Technologies, Canada) was used with the special primers containing (U). PCR was performed in an Eppendorf thermal cycler using the following protocol: an initial denaturation at 94°C for 30 sec, followed by 37 cycles with melting at 94°C for 30 sec, annealing at 54-58ºC (depending on the primers used) for 30 sec, extension at 72°C for 1.5 min, then a final extension for 10 min at 72°C; amplified samples were kept at 10°C once the reaction was terminated. For confirmation of fragment size, 5µl of the PCR amplification (~20 ng/ µl) was run on 1.5% agarose gel in 1X TAE buffer. All buffer and media recipes are provided in Appendix, Table A6, supplemented with ethidium bromide (0.6 µg/ ml) for 45 min at 145 V. Gel was photographed using Gel Doc XR+ with "image lab" software (BIO-RAD, Canada). PCR amplicons needed for cloning were purified using QIAquick PCR purification kit (Qiagen Science, Canada), following the manufacturer's instructions. DNA concentration was measured for all purified PCR amplicons using a Nanodrop 1000 Spectrophotometer (Thermo Scientific, USA). Each amplicon contained (~20ng/ µl) DNA. To reach the required DNA concentration of 250 ng in a small volume of ~5 µl, a large volume of ~ 50 µl containing 1200 ng was dried down using a DNA speed vac, DNA 120 (Savant, Thermo scientific, Canada).

Table 2: Oligonucleotide primers used for PCRs in this study. The underlined sequences are the overhangs added on the U-containing primers and are homologous to specific positions in the PRF-HU2 vector**.** The overhangs in the upstream primers of the gene of interest are located close to the left border (LB) site of the pRF-HU2 vector, and the overhangs in the downstream primers are located close to the right border (RB) site of the pRF-HU2 vector (Appendix, Figure A1). *Hph* primers *hph* p1, *hph* p2 and *hph* p3 are located at the 3' end, in the middle, and at the 5' of the *hph* gene, respectively.

Target gene	Forward	Reverse	Expected size
FGSG-09061 Upstream	<u>GGGTTTAAU</u>GAGCCTGAGCCGAAAGAGAACAC	<u>GGACTTAAU</u>GCAAAGCTACCTGGCGGATAAAG	614
FGSG-09061 Downstream	<u>GGCATTAAU</u>AAACCAAACCCAAATCCGTCTTAT	<u>GGTCTTAAU</u>ACTGGGGTTTCACTGTTGCTGGTA	666
FGSG-09061 target gene	AGAGCACATTCCCTTTGACA	CACCAACTTCACCCAGACAG	177
FGSG-09063 Upstream	<u>GGGTTTAAU</u>CTTGTGTTTGGCGCTGGACTAAT	<u>GGACTTAAU</u>AATAAATATAGAGGTTGGGTTGAA	960
FGSG-09063 Downstream	<u>GGCATTAAU</u>GTTTATTATTTGATTTGGCGTGAT	<u>GGTCTTAAU</u>CACCCGCTCCCTGATGACA	119
FGSG-09063 target gene	CCAAGAAGGCAAGTGGGATA	GTGGGTAGGGCTTTAGGAG	159
FGSG-03657 Upstream	<u>GGGTTTAAU</u>AGCTGCGGCATCTTCGTCAA	<u>GGACTTAAU</u>ACCCCATTCCTTCCGTCATAGA	753
FGSG-03657 Downstream	<u>GGCATTAAU</u>TTCTAGCCGGGTGTAAAATAATA	<u>GGTCTTAAU</u>TCGCGCCGTGGATAACT	774
FGSG-03657 target gene	GCTGCCCATGCCACAAGTCC	CACAAGCCATTGCGTCCTCT	175
FGSG-03667 Upstream	<u>GGGTTTAAU</u>ATTGAGGGCATTGATGTTGGATTC	<u>GGACTTAAU</u>AAGGGCTTCTCAGGAGTTGGATTT	671
FGSG-03667 Dow stream	<u>GGCATTAAU</u>GAGTCAGCCACAGATAAACAAGTA	<u>GGTCTTAAU</u>GAGAGCGAAAACCAGGAAATA	616
FGSG-03667 target gene	ATGTCCTCGTTCATCCAGC	CTCATTTGACCAGCCCAGT	108
FGSG-08358 Upstream	<u>GGGTTTAAU</u>CTCAGCCCACAGCCACAA	<u>GGACTTAAU</u>CCCCATAGCGATCAAA*AGGTT	603
FGSG-08358 Downstream	<u>GGCATTAAU</u>CAGCGCAAACATCCATAACAAAGA	<u>GGTCTTAAU</u>ACGGGGGCGAAGAAGAAGTG	664
FGSG-08358 target gene	GCAGCATCTCATTCGACCAC	CCTTCTTCGCATCGTAGCC	208
FGSG-08037 Upstream	<u>GGGTTTAAU</u>TCTCGCCGAATCTATCACCCTACA	<u>GGACTTAAU</u>TTCCGGCGTCTATCAACTTCCTG	624
FGSG-08037 Downstream	<u>GGCATTAAU</u>CCTATTACTGCGACGGGAAGATGT	<u>GGTCTTAAU</u>ACCCGCCTGGCTATGTCAAGTAAT	720
FGSG-08037 target gene	TGCCGAGACTCTGTTTGCTGGAC	GGTAGTGCGGCCGGTGTAGTG	416
hph p1	AAATTGCCGTCAACCAAGC	GGTTGGCTTGTATGGAGCA	135
hph p2	GCTCCATACAAGCCAACC	GGTCATTGACTGGAGCGAG	100
hph p3	CAGGCTCTCGCTGAATTCC	AGAAGTTTCTGATCGAAAAGTTCGAC	226

2.2.2 Vector construction

The binary pRF-HU2 vector, used in this project, was provided by the lab of Dr. Gopal Subramaniam of Agriculture and Agri-Food Canada, Ottawa, Ontario. A bacterial strain containing pRF-HU2 was cultivated in LB-Miller broth (LB) supplemented with 30µg/ml kanamycin at 37^{o}C with shaking at 200 RPM overnight. Vector DNA was isolated using a QIAprep Spin miniprep Kit (Qiagen Science, Canada) according to the manufacturer's instructions except that the elution was done with water. Vector DNA (2.35µg/30µl) was then digested using the restriction enzyme PacI, followed by the nicking enzyme Nt.BbvCI (New England Biolabs, Canada) in 10µl buffer to produce two fragments. Complete digestion was verified by running 2µL (~5µg) of digested vector on 1.2% agarose gel, and then the rest of the fragments were purified using QIAquick PCR Purification Kit (Qiagen Science) according to the manufacturer's instructions except that the elution buffer was water. Quantification of the DNA was done using the Nanodrop 1000 Spectrophotometer.

2.2.3 Assembly of gene replacement cassette and *E. coli* transformation

Assembly:

Based on Frandsen et al. (2012), assembly of the upstream and the downstream fragments (HRSs) together with the two pRF-HU2 binary vector fragments was done in only one step (Figure 3). PCR amplicons of the upstream and downstream regions of each GOI were cloned into the pRF-HU2 vector by the following "Uracil-specific excision reagent (USER) reaction": 260 ng each of upstream and downstream PCR products, 100 ng of pRF-HU2 vector fragments, 3 µL of 10X Pfu turbo buffer, 1 µL of USER enzyme mixture (containing Uracil DNA glycosylase and the Endonuclease VIII); mix and bring final volume to 30.0 μL with H_2O. The mixture was then incubated at 37°C for 20 min, and then at 25°C for 20 min.

E. coli transformation:

Five μL of USER reaction were used to transform the deletion cassette into *E. coli* Top 10 Competent cells (Invitrogen Life Technologies, Canada). Transformation was done by placing the USER reaction and the *E. coli* Top 10 cells on ice for 30 min followed by heat shock at 42°C for 30 sec, and then place on ice immediately for 2 min. Then, 250 μL of SOC medium were immediately added and the cells incubated at 37°C with shaker at 200 RPM for 1.5 hrs. Cells were then plated onto LB agar plates supplemented with 30 μg/mL of kanamycin and grown at 37°C overnight.

2.2.4 *E. coli* colony screening and sequencing:

Twenty-four transformed colonies were grown and plasmid DNA isolated as described in Section 2.2.2. Screening was done by PCR as described in Figure 4, looking for the presence of the upstream and downstream fragments and of hygromycin B resistance gene, *hph,* as well as a proper orientation of the fragments. Colonies that contain valid gene replacement cassette were chosen for sequencing.

Sequencing reactions were set up as following: 700 ng of plasmid DNA, 0.5 μL of 3.2 μM primer, 2 μL of 5x sequencing buffer, 0.5 μL of 2.5x BDT mix (BigDye® Terminator), enough water to bring up the volume to 10 μl. Primers used for sequencing are: GOI upstream forward, GOI downstream reverse, hph p2, hph p1 forward and hph p3 reverse. Sequencing was performed by the molecular microbiology technology lab (MMTL) group at

ECORC (Ottawa) using an ABI 3130xl Genetic Analyzer (Life Technologies). Sequence analysis was done using the software Chromas (Technelysium Pty Ltd, Brisbane, Australia).

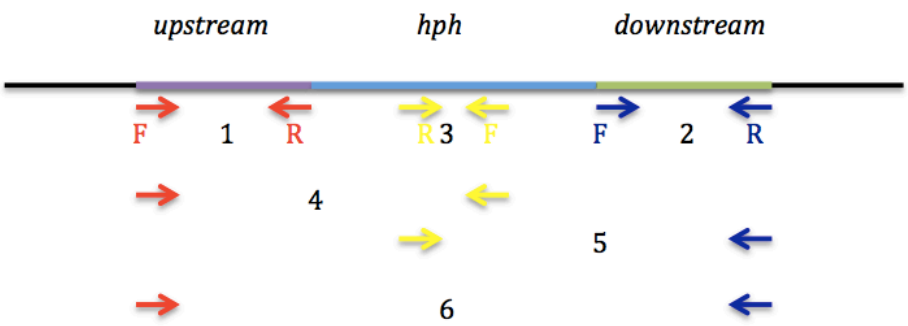

/Primer pair	1	2	3	4	5	6
Valid gene replacement cassette	+	+	+	+	+	+
Invalid gene replacement cassette	+/-	+/-	+/-	+/-	+/-	-

Figure 4: Screening and verification of gene replacement cassette in *E. coli*. Red arrows represent GOI upstream primers, yellow arrows represent *hph* primers and blue arrows represent GOI downstream primers. Primer pair (1) was used to test the insertion of the upstream fragment, primer pair (2) that of the downstream fragment, and primer pair (3) for the present of the *hph* gene. Primer pair (4) and (5) were used to test for fragment integration in the proper loci (LB or RB). Primer pair (6) was used to confirm the presence of the whole fragment including the upstream, downstream, and *hph*. A valid gene replacement cassette should show a positive band in the agarose gel for all PCR assays as shown in the table. +, expected positive result; -, expected negative result.

2.2.5 Transformation into *Agrobacterium tumefaciens*

A valid gene replacement cassette from one *E. coli* colony was introduced into *A. tumefaciens* strain LBA4404 cells by electroporation for 4-6 sec in 1.7 KV. Transformants were selected on LB plates supplemented with 100 µg/mL of kanamycin + 10 µg/mL rifampicin and stored at -80^{o}C.

2.2.6 *Agrobacterium tumefaciens* mediated transformation (ATMT)

A. tumefaciens mediated transformation was used to transfer the gene replacement cassettes to *F. graminearum* following the methods of Frandsen et al. (2012). An *A. tumefaciens* strain containing a gene replacement cassette was grown in LB supplemented with 50 µg/mL of kanamycin and 10µg/mL of rifampicin for 2 days in a 28^{o}C shaker at 100 RPM. One hundred fifty µL of that growth was used to inoculate 10 ml IMAS medium supplemented with 50 µg/mL of kanamycin and grown overnight in a 28^{o}C shaker at 100 RPM. When the culture reached the desired OD600 = 0.5 – 0.7, it was mixed with 2.0 X 10^6 *F. graminearum* conidia also in liquid IMAS. The mixture was then transferred onto the top of sterile black filter paper sitting on IMAS plates with no antibiotic and incubated at 28^{o}C in the dark for three days to allow the growth of both *A. tumefaciens* and *F. graminearum.* The black filter paper containing both *A. tumefaciens* and *F. graminearum* was then transferred to defined fusarium medium (DFM) plates supplemented with 150 µg/mL hygromycin and 300µg/mL cefoxitin, and incubated at 28^{o}C in the dark for three days to eliminate the growth of *A. tumefaciens* and to allow only *F. graminearum* containing *hph* to grow. The black filter paper was then transferred to another DFM plate supplemented with only 150 µg/mL hygromycin as described above and incubated in the same conditions for three days.

Following this, the black filter paper was discarded and the plates reincubated in the same conditions as above for one or two days until colonies could be observed. Transformant colonies were then individually transferred to and grown on PDA plates supplemented with 150µg/mL hygromycin. *F. graminearum* genomic DNA was extracted from an aliquot of each transformed colony. Around 100 mg of mycelium from each colony were harvested by scratching the mycelium from the agar surface and transferred to a lysing matrix tube. The mycelium was processed using the E.Z.N.A Fungal DNA Mini Kit (OMEGA bio-tek, USA) and the resulting DNA used for PCR screening.

PCR screening was performed as described in Figure 5, to determine if the transformants had the proper gene replacement configuration (knockout) or if they were ectopic insertion transformants (ect), by testing for the absence of the target gene specific fragment, the presence of the Hygromycin B resistance gene, as well as the proper orientation of the HRS fragments.

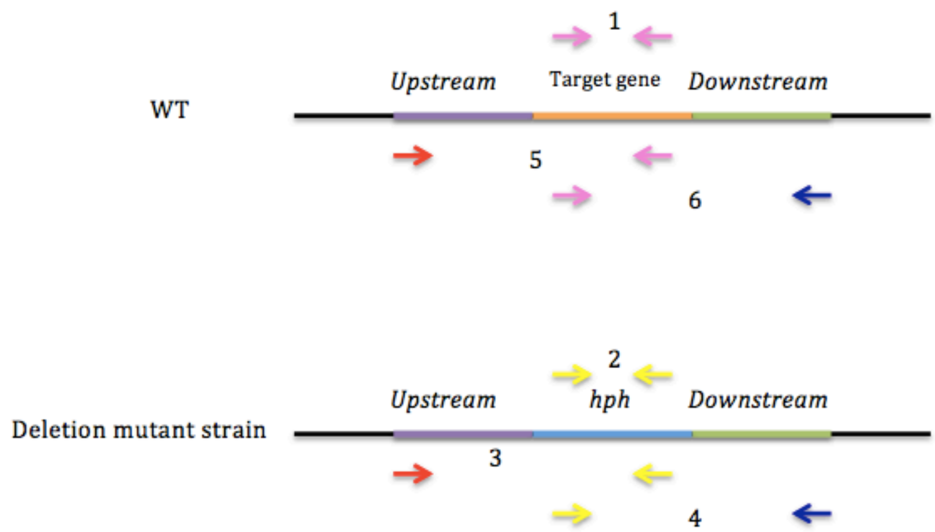

/primer pairs	1	2	3	4	5*	6*
Deletion mutant strain	-	+	+	+	-	-
Ectopic insertion strain	+	+	+/-	+/-	+/-	+/-

Figure 5: Screening and confirmation of gene replacement by homologous recombination. Red arrows represent GOI upstream primers, yellow arrows represent *hph* primers, pink arrows represent GOI specific primers and blue arrows represent GOI downstream primers. Primer pair (1) was used to test for the absence of the target gene and primer pair (2) for the presence of the *hph* gene. Primer pair (3) and (4) were used to test the proper orientation of *hph* in relation to the upstream and downstream regions. Primer pair (5) used to test the right orientation of target gene with the upstream region. Primer pair (6) used to the right orientation of target gene with the downstream region. Successful target gene replacement by *hph* showed negative result with PCRs 1, 5 and 6 and positive for the other assays**.** +, expected positive result; -, expected negative result.

2.2.7 Isolation of single spores:

Single spores were isolated from each transformant in order to get a single genotype for each transgenic strain. For each transformant, a spore suspension in sterilized water was poured onto a 2% water agar plate and left to dry. Single spores were then identified and isolated under the microscope. For each transformant, three single spores were picked up using a sterilized needle cutting out the agar area around the chosen spore, and transferred to individual fresh PDA plates supplemented with 150 μg/mL hygromycin to produce single spore colonies. Transformants obtained from single spores were then tested for the absence of the target gene as described in Figure 5.

Three knockout transformants and three ectopic transformants were chosen for further investigation for each GOI, and preserved in glycerol at -80^{o}C.

2.3 The ability of *F. graminearum* to use SA as a carbon source

In order to examine whether or not the knockout of candidate genes for SA degradation affected the ability of *F. graminearum* to use SA as a carbon source, transgenic strains (knockout, ectopic and WT strains) were grown on modified SNA plates (1 g KH2PO4, 1 g KNO3, 0.5 g MgSO4, 0.5 g KCl, 1 g glucose, 1 g sucrose, and 20 g agar per liter). This medium was supplemented with different concentrations of sugar or SA as the main carbon source: 1: no SA, 1 g/l each sugar; 2: no SA, 0.2 g/l each sugar (1 and 2 as positive controls); 3: no SA, no sugars (negative control); 4: 1.5 mM SA, no sugars; 5: 6 mM SA, no sugars; 6: 12 mM SA, no sugars; all media were adjusted to pH 8, using 5 M KOH, when including SA. Plates were inoculated with a 6 mm plug cut from the edge of 3-5 days old colonies grown in modified SNA plates and incubated at 28^{o}C in the dark. The growth area of the transgenic strains and of the *F. graminearum* WT was measured over a 4-day period by mapping the edge of the mycelium each day with a waterproof marker pen. At day 4, pictures were taken of each plate (both sides) with a Nikon camera D90 with AF Micro-Nikkor 60mm lens. The mycelium growth area and density of growth for each plate were measured by processing the images with ImageJ software (Rasband, 1997–2014). In the growth area, the scale was set for each plate based on the diameter of the plate, 10 mm. The growth area was measured automatically by superposing a circle on top of each day's growth edge. For growth density, a medium size circle was drawn and saved in the program to be used as a default measuring. This circle was then applied for all the plates and the integrated density was automatically measured.

2.4 Statistic analysis:

Statistical analysis was performed in Microsoft Excel 2013 using one-way ANOVA (Analysis of variance) comparing three biological replicates, each containing three technical replicates for all strains within the gene. The alpha was set to 0.05 before measuring the variation. P value <0.05 indicated as a significant difference between deletion mutant strains and ectopic mutant strains as shown in graphs as an asterisk.

2.5 High Performance Liquid Chromatography analysis:

In order to examine the enzymatic activity of each knockout gene toward the degradation of SA, *F. graminearum* WT and mutant strains were growth in liquid culture in the presence of SA and the residual amount of SA in the culture supernatant was measured using HPLC. A modified two-stage protocol from Miller & Blackwell (1986) was used to grow *F. graminearum* WT and mutant strains. A schematic representation of the growth and sampling procedure is illustrated in Figure 6A and B.

In a first experiment, the rate of degradation of SA over time by the wild type parental strain of *F. graminearum* was tested in presence and absence of sugars, to determine how fast *F. graminearum* can metabolize SA in the growth conditions used and investigate if simple sugars affect metabolism of SA. The second stage medium was supplemented with different concentration of sugar: 1) 40 g sucrose and 10 g glycerol (standard amount); 2) 20 g sucrose and 5 g glycerol; 3) 0 g sucrose and 0 g glycerol. All media were also amended with 1mM SA. Cultures were harvested at the following time points: 0, 2, 4, 6, 8, and 24 hrs, and aliquots of supernatant analyzed by HPLC.

After optimization experiments, the following conditions were chosen for mutant testing. For each strain and well, $5x10^5$ spores were inoculated in 4 ml of first stage medium and incubated in the dark in a 6-well culture tray (Falcon Multiwell, cat.#35304) at 28^{o}C with the shaker at 170 rpm for 24hr. Cultures from each well were then transferred to sterile 15 ml Falcon tubes and centrifuged at 4000 RPM in Eppendorf centrifuge 5804R for 10 min to collect pelleted mycelia. Pellets were washed with sterile water and centrifuged at 4000 RPM for 10 min. Pellets were then resuspended in 4 ml of second stage medium, without sucrose or glycerol, supplemented with 1 mM SA at pH 8, transferred to new 6-well culture trays and incubated at 28^{o}C with shaker at 170 RPM in dark for 0, 2, 4 and 6 hr. For each fungal strain, sufficient wells were inoculated to allow three biological replicates (one per well) for each sampling time point. Mycelium and supernatant were collected after each time point and separated by filtration under vacuum using Whatman filter paper 1 (Sigma-Aldrich).

Mycelium was dried overnight at room temperature and its dry weight was measured. Filtrate supernatants were collected after each time point and 5% acetonitrile were added to each 95% volume of supernatant. Filtrate supernatant was stored at -20˚C for SA measurement.

One hundred µl of the liquid cultures filtrate was injected into an ATKA P-10 HPLC system (GE Healthcare, Canada) with 150 X 4.6 mm 5 µ Hypersil ODS column (Thermo-Electron Corp). The compounds in the samples were separated on a gradient of 05:95 to 95:05 acetonitrile: water supplemented with 0.1% Trifluoroacetic acid (TFA) over 25 min at a flow rate of 1 ml min^{-1}. The column was then washed with 100% acetonitrile for 5 min followed by 05:95 acetonitrile: water with 0.1% Trifluoroacetic acid for 15 min. HPLC-grade SA, catechol and gentisate (Sigma-Aldrich, Canada), the predicted first intermediates in degradation of SA, were used as reference compounds. SA concentration was monitored by UV at 210, 280 and 300 nm, and the data at 300 nm was analysed by UNICORN software (GE Healthcare, Canada). SA was quantified based on the area under the curve (mAU*min).

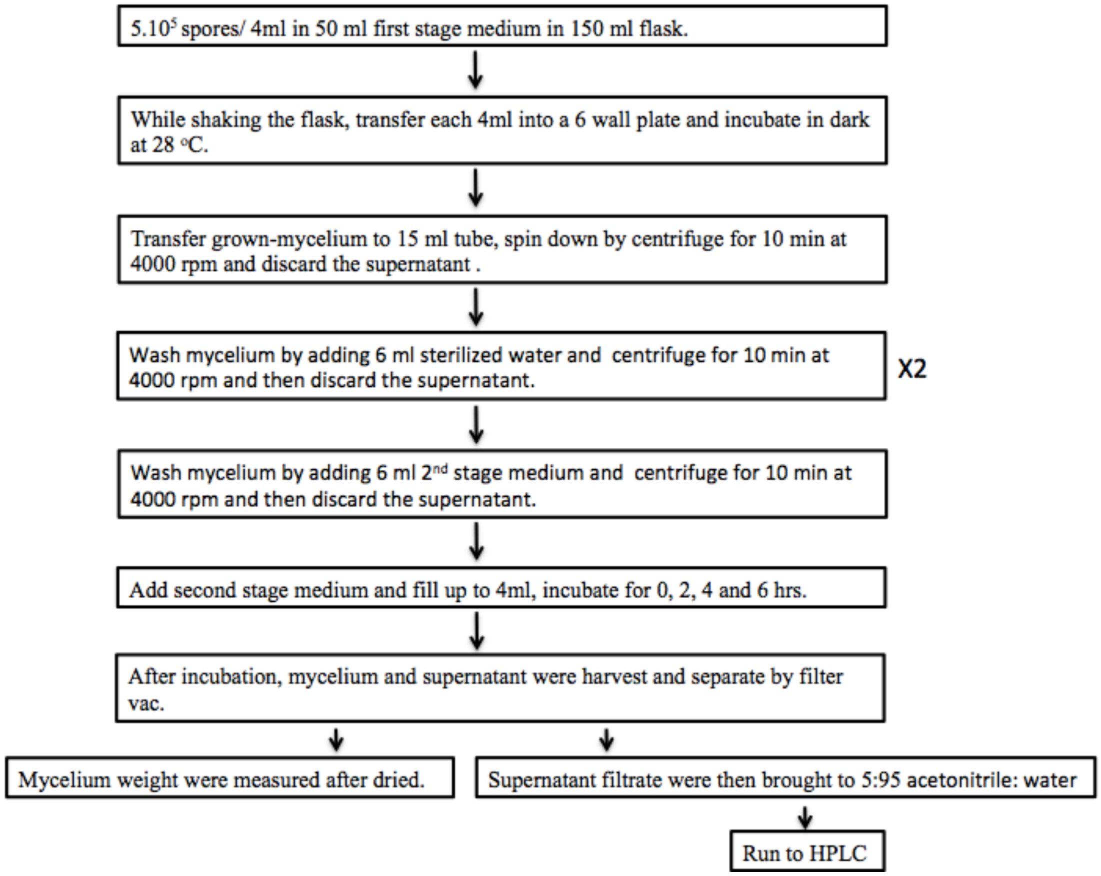

Figure 6A: Flow chart for the growth and sampling procedure for the HPLC assay.

Reproduced from (Miller & Blackwell, 1986)

1

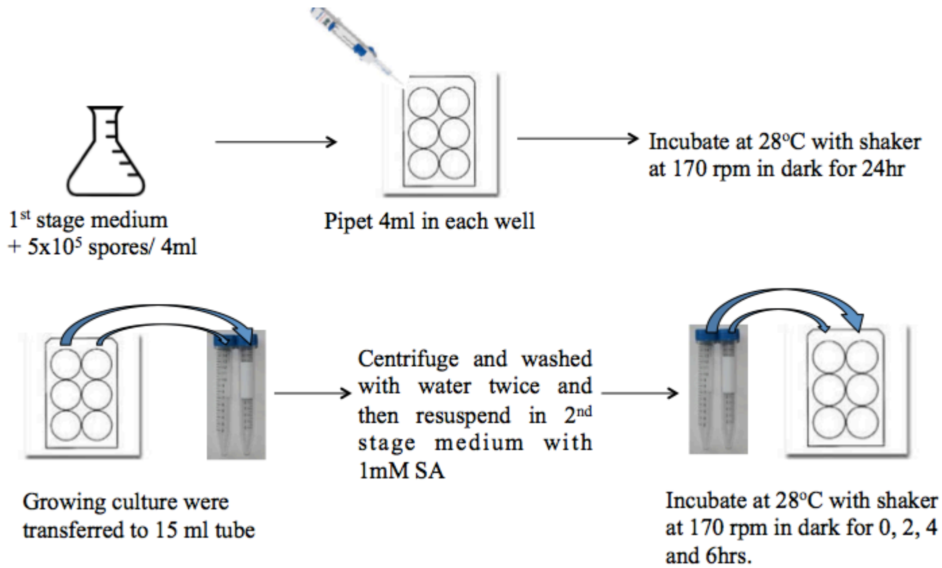

2

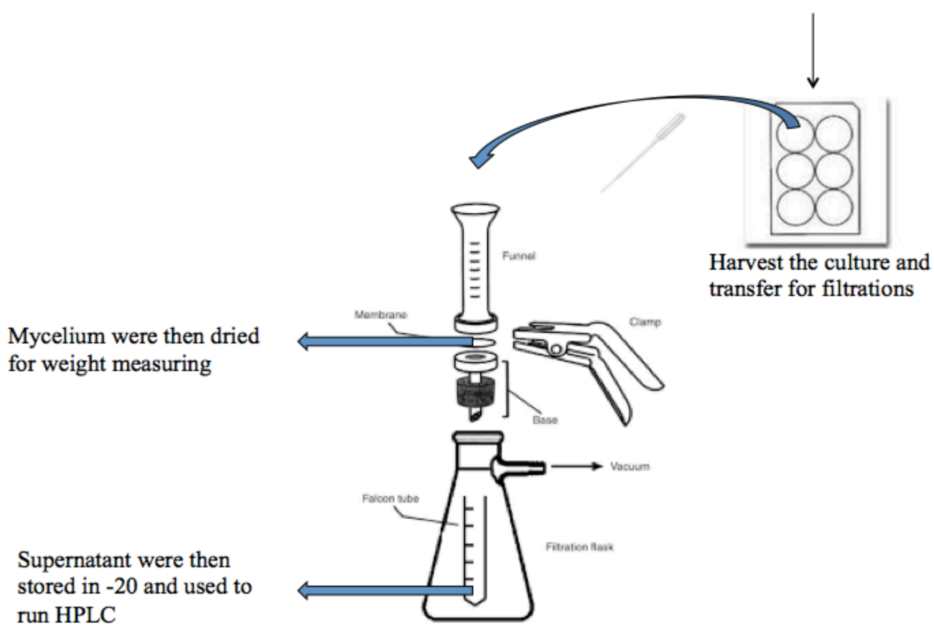

Figure 6B: Visual representation of the growth and sampling procedure for the HPLC assay. 1) Culture procedure in 1st stage medium and transfer to 2nd stage medium. 2) Harvesting process and the use of the mycelium and filtrate fractions.

Chapter 3 – Results

This project aimed at characterizing a set of *F. graminearum* genes induced by growth in the presence of SA; the candidate genes selected are predicted to code for enzymes involved in the catalysis of the initial and second step in the SA degradation pathway by fungi. Deletion mutant strains were obtained for the following genes: FGSG_09063, FGSG_03657, FGSG_09061, FGSG_08037, FGSG_08358 and FGSG_03667, by using gene replacement by homologous recombination. All strains were tested for their ability to grow on solid media when SA was the main source of carbon, and a subset of the strains were tested for their ability to use SA in a liquid medium.

3.1 Production of gene-replacement mutants for candidate genes for degradation of SA

To identify genes that are involved in the degradation of SA, we inactivated candidate genes by gene replacement for the first two predicted enzymatic steps. For the initial step, conversion of SA to catechol, the following genes were inactivated: predicted salicylate 1-monooxygenases FGSG_09063 and FGSG_03657, and predicted 2,3-dihydroxybenzoic acid decarboxylase FGSG_09061. For the second step, cleavage of the ortho ring, predicted intradiol 1,2-dioxygenase FGSG_08037, predicted homogentisate 1,2-dioxygenase FGSG_08358, and predicted hydroxyquinol 1,2-dioxygenase FGSG_03667 were inactivated (Figure 7). For each target gene, the coding portion of the gene was replaced by the hygromycin-resistance gene, hygromycin phosphotransferase or *hph*, as a selectable marker, using homologous recombination as facilitated by the USER-friendly cloning technique and *A. tumefaciens*-mediated transformation (Figure 3; Frandsen et al., 2008). The deletion cassettes were produced by the annealing of the digested pRF-HU2 vector with PCR-amplified homologous recombinant segments (HRSs) located in the upstream and downstream non-coding regions of each target gene, and then the ligated material was transformed into *E. coli*. For each target gene, a complete deletion cassette was transferred into *A. tumefaciens* and used to mediate transformation into *F. graminearum*. Since this process was applied to all target genes, the results for a randomly chosen gene, FGSG_09063, are presented in the following subsections as an example. The results for other genes are summarized in (Table 3).

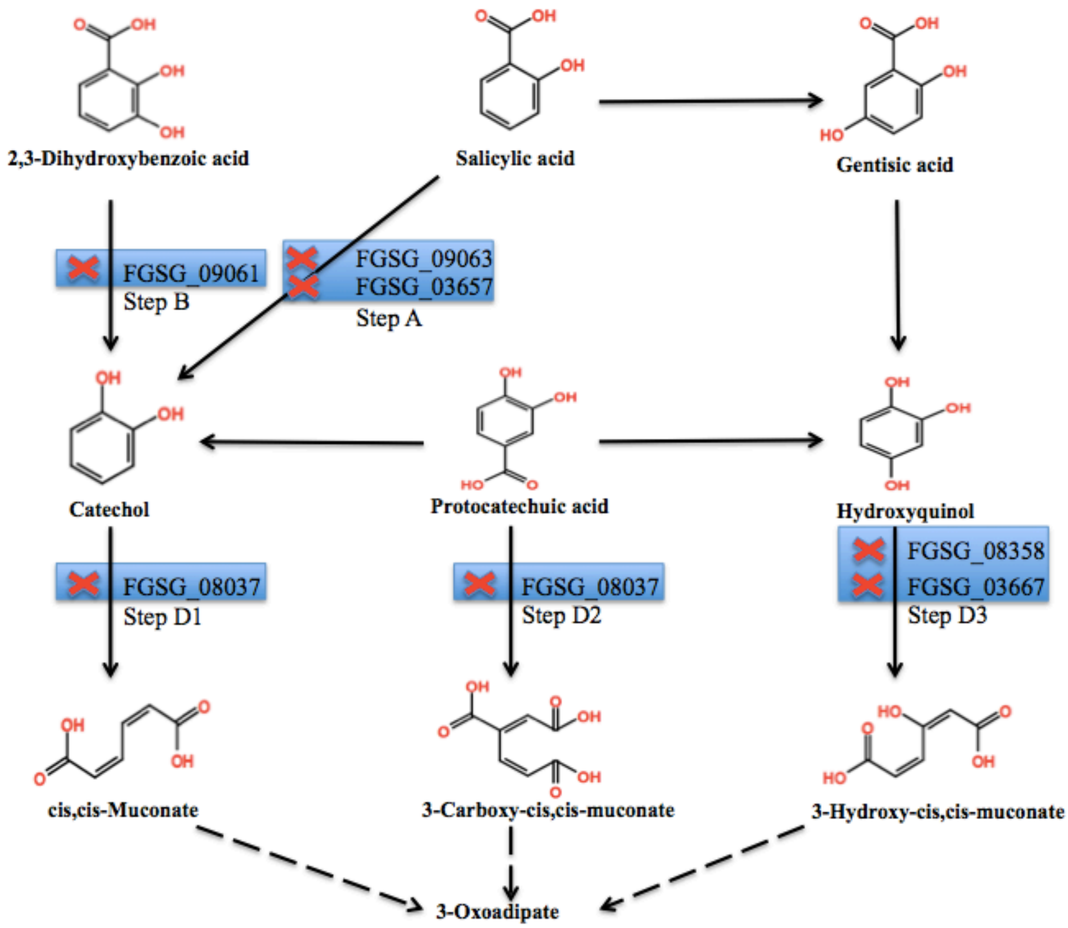

Figure 7: Postulated initial degradation steps for SA in fungal species. Candidate genes chosen for this study are tentatively assigned to individual reactions. Dashed lines indicate that there are additional catabolic steps to the final compound in the degradation pathway, 3-oxoadipate. Modified from Qi et al. (2012).

Table 3: Summary of the results for target gene replacement. The colony number for the confirmed positive colonies in each step of the knockout process is indicated. Underlined colony numbers correspond to the source colonies for construct used to proceed to next step. The last two rows represent colony numbers for deletion and ectopic mutant strains used in tests for ability to utilize SA as a carbon source.

	FGSG_03657	FGSG_09061	FGSG_03667	FGSG_08358	FGSG_08037
E. Coli colonies	4, 12, 14, 17	1, 2, 7, 10	3, 4, 8, 6, 14	1, 4, 11	1, 2, 6, 7
Sequencing	4, 12	1, 7	3, 4	1, 11	1, 7
A. tumefaciens	12	1	3	11	1
F. graminearum deletion mutant colonies	12, 14, 16	2, 7, 6, 15,	2, 3, 7	4, 8, 9	16, 17, 19
F. graminearum ectopic insertion colonies	6, 8, 51	8	1, 4, 6	2, 3, 5	12, 15, 18

3.1.1 Cloning and screening of *E. coli* transformants

Prior to cloning, HRSs and pRF-HU2 digested fragments were prepared. HRSs were amplified using upstream and downstream specific primer pairs (Table 2) and amplification was confirmed by separating the PCR amplicons on agarose gel. The expected size for amplicons was around 1000 bp (see Figure 8 as an example). The pRF-HU2 vector was digested using a restricted enzyme (*PacI*) and a nicking enzyme (*Nt.BbvCI*), to yield two fragments of DNA. Digestion was confirmed by running digested and undigested vectors side by side on agarose gel (Figure 9). For cloning, gene specific upstream and downstream HRS amplicons and the two fragments of pRF-HU2 vector were annealed together, allowing the upstream and downstream HRSs to be inserted respectively upstream and downstream of the *hph* gene; this was followed by transformation into *E. coli*. Transformed colonies were randomly chosen for plasmid DNA extraction; Figure 10 shows an example of extracted plasmid DNA. DNA bands appeared in three different groups. It is presumed that the higher molecular weight bands represented plasmid DNAs containing two HRS insertions, the intermediate molecular weight bands represented DNAs with only one HRS insertion, either the upstream or downstream of the target gene, and the lower molecular weight bands represented DNAs without HRS insertion or undigested vector. Extractions containing plasmid DNA visible on gel were selected for PCR screening.

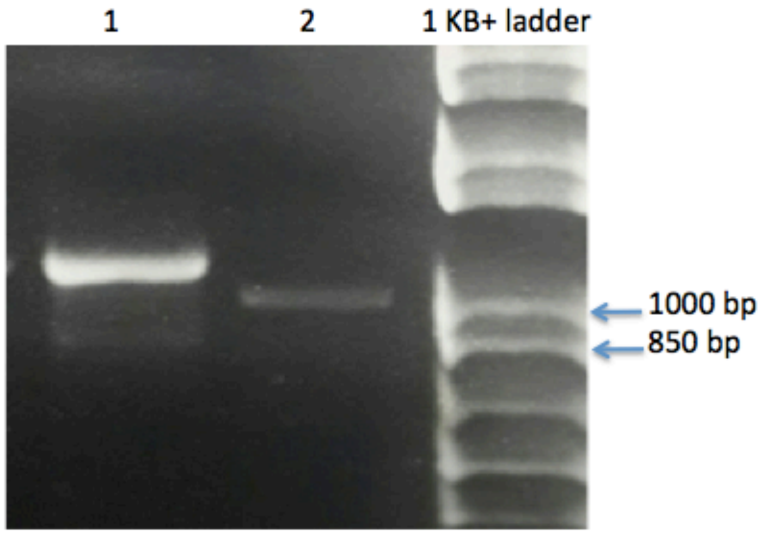

Figure 8: PCR amplicons of the upstream and downstream homologous recombination segments (HRSs) flanking the coding sequence of FGSG_09063, separated in 1.5% agarose gel. Column 1 and 2 show PCR amplification bands of the downstream and upstream fragments, respectivly, from genomic DNA strain DAOM 233423 with expected size around 1000 bp. The lane on the right contains linear DNA fragments of known sizes from a commercial source.

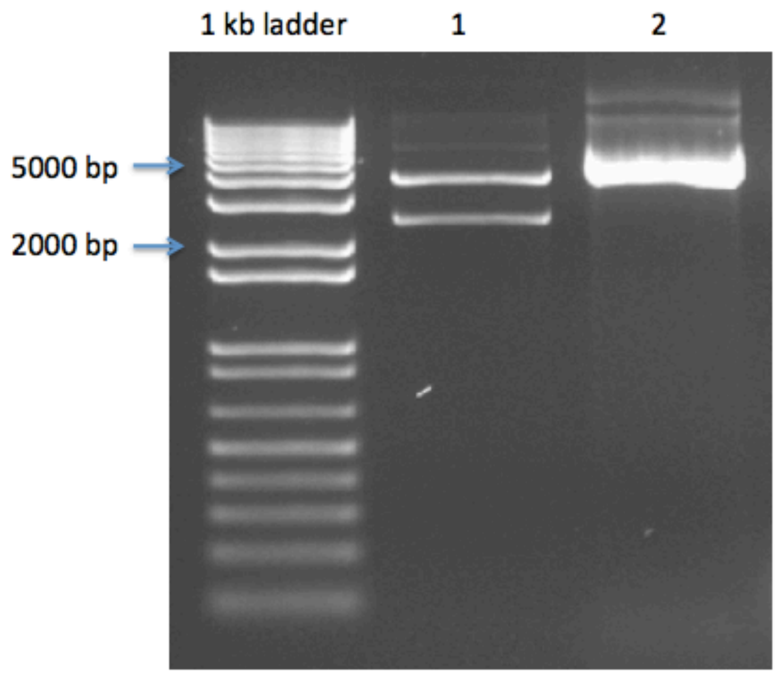

Figure 9: pRF-HU2 vector after digestion with a restricted enzyme (PacI) and a nicking enzyme (Nt.BbvCI), and separation on 1.5% agarose gel. Column 1 represents the digested pRF-HU2 bands with expected size of approximately 2489 bp and 3834 bp. Column 2 represents undigested pRF-HU2 DNA. The lane on the left contains linear DNA fragments of known sizes from a commercial source.

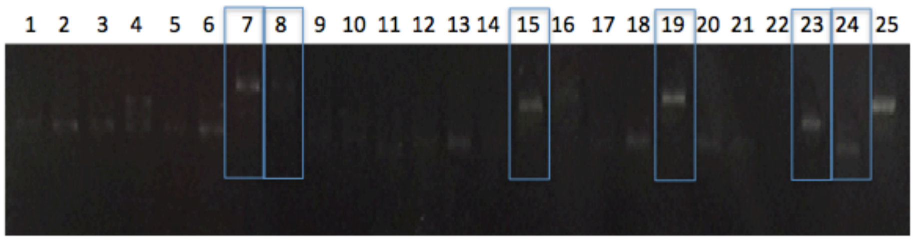

Figure 10: Circular plasmid DNA extracted from transformed *E. coli* colonies, separated on 1% agarose gel. Columns 1 to 25 contain 5ul of plasmid DNA extraction from each of 25 *E. coli* colonies. Columns 7, 8, 15, and 19, 23 and 24 contain plasmid DNAs of different sizes, possibly representing deletion cassettes with complete and partial assembly of the four fragments during ligation.

PCR screening was done on plasmid DNA extracted from *E. coli* colonies, as well as wild type *F. graminearum* genomic DNA as control, using the strategy described in Figure 4. The first two PCR assays were designed to test for the presence of the upstream and downstream HRS using the appropriate gene-specific primers (Table 2). Figure 11 presents an example of PCR screening for gene FGSG_09063. It shows that both HRS were successfully inserted in plasmid DNAs from colonies # 7, 8 and 19. DNAs from colonies #15 and #23 had only one of the HRS inserted, downstream and upstream, respectively. DNA from colony #24 contains neither upstream nor downstream HRS fragments. The following three PCR assays were designed to test for the proper orientation of the HRS insertions, as described in Figure 4 as well as the integrity of the deletion cassette. As we can see in Figure 12, the upstream and downstream HRSs were successfully integrated within the pRF-HU2 vector in the desired sites and orientation. However, the presence of a full deletion cassette including upstream HRS, *hgh* gene and downstream HRS could not be confirmed for colony #8.

For further verification of the location and integrity of the HRS fragments, plasmid DNAs from colonies 7 and 19, containing a possible complete deletion cassette for FGSG_09063, were then sequenced using primers FGSG_09063 upstream forward, FGSG_09063 downstream reverse, Hph p2, Hph p1 forward and Hph p3 reverse (Table 2). The sequences obtained were manually aligned with the published sequence for the HRS fragments from *F. graminearum* strain Ph1 (Cuomo et al., 2007).

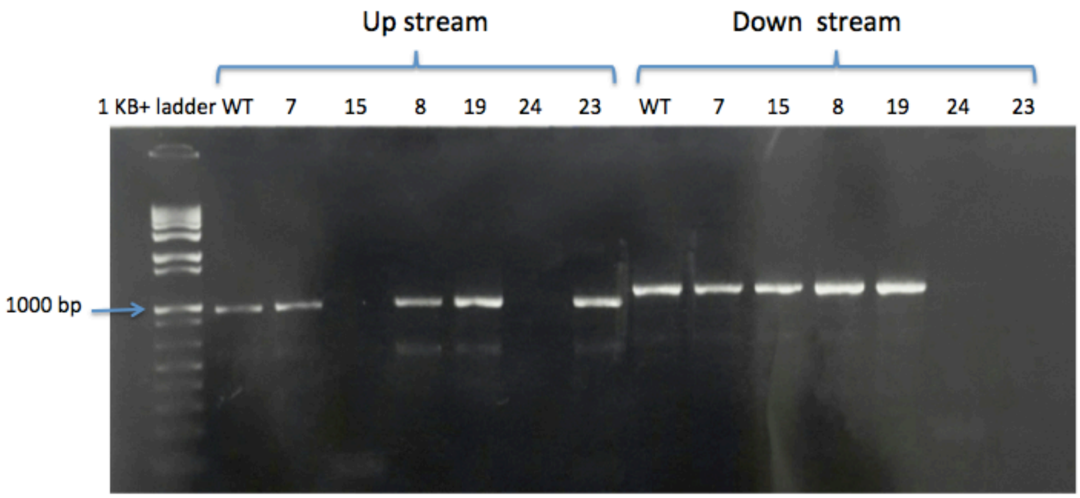

Figure 11: PCR screening for the presence of upstream and downstream HRSs into the plasmid DNA isolated from transformed *E. coli* colonies. PCR amplification was performed using FGSG_09063 upstream and downstream primer pairs. Column numbers refer to the same colony numbers as used in Figure 10; WT, wild type *F. graminerum* genomic DNA used as control. Amplicons were run on 1.5% agarose gel.

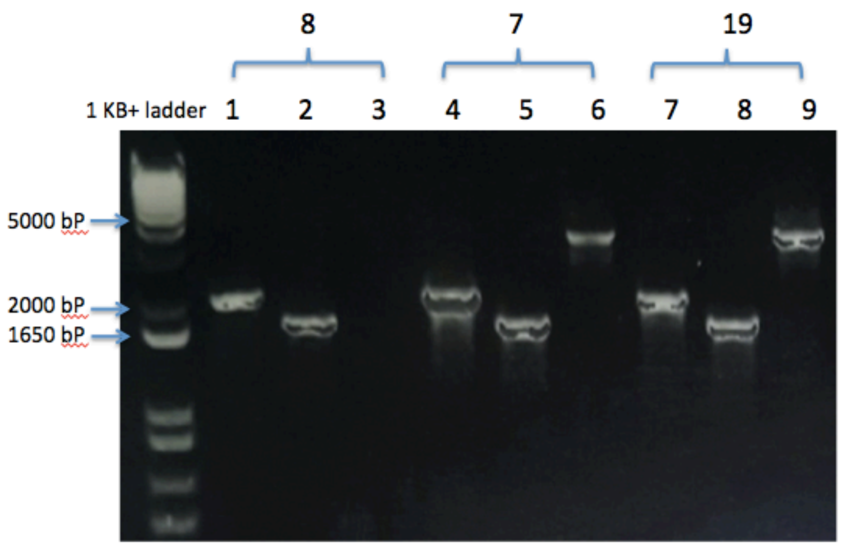

Figure 12: PCR screening for proper HRSs orientations in deletion cassettes from 3 distinct *E. coli* colonies, #7, 8 and 19. Amplicons were separated in 1.5% agarose gel. Column 1, 4 and 7: test for the insertion of the upstream HRS in 5' of the hygromycin resistance gene using primer pair 5 of Figure 4; amplicons of about 2455 bp in size were expected. Column 2, 5 and 8: test for the integration of downstream HRS in 3' of the hygromycin resistance gene using primer pair 4 of Figure 4; amplified bands with size around 1783 bp were expected. Column 3, 6 and 9: test for the presence of a full deletion cassette including the *hph* gene in between the two HRSs using primer pair 6 of Figure 4; bands of size around 3798 bp were expected.

3.1.2 *Agrobacterium tumefaciens* mediated *F. graminearum* transformation (ATMT)

Agrobacterium tumefaciens is well known for its ability to transfer part of its DNA, the T-DNA, to several plants and fungal species. The plasmid DNA from colony #7 for the deletion cassette of FGSG_09063 was introduced into *A. tumefaciens* LBA4404 by electroporation. Subsequently, a transformed *A. tumefaciens* colony was used for transformation of *F. graminearum* strain DAOM 233423.

Fusarium graminearum transformation yielded colonies of various size and colors. Colonies were frequently observed as white, filamentous, pulvinate colonies (see Figure 13 for examples). Occasionally, some colonies were yellowish, orangey, or much smaller in size. However, once the colored colonies were transferred to fresh PDA plates, they grew nice and white. Small colonies needed more time of incubation in the original plates to reach the size of other colonies prior to transfer to fresh PDA. Ten colonies were randomly selected for PCR screening to test for integration of the deletion cassette at the target gene and gene replacement.

Screening of *F. graminearum* transformant colonies was done to distinguish deletion mutants (also referred to as knockout or KO), where the gene of interest was replaced by the gene *hph*, from ectopic insertion mutants (Ect) in which part or the whole deletion cassette plasmid was inserted somewhere else in the genome. Four PCR assays were performed for that screening. The first, key PCR assay was performed to test for the absence of the target gene in the transformed colonies. Figure 14 shows an example for gene FGSG_09063. Result showed that four colonies out of nine had a successful deletion of the target gene, as there was no band of amplification when using their DNA as a template. However, five colonies showed no deletion of the target gene.

A second PCR assay was performed to test for the presence of the *hph* resistance gene. Figure 15 shows that the *hph* fragment was amplified in all tested colonies transformed with the deletion cassette for FGSG_09063. It confirms that the *hph* gene was present in both, deletion and ectopic insertion transformants. A third and fourth PCR assay were performed on the four FGSG_ 09063Δ deletion mutant strains, to confirm the correct orientation of the deletion cassette at the target gene site. This can be possible only if the gene was correctly replaced by homologous recombination. Result showed that all *F. graminearum* FGSG_09063Δ deletion mutant strains were correctly generated through homologous recombination (Figure 16).

After all PCR assays, for each gene, three deletion mutant strains (KO) and three ectopic insertion mutant strains (Ect) (as controls) were selected for further characterization, except for gene FGSG_09061 for which only one ectopic insertion strain was identified.

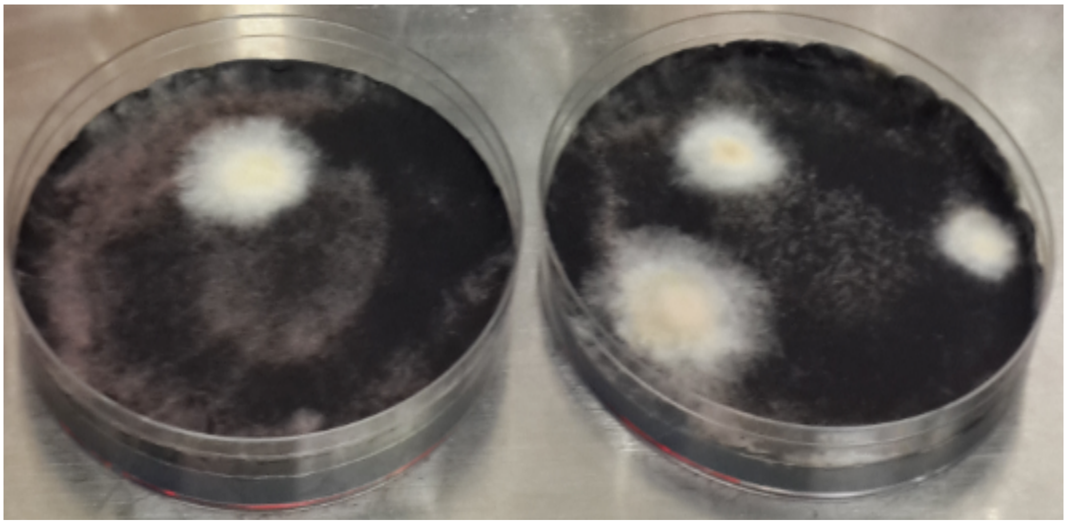

Figure 13: *F. graminearum* transformants colonies for deletion of FGSG_09063. Colonies are growing on sterile black paper deposited on PDA agar plates supplemented with 150µg/mL hygromycin. The number of hygromycin-resistant colonies was different from plate to plate, with a total of about 25 colonies in 10 plates (transformation for one gene).

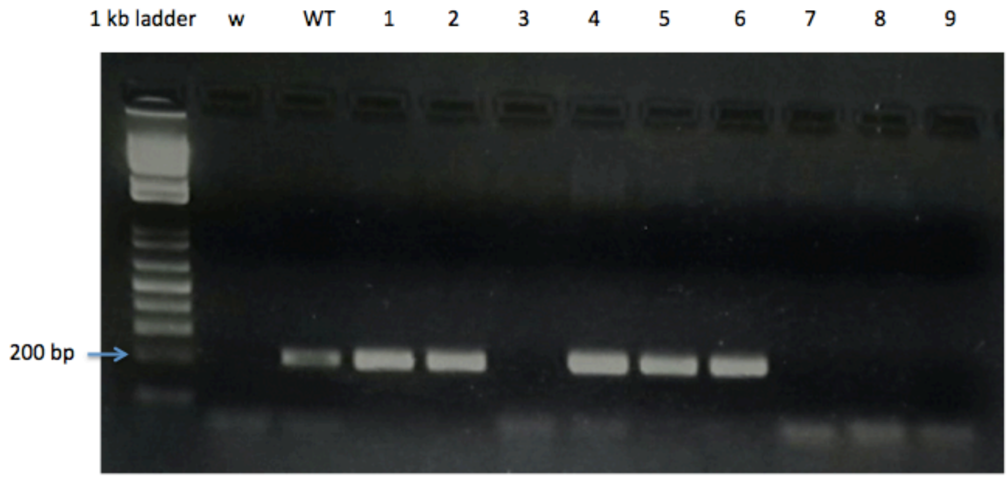

Figure 14: Testing for the disruption of gene FGSG_09063 in *F. graminearum* transformants. PCR amplification of the target gene was performed using primer pair FGSG_09063 target gene forward and reverse (Table 2); amplicons of about 200 bp were expected in presence of the target gene. Amplicons were separated on 1.2% agarose gel. Lanes w and WT represented negative and positive controls, using water and wild type *F. graminearum* genomic DNA as a templates, respectively. Columns 1 to 9 show amplification from *F. graminearum* transformant colonies. Columns 1, 2, 4, 5 and 6 showed bands, indicating that they still contain the target gene; the corresponding colonies were identified as ectopic strains. Columns 3, 7, 8 and 9 showed no amplification of the target gene and identified as potential deletion strains.

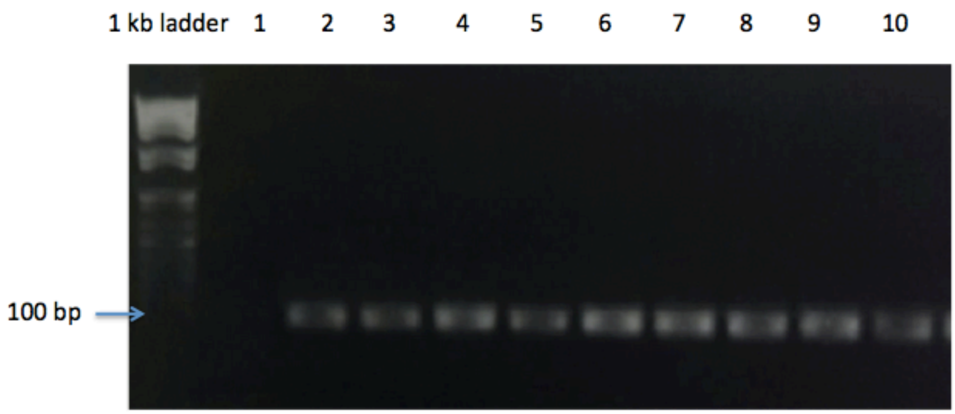

Figure 15: Testing for the presence of the hygromycin resistance gene in FGSG_09063 transformant strains. Amplicons of about 100 bp were expected; separation was on 1.2% agarose gel. Column 1 represented a negative control using wild type *F. graminearum* genomic DNA as a template. Columns 2 to 10 showed insertion of hygromycin resistance gene in all transformant strains.

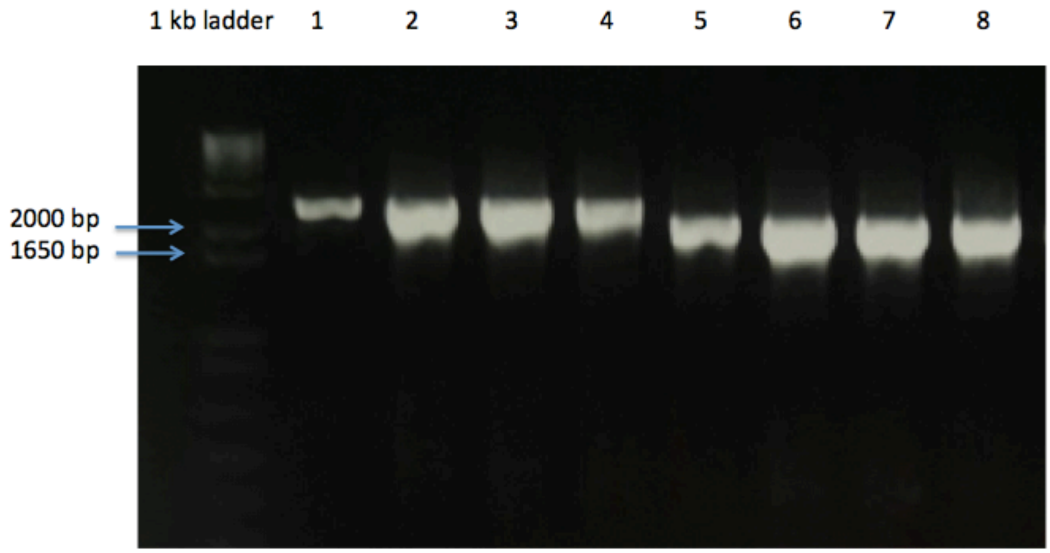

Figure 16: PCR assays to confirm the correct HRS orientations in 4 deletion strains for gene FGSG_09063. Amplicons were separated on 1.5% agarose gel. Columns 1 to 4: integration of downstream HRS in 3' of hygromycin resistance gene was tested using primer pair 5 of Figure 4; Bands of the amplification were expected to be around 2455 bp. Columns 5 to 8: integration of upstream HRS in 5' of the hygromycin resistance gene was tested using primer pair 4 of Figure 4; amplicons were expected to be around 1780 bp.

3.2 Ability of the deletion and ectopic insertion mutant strains and wild type *F. graminearum* to use SA as a carbon source in solid medium

To assess if one or more of the genes deleted is required for SA degradation, two tests were performed: 1) measurement of the ability of *F. graminearum* strains to use SA as the main carbon source in solid media, and 2) measurement of the ability of *F. graminearum* strains to degrade SA in liquid medium (see next section).

As a preparatory step towards the determination of the ability to use SA as the main carbon source in solid media, we compared the ability of two *F. graminearum* wild type strains to grow on modified SNA agar plates containing different carbon sources, including a) no sugar or SA (negative control), b) 0.2 g/L sucrose and 0.2 g/L glucose, c) 1 g/L sucrose and 1 g/L glucose (b and c as positive controls), d) neither sucrose nor glucose, however supplemented with either 1.5, 6 or 12 mM SA as a carbon source. Of the two strains compared, DAOM233423 was used in this project as the parent strain to generate the mutants while DAOM180378 was used in a previous publication characterizing the effect of SA on *F. graminearum* growth (Qi et al. 2012). Results showed that the strain DAOM180378 grew slightly faster than DAOM233423 in all conditions, however both strains responded similarly to the changes in growth conditions (Figure 17).

Deletion and ectopic insertion mutant strains for each gene and the wild type parental *F. graminearum* strain were grown on the same treatments as above to compare their ability to use SA as a carbon source. The rate of growth of the wild type strain, deletion mutant strains and ectopic insertion mutant strains on SNA plates supplemented with sugars was not affected by any gene deletion (Appendix, Table A1). All strains grew at a similar rate on SNA plates supplemented with SA in different concentration. Interestingly, the mycelium of all strains also spread at the same rate in SNA plates without sugar or SA; it is presumed that *F. graminearum* strains, the only other potential source of carbon in the medium.

However, it could be visually observed that there were differences in mycelium density between conditions. For all strains, wild type, deletion mutant and ectopic insertion mutant strains, the mycelium was denser on SNA plates supplemented with sugars, especially with the higher amount of sugars (which is the amount in the standard SNA medium) (Figure 18). The lowest density of mycelium was observed on SNA plates with no added carbon source except for the agar, which is not easily used by *F. graminearum*. Interestingly, the mycelium density was remarkably affected in some deletion mutant strains when grown on SNA supplemented with SA as a carbon source. Results showed that mycelium density of deletion mutant strains for genes FGSG_03667 and FGSG_09061 was noticeably reduced in all SNA plates supplemented with SA when compared with the ectopic insertion mutant strains for the same genes (Figure 18, Appendix, Table A2). However, there was no effect on the mycelium density between deletion mutant strains and ectopic insertion mutant strains for genes FGSG_ 09063, FGSG_03657, FGSG_08358, and FGSG_08037 when grown on SNA plates supplemented with SA (see Figure 19 for an example).

For a semi-quantitative estimation of the changes in mycelia density, integrated pixel density within marked growth areas was determined from pictures of the agar plates. After an examination of the means and standard deviation in each treatment for all mutant strains of each gene, two growth conditions were chosen for further statistical analysis between the deletion mutant strains and ectopic insertion strains: 1) no SA, 0.2g glucose, 0.2 g sucrose and 2) 12mM SA, no sugar. Those conditions were chosen for the higher consistency of the *F. graminearum* growth when compared with other conditions. As expected, on SNA plates supplemented with 0.2g glucose and 0.2 g sucrose, there was no statistical difference (p value >0.05) in mycelium density between deletion mutants and ectopic insertion mutant strains for any of the genes, indicating that deletion of target genes did not affect the ability of *F. graminearum* to use simple sugars as the main source of carbon (Figure 20, upper row of panels). The statistical analysis confirmed that there was a significant reduction (p value < 0.05) in density of mycelium only for *FGSG*_09061Δ and *FGSG*_03667Δ strains, when compared to ectopic insertion mutants for the same gene, when growing on SNA plates supplemented with 12mM SA as a carbon source (Figure 20, lower row of panels) (Appendix, Table A3). This result suggests that those two genes play a significant role in SA degradation by *F. graminearum* strains. One of them, FGSG_09061Δ, is predicted to be a 2,3 dihydroxybenzoic acid decarboxylase postulated to be involved in the first step in SA degradation. The other gene, FGSG_03667Δ is predicted to be a hydroxyquinol 1,2-dioxygenase, and postulated to be involved in the first step in the ortho ring-cleavage part of the degradation pathway.

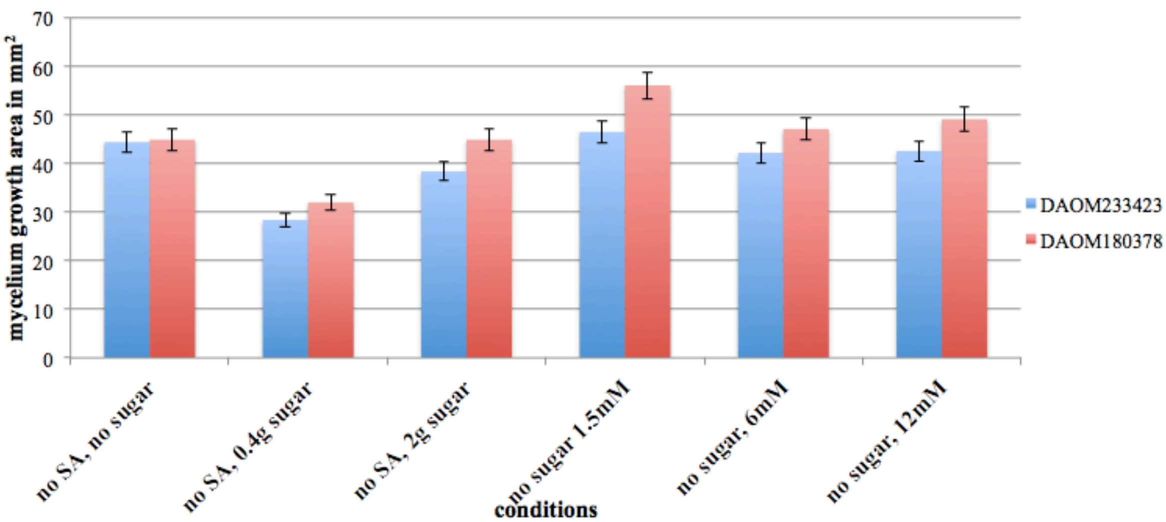

Figure 17: Growth of *F. graminearum* strains DAOM233423 and DAOM180378 on SNA plates with different carbon sources. The advancing edge of the mycelium growth area was measured after 3 days of incubation in the dark at 28^{o}C. The values represent the means of 3 biological replicates**.**

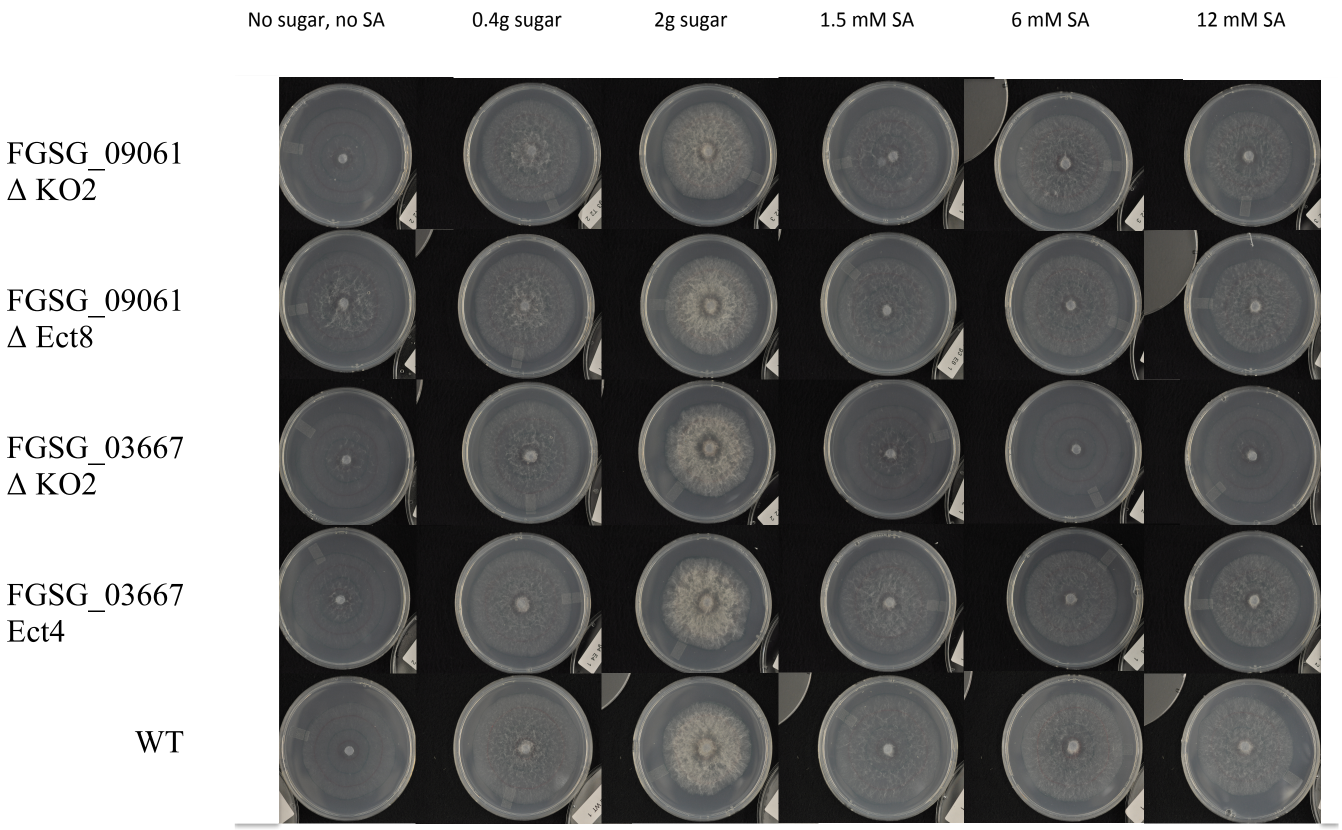

Figure 18: Comparison of the growth between a deletion mutant and an ectopic insertion strains for FGSG_03667 and FGSG_09061 with the wild type parental strain. Strains were inoculated on modified SNA media supplemented with sugars (sucrose and glucose) or SA as carbon source. Columns represent modified SNA plates with different carbon sources. Rows show a deletion mutant strain (*FGSG_03667*ΔKO2) and an ectopic insertion strain (FGSG_03667Ect4) for gene FGSG_03667, a deletion mutant strain (*FGSG_09061*ΔKO2) and an ectopic insertion strain (FGSG_09061Ect8) for gene FGSG_03667and the wild type (WT) parental strain DOAM 233423. Pictures were taken after 4 days of growth in the dark at 28 C**.**

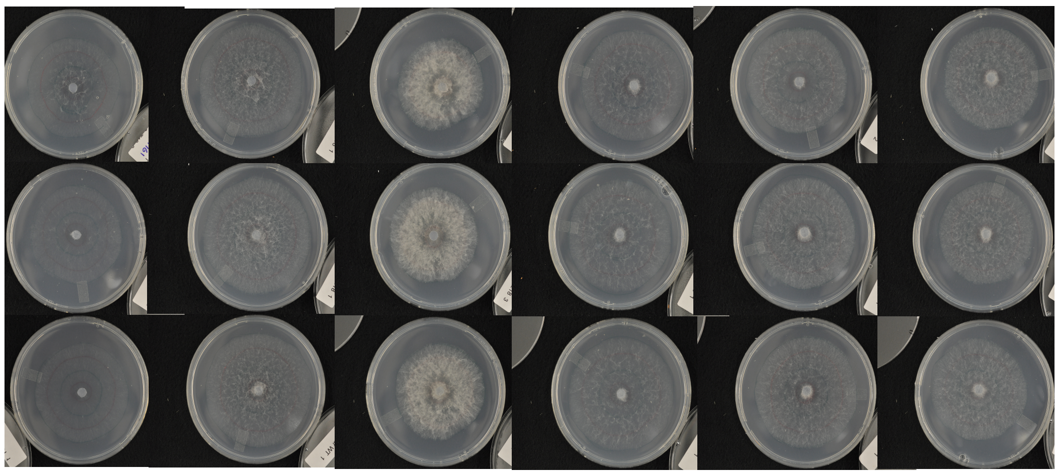

Figure 19: Comparison of the growth of a deletion mutant and an ectopic insertion strains for FGSG_08037 with the WT parental strain. Strains were grown on modified SNA media supplemented with sugars (sucrose and glucose) or SA as a carbon source. Columns represent modified SNA plates with different carbon sources. Rows show a deletion mutant strain (FGSG_08037ΔKO16) and an ectopic insertion strain (FGSG_08037Ect18) for gene FGSG_08037, and the wild type (WT) parental strain DOAM 233423. Pictures were taken after 4 days of growth in the dark at 28 C.

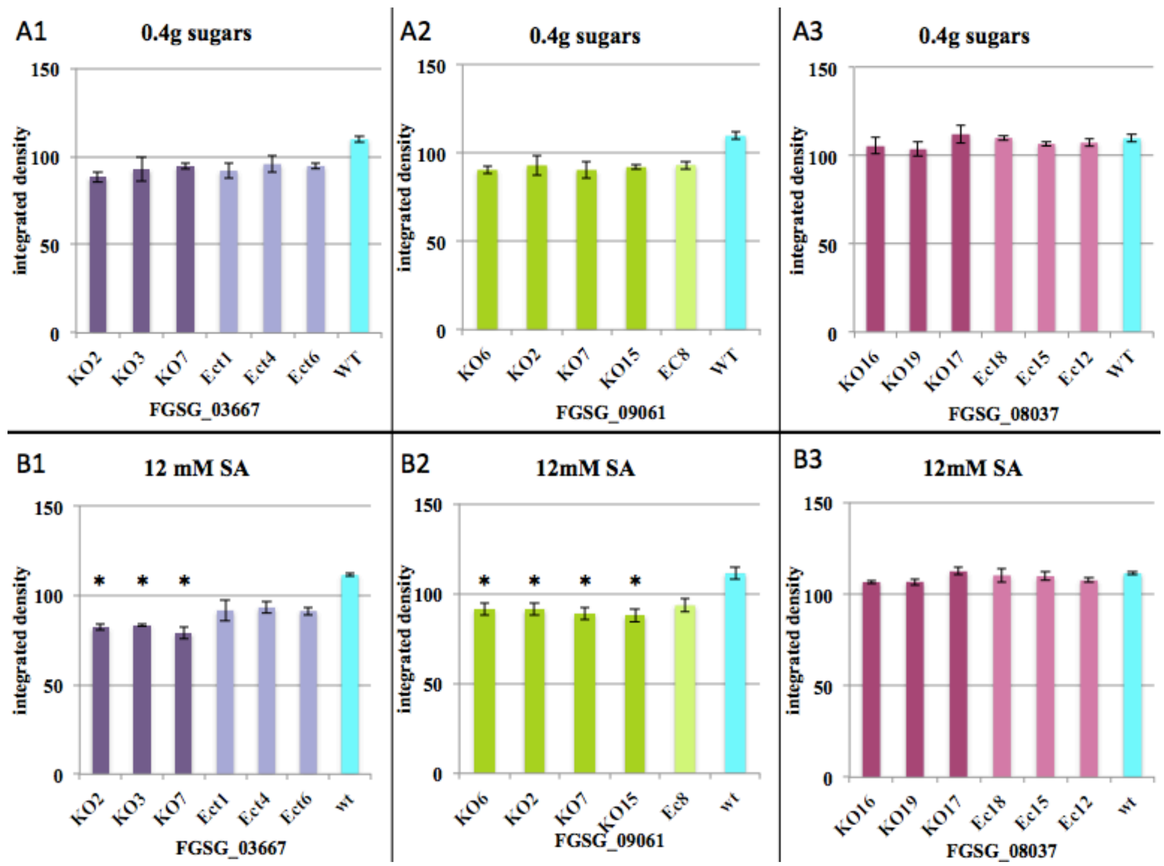

Figure 20: Estimated integrated density of mycelia growth for deletion mutant and ectopic insertion strains for genes FGSG_03667, FGSG_09061 and FGSG_08037. Mycelia density was measured after 4 days of growth on modified SNA containing either 0.4 g of sugars (Panels A1, A2 and A3) or 12 mM of SA (Panels B1, B2 and B3). The values represent means of 3 biological replicates ± standard deviation. Asterisk represents statistically significant differences ($P < 0.5$) between KO and Ect strains for a given gene.

3.3 Ability of mutant and wild type strains of *F. graminearum* to degrade SA in liquid medium

To quantify more precisely the ability of *F. graminearum* mutant strains to catabolize SA, the amount of SA in the supernatant of fungal cultures grown in liquid medium was measured over time by HPLC. The growth and sampling procedure for this assay is described schematically in Figure 6. Identification of the SA peak in the culture supernatant was made by comparison of HPLC retention time for the peaks observed with those for the reference compounds SA, catechol, and gentisate (Figure 21).

In a first experiment, the rate of degradation of SA over time by the wild type parental strain of *F. graminearum* was tested in presence and absence of sugars, to determine how fast *F. graminearum* can metabolize SA in the growth conditions used and investigate if simple sugars affect metabolism of SA (Figure 22). With 40 g sucrose and 10 g glycerol as starting amounts of sugars in the cultures, SA remained at about the same level, 100%, in supernatants from the 0, 2, 4, 6 and 8 hr cultures; a much smaller amount of SA, approximately 2.5%, was detected at 24 hrs after inoculation. In similar growth conditions, Qi et al. (2012) had observed a complete disappearance of SA at 24 hrs after inoculation; this difference could be explained by the slight growth differences between the strain they used, DAOM180378, and the one used here, DAOM233423, as shown in the previous section.

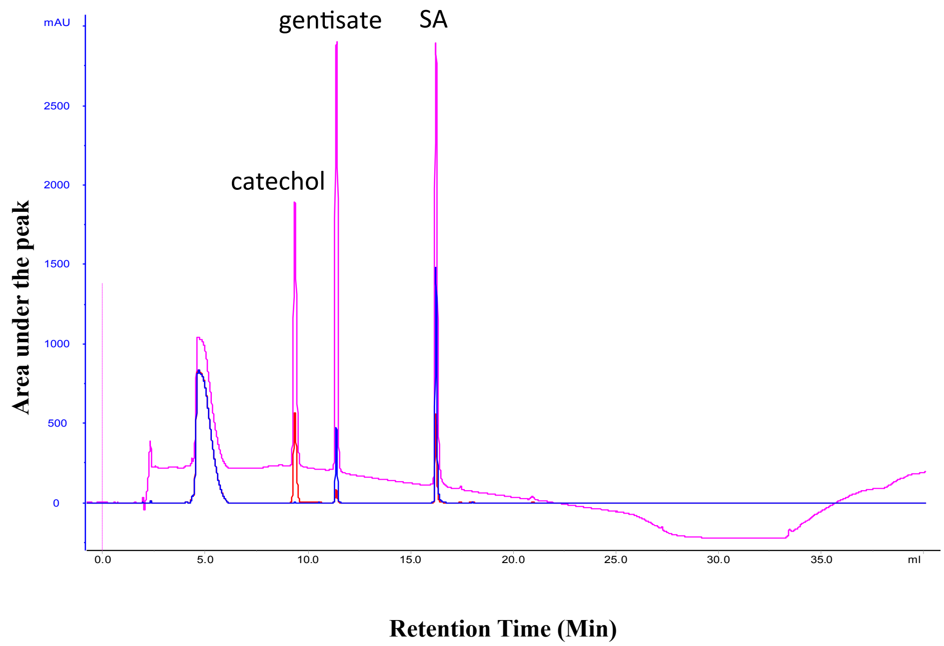

Figure 21: HPLC chromatogram of the reference compounds SA, catechol and gentisate. The blue line represent absorbance at 300 nm, the red line represent absorbance at 280 nm and the pink line represent absorbance at 210 nm. Absorbance at 300 nm was used for calculations.

With half the amount of sugars, 20 g sucrose and 5 g glycerol, at the start of the cultures, SA levels dropped to 0.03% of the starting amount at 8hrs after inoculation. Interestingly, in second stage media supplemented with 1mM SA as the sole carbon source, SA levels dropped even earlier, with only 0-2% of the starting amount of SA being detected at 4 hrs after inoculation.

In that first experiment, variation between biological replicates was found to be larger than desired. Technical problems occurred during the washing and transferring of the mycelia to the second stage medium (see schema of the procedure in Figure 6A and B). It was interpreted that the density of the mycelium after the first 24 hrs of growth was not optimal, creating problems with the subsequent manipulation of the mycelia. To test this possibility, an experiment was devised to test the effect of increasing the amount of spores used to inoculate the first stage media. So, 5×10^4 (original amount), 5×10^5, and 5×10^6 spores/ml were used as starting inoculum. A second stage media supplemented with 1mM SA as the sole carbon source was used. Result showed that by increasing the amount of spores inoculated in the starting media, the variation in measurements of SA levels between biological replicates was 30-40% less (Appendix Table A4). Inoculation of the first stage media with 5×10^5 amount of spores/ml and use of a second stage media with SA and no simple sugars were chosen as parameters for the following experiments.

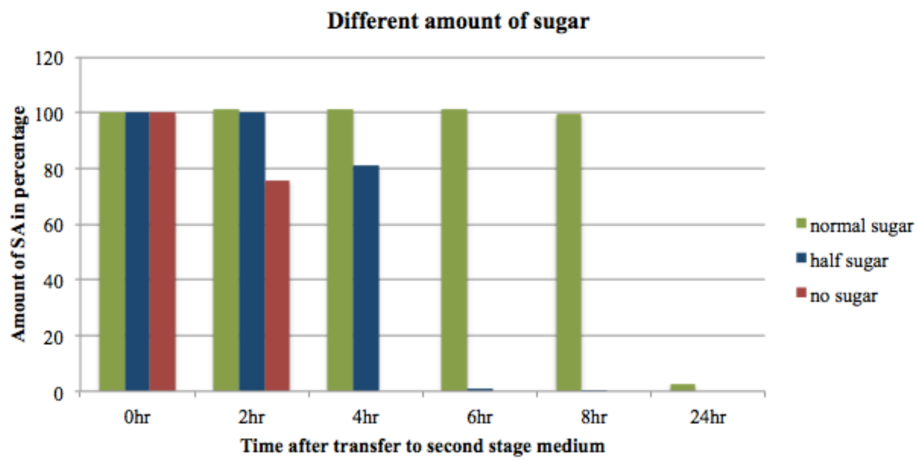

Figure 22: Degradation of SA over a period of 24 hrs of growth in presence or absence of sugar. SA values represent the percentage of SA relative to the amount detected at 0 hr in the same treatment. Normal sugar represented a 2nd stage media containing 40 g sucrose and 10 g glycerol, half sugar represented a 2nd stage media containing 20 g sucrose and 5 g glycerol and no sugar represented a 2nd stage media containing 0 g sucrose and 0 g glycerol. All media were also amended with 1mM SA.

Using a protocol optimized for treatment conditions and HPLC analysis (see Chapter 2, section 2.5), the wild type parental strain and a subset of the mutant strains produced (one deletion mutant strain per gene) were tested for their ability to degrade SA (Figure 23, Appendix Table A5). For the ortho ring cleavage step, results showed that the deletion mutant for one gene, FGSG_03667ΔKO2, had lost its capacity to use SA as a carbon source. No reduction in the levels of SA were observed even after 6 hours of treatment while the wild type strain had consumed 100% of SA after 4hrs (Figure 23). This was a bit of a surprise because the presence of some intermediate compound (such as catechol or gentisate) was expected because FGSG_03667 is predicted to catalyze the second step in degradation of SA. Blocking of that second step could have caused accumulation of the product from the first step of SA degradation. Deletion mutants for genes FGSG_08358ΔKO4 and FGSG_08037ΔKO16 showed similar ability to degrade SA when compared to the wild type strain grown at the same time (Figure 23). These results suggest that FGSG_03667 is fully responsible for the 1,2-dioxygenase activity in our testing conditions.

For the first step in SA degradation, the deletion mutants for 2 genes, FGSG_09061ΔKO15 and FGSG_03657ΔKO14, showed significant delay in SA degradation when compared to the wild type strain grown in parallel, with 90% and 72%, respectively, of the SA present at 0 hr being consumed after 4 hrs of treatment (Figure 23). The deletion mutant for gene FGSG_09063ΔKO2 showed a slight delay in SA degradation when compared to the wild type strain grown in parallel, however the difference was not significant (Figure 23). These results suggest that FGSG_09061 and FGSG_03657 contribute to SA degradation in our testing conditions presumably by converting SA into catechol.

To confirm the findings for the gene FGSG_09061, two additional deletion mutants and one ectopic insertion mutant were tested (Figure 24, Appendix Table A5). Results showed that in FGSG_09061ΔKO9 and FGSG_09061ΔKO6 cultures, SA was decreased by 2 and 8% after 4 hrs and by 72% and 47% after 6 hrs, while in FGSG_09061Ect8 and WT cultures, SA was decreased by 82% and 100% after 4 hrs, respectively. These results confirm those obtained with the mutant FGSG_09061ΔK15. Findings for gene FGSG_03667 were confirmed by another laboratory member; two more deletion mutants showed 80% and 90% of SA remaining after 4 and 6 hours while the 3 ectopic insertion strains showed 0.5 to 11% and the WT 0.2% of SA remaining (data not shown). Findings for gene FGSG_03657 remain to be confirmed with additional deletion and ectopic insertion mutants to confirm its contribution to SA degradation.

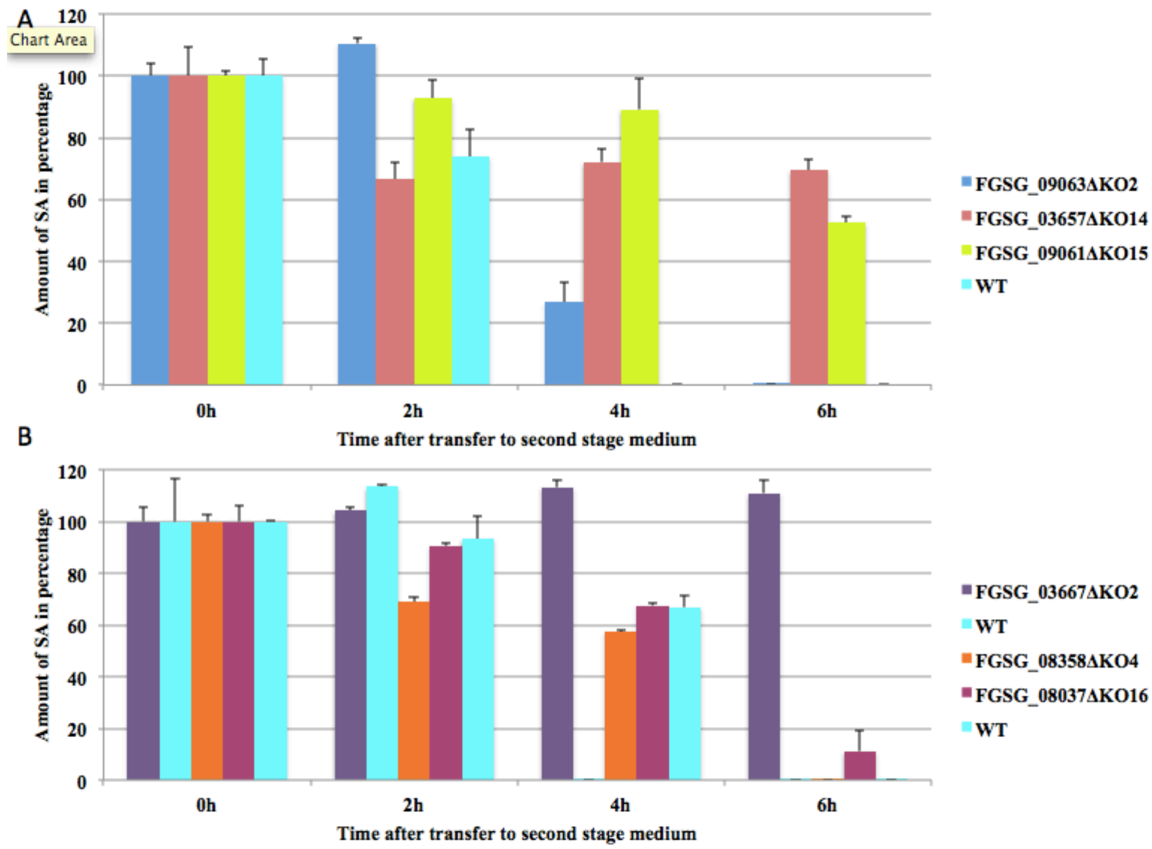

Figure 23: Degradation of SA in liquid culture for one deletion mutant strain of each gene and WT in 2nd stage medium supplemented with 1mM SA as sole carbon source. SA values represent the percentage of SA relative to the amount detected at 0 hr with the same strain. Panel A represented the first group of three genes; FGSG_09063Δ, FGSG_03657Δ and FGSG_09061Δ. Panel B represented the second group of three genes; FGSG_03667Δ, FGSG_08358Δ and FGSG_08037Δ. Time-course experiments were performed with two strains at a time, by inoculating individual wells in parallel plates and sampling 3 wells (as three biological replicates) per strain per time point. In Panel B, two WT strains are shown for each time point, each one being located right of the mutant strain(s) that should be compared to it.

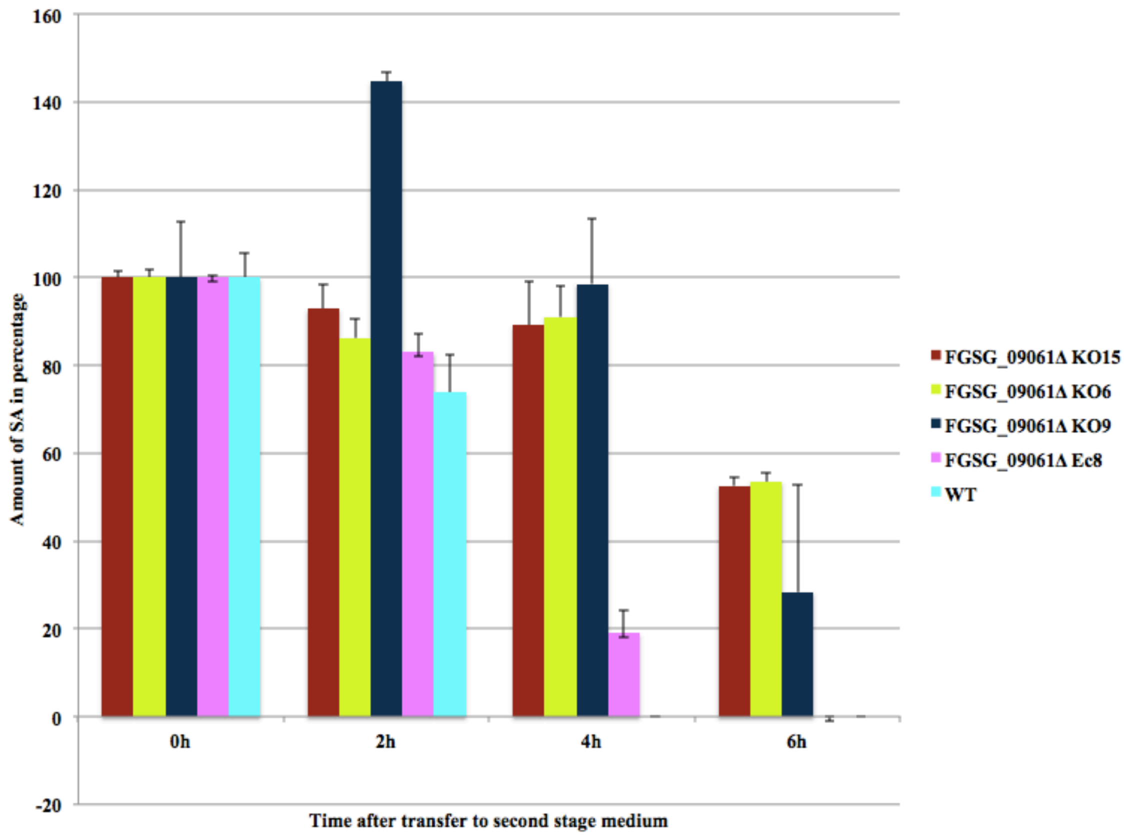

Figure 24: Degradation of SA in liquid culture for four mutant strains of gene FGSG_09061 in 2nd stage medium supplemented with 1mM SA as sole carbon source. SA values represent the percentage of SA relative to the amount detected at 0 hr for the same strain. Time-course experiments were performed with two strains at a time, by inoculating individual wells in parallel plates and sampling 3 wells (as three biological replicates) per strain per time point.

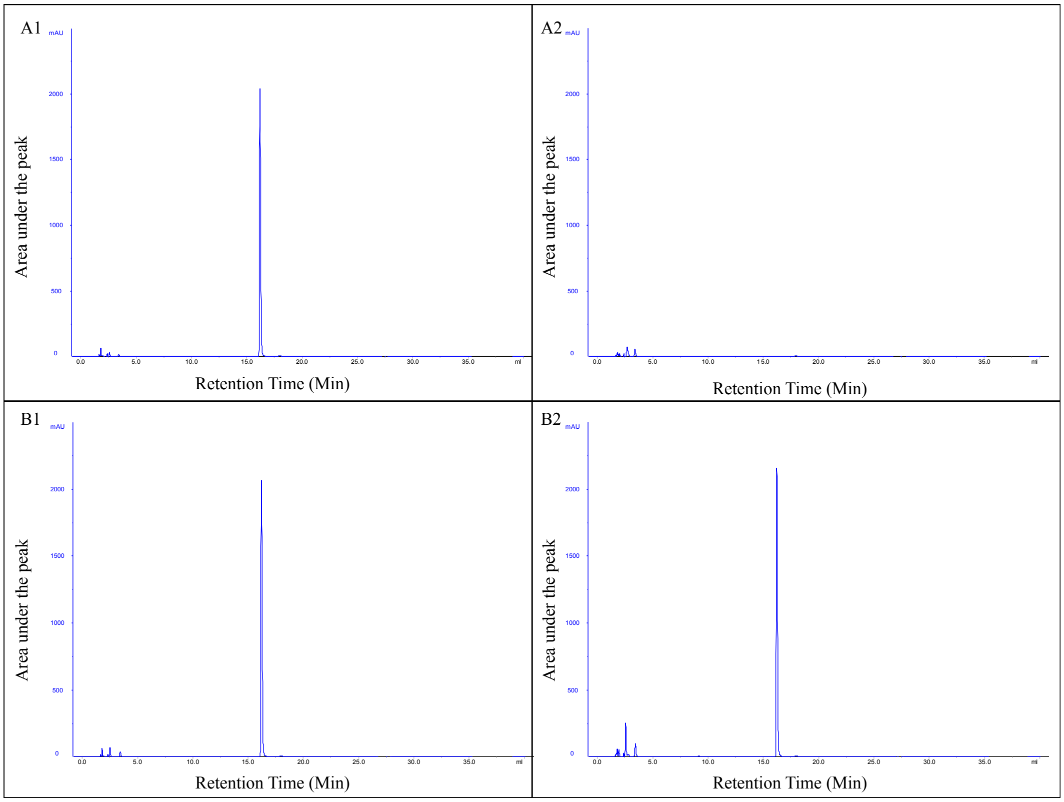
A1
A2
B1
B2
mAU
Area under the peak
Retention Time (Min)

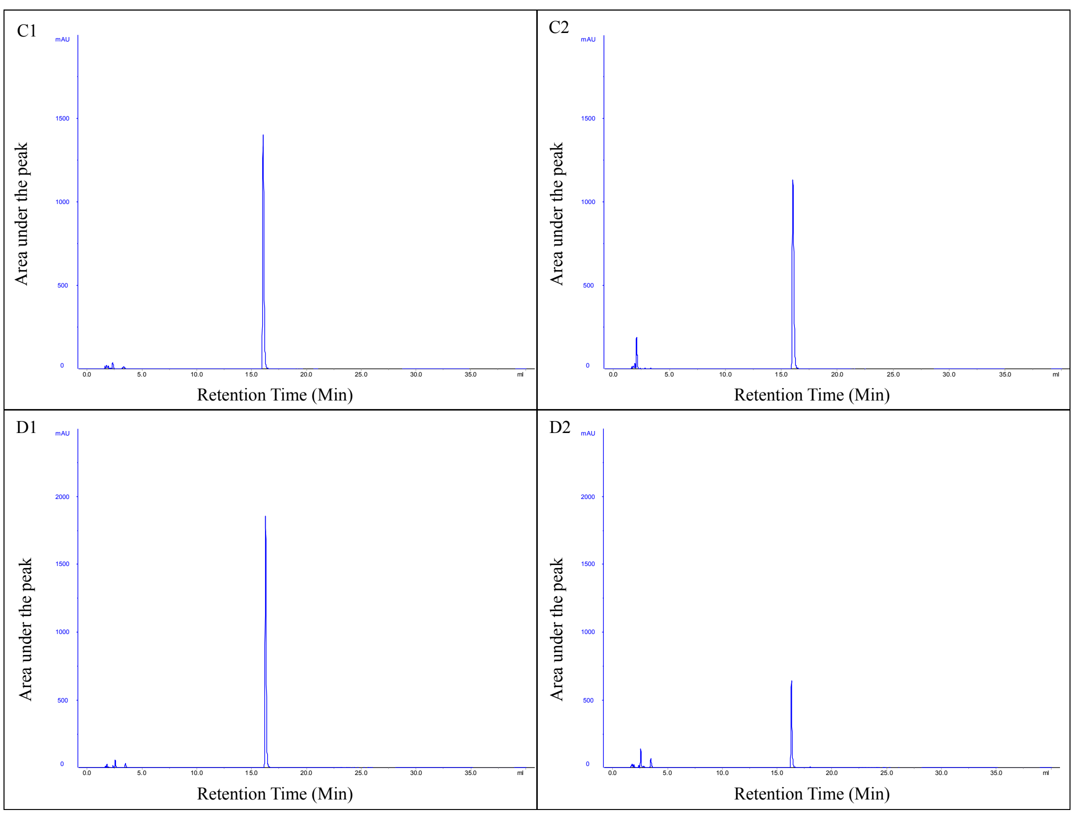
C1
C2
D1
D2
mAU
Area under the peak
Retention Time (Min)

Figure 25: HPLC chromatograms of the filtrates from SA-treated deletion mutant strains of 3 genes and WT at the same time points. Panel A1, B1, C1 and D1 represent filtrates from SA-treated WT, FGSG_03667Δ, FGSG_03657Δ and FGSG_09063Δ strains at 0hr post inoculation, respectively. Panel A2, B2, C2 and D2 represent filtrate from same strains at 4hr post inoculation.

Chapter 4 - Discussion

Salicylic acid is one of the plant phytohormones that regulates plant defense response, particularly against biotropic and hemibiotropic pathogens (De Vos et al., 2005). *Fusarium graminearum* is one of the fungal species able to degrade SA and use it as a carbon source (Qi et al., 2012). When the effect of SA on *F. graminearum* genes was first investigated, both up-regulated genes and down-regulated genes were identified in SA-treated cultures. Among the up-regulated genes, 15 were found to encode predicted enzymes for aromatic compound degradation including SA (Qi et al., 2012). The purpose of the present study was to confirm a role for six of those genes in the SA degradation pathway by *F. graminearum*. Those candidate genes were divided into two groups. The first group contains candidate genes for the catalysis of the first step of the SA degradation, and included two genes predicted to function as salicylate 1-monooxygenases and one as 2,3 dihydroxybenzoic acid decarboxylase. The second group contains candidate genes for the catalysis of the second step of the SA degradation pathway, which is the first step in the ortho-ring cleavage pathway, and included genes predicted to function as hydroxyquinol-1,2-dioxygenase, intradiol dioxygenase, and homogentisate 1,2-dioxygenase. Identification of those genes in *F. graminearum* was based on BLASTn homology to sequence for genes with known function in SA and aromatic compound degradation in fungi.

Testing the ability of wild type *F. graminearum* to utilize SA in a 2nd stage medium containing different amounts of sugar showed a delaying of SA consumption correlated with the amount of sugar in the medium. This result suggested that SA degradation occured only after the consumption of all or a significant amount of the simple sugars in the medium. That experiment also showed that a lapse of time was required before *F. graminearum* could use SA as a source of carbon once it was exposed to it.

In fungi, the degradation of SA is initiated with the conversion of SA to one of the following intermediates: catechol, gentisate, or protocatechuate. Those three intermediates then enter the ortho-ring cleavage pathway (Wright, 1993). The first step of SA conversion requires a hydroxylase or monooxygenase enzyme. Salicylate-1 monooxygenase enzymes have been shown to play an important and direct role in converting SA to catechol in *Fusarium* sp. strain BI, *Trichosporon cutaneum* as well as *Rhodotorula graminis* (Anderson & Dagley, 1980; Dodge & Wackett, 2005; Durham, 1984). In *F. graminearum*, two genes are predicted to encode a salicylate-1 monooxygenase enzyme, FGSG_09063 and FGSG_03657, with their closest match in databases being a salicylate 1-monooxygenase from *Pseudomonas putida* (You et al., 1991) Both genes were induced by treatment with SA (Qi et al., 2012). Those genes were chosen as best candidate genes for step A in the SA degradation pathway converting SA directly to catechol (Figure 7).

In addition, one *F. graminearum* gene, FGSG_09061, was predicted to encode a 2,3 dihydroxybenzoic acid decarboxylase with its closest BLASTn match being an homolog gene from *Aspergillus nidulans* (Santha et al., 1995). This gene was also induced by treatment with SA, and was included as a third candidate gene for the first step in SA degradation. In some fungal species, 2,3 dihydroxybenzoic acid, which is closely related to SA, was found to be directly converted to catechol by a 2,3 dihydroxybenzoic acid decarboxylase (Figure 7, step B) (Anderson & Dagley, 1980; Wright, 1993; Santha et al., 1995). This enzyme has been found in many aromatic degradation pathways because of its ability to utilize several substrates, including SA, vanillate, orsellinate, 2,4-dihydroxybenzoic acid and 2,6-

dihydroxybenzoic acid (Santha et al., 1995)

Testing of one FGSG_03657Δ mutant strain showed a reduction in SA degradation in liquid medium when compared to the wild-type strain, even though there was no significant differences observed between the FGSG_03657Δ mutation strains, the ectopic insertion strains and the wild type strain when growing on solid medium. These results suggest that the HPLC assay is a more sensitive assay than the plate assay to detect SA use by *F. graminearum*, and that this gene is important for the first step of the SA degradation pathway. Further confirmation of the HPLC results should be done by comparing the three FGSG_03657Δ mutant strains and 3 ectopic insertion strains produced for this gene in this study.

Testing of mutant strains for *F. graminearum* gene FGSG_09061, a predicted 2,3 dihydroxybenzoic acid decarboxylase, showed that this gene also contributes to SA degradation. Growing FGSG_09061Δ mutant strains in solid medium in presence of SA showed a significant reduction of the mycelium density comparing with FGSG_09061 the ectopic and wild type strains. The result from the HPLC assays also showed a significant delay in utilizing SA in FGSG_09061Δ mutant strains in liquid medium. In contrast, deletion of the other predicted salicylate-1 monooxygenase gene, FGSG_09063, showed no significant effect on SA degradation, suggesting that this gene does not contribute to SA degradation in our experimental conditions.

Taken together, the results of characterization of deletion mutant strains for candidate genes for the catalysis of the initial step of SA degradation pathway in *F. graminearum* indicated that two genes, FGSG_03657 and FGSG_09061, are mainly responsible to initiate the degradation of SA in our experimental conditions. Results from independent deletion of each of these two genes suggest that each of them can provide more than half of the catalytic activity required for the first step of SA degradation. In the absence of FGSG_03657, only 30% of SA was consumed after 4hrs, while in the absence of FGSG_09061 only 10% of the SA was consumed. In comparison, wild type and ectopic insertion strains depleted 75 to 100% of SA during the same time period. Double deletion mutants for FGSG_09061 and FGSG_03657 should be created to confirm that these two genes account for 100% of the catalytic activity required for the first step of SA degradation. Based on their predicted function, it is expected that those two genes catalyze the conversion of SA to catechol. Biochemical experiments would be required to confirm this. An enzymatic activity assay could confirm the function of the enzymes coded by these two genes and measure the capacity to degrade SA into catechol (or another phenolic compound). Use of purified proteins would be preferred. As an example, protein extracts would be mixed with SA as a substrate in a phosphate buffer, the mixture would be incubated at 28^{o}C, the reaction would be stopped by the addition of 12 M HCl, and the amount of SA and reaction product would be measured by HPLC as done by Iwasaki et al., (2009).

The second step of the SA degradation pathway is the ortho ring cleavage. In fungi, many intradiol dioxygenase genes have been described, including catechol 1,2-dioxygenase, hydroxyquinol 1,2-dioxygenase, protocatechuate 3,4-dioxygenase, and homogentisate 1,2-dioxygenase (Wright, 1993). In *F. graminearum,* three SA-up regulated genes were identified encoding predicted intradiol dioxygenases (Qi et al., 2012). FGSG_03667 is predicted to encode a hydroxyquinol 1,2-dioxygenase (1,2-HQD) and the closest homologous gene for it was from the bacterium *Nocardioides simplex* (Ferraroni et al., 2005). 1,2-HQD catalyze the step D3 in the SA degradation pathway, converting hydroxyquinol to 3-hydroxy-cis,cis-munocate (Figure 7). FGSG_08358 is predicted to encode a homogentisate 1,2-dioxygenase and the closest homologous gene with annotated function was from *Aspergillus nidulans* (Fernandez-Canon & Penalva, 1995). In that species, homogentisate 1,2-dioxygenase was essential to catalyze the reaction of the ring cleavage in the degradation of the aromatic compound phenylacetate (Fernandez-Canon & Penalva, 1995). FGSG_08037 has homology to uncharacterized potential intradiol 1,2-dioxygenases (Ferraroni et al., 2005). Those 3 genes were chosen as best candidate genes for step D in the SA degradation pathway (Figure 7).

Our result indicates that FGSG_03667 is an essential gene in the SA degradation pathway by *F. graminearum*. Deletion of FGSG_03667 resulted in complete loss of ability for *F. graminearum* to metabolize SA. Analysis of FGSG_03667Δ mutant strains grown on modified solid SNA medium supplemented with SA as the main carbon source showed a significant reduction in the mycelium density comparing with FGSG_03667 ectopic strains and WT strain. More importantly, the HPLC assay using culture filtrate from FGSG_03667Δ mutant strains showed that they were unable to utilize SA under conditions where the wild type strain consumed 100% of the SA amount in only 4 hrs post inoculation. These results suggest that *F. graminearum* may degrade SA via the hydroxyquinol branch of the degradation pathway. Similarly, previous studies in *Trichosporon cutaneum* and *Phanerochaete chrysosporium* indicated that 1,2-HQD is one of the key enzymes responsible for the ortho ring cleavage, catalyzing hydroxyquinol to 3-hydroxy-cis,cis-muconate (Anderson & Dagley, 1980; Sze & Dagley, 1984). It was found that hydroxyquinol is a product of oxidation of gentisate in *T. cutaneum* cultures grown in salicylate as a carbon source, or a product of hydroxylation of protocatechuate in *T. cutaneum* cultures grown in benzoate and other aromatic compounds; similar observations were made in some other fungi

(Anderson & Dagley, 1980; Wright, 1993). Similarly, Sze and Dagley (1984) found that salicylate-grown cultures of *T. cutaneum* could rapidly utilize gentisate to produce hydroxyquinol. Their results indicated that hydroxyquinol was the most important catabolitic product for many phenolic compounds in *T. cutaneum*, including for benzoate, protocatechuate, gentisate and resorcinol (Sze & Dagley, 1984).

Inactivation of the genes FGSG_08358 and FGSG_08037 had no effect on the ability of *F. graminearum* to utilize SA. Deletion mutant strains for either gene showed similar results to ectopic mutant strains and WT in both solid and liquid assays. This indicates that those two genes have no role in SA degradation, at least in our experimental conditions.

Taken together, our results suggest the involvement of two different branches or pathways in the degradation of SA by *F. graminearum*. First, our results indicated that the initial step of SA degradation by *F. graminearum* was mediated by two genes, FGSG_03657 and FGSG_09061. Both genes are predicted to encode enzymes that catalyze the conversion of SA to catechol, suggesting that catechol is an intermediate product of SA degradation. The importance of this step was previously proven in bacteria, yeasts and other fungi (Wright, 1993). In addition, Dodge et al. (2005) found that, in a *Fusarium* isolate (species undetermined), SA was degraded via catechol as an intermediate, supporting our findings. Second, our results indicated that FGSG_03667 was the only essential gene for the predicted second step of SA degradation by *F. graminearum*. This gene is predicted to encode an enzyme that catalyzes the ortho ring cleavage via the conversion of hydroxyquinol to 3-hydroxy-cis,cis-muconate, suggesting that hydroxyquinol is an intermediate substrate in SA degradation. Previous studies in yeast and fungi found those organisms able to use hydroxyquinol following a period of growth in medium supplemented with SA or some other aromatic compounds such as benzoic acid and vanillate (Anderson & Dagley, 1980; Rieble et al., 1994)

Based on our findings, there appear to be a discrepancy between our results for the first and second steps of SA degradation, because the predicted function of the genes involved in the first step suggested catechol to be the first intermediate product while the predicted function of the gene involved in the second step suggested hydroxyquinol to be the intermediate substrate for the ortho ring cleavage. One possible explanation is that the 1,2_HQD enzyme is not a substrate specific enzyme and can use catechol as a substrate. Despite the fact that intradioal dioxygenases are highly substrate specific enzymes, some studies have shown that they can use additional substrates. In *T. cutaneum*, it was shown that catechol 1,2-dioxygenase had the ability to readily utilize hydroxyquinol; while 1,2-HQ uses catechol only at 1% of the rate it uses HQ (Sze & Dagley, 1984; Varga and Neujahr, 1970). Rieble et al. (1994) has also shown in *P. chrysosporium* that the 1,2-HQD was able to utilize catechol, although it used catechol with an efficiency of about 20% when compared with HQ. It was also found in the *Arthobacter* species strain BA-5-17 that 1,2 HQD had the ability to use catechol at 15% of the rate it uses HQ via ortho or meta cleavage (Murakami et al., 1999). Amino acids sequences and characterizations of 1,2 HQD and catechol 1,2 dioxygenases have classified those two groups as the most similar dioxygenases (Ferraroni et al., 2005). An alternate explanation to the apparent discrepancy in pathway branches could be that the predicted function of FGSG_03667 is not as accurate as desired because of the phylogenetic distance between *F. graminearum* and the bacterium species *Nocardioides simplex*, which was used for annotation in Qi et al (2012). Recent BLASTn alignment of FGSG_03667 against fungal species results in high similarity to both catechol dioxygenase and to hydroxyquinol 1,2-dioxygenase (Appendix Table A7). Biochemical experiments will be required to define the substrate(s) for the enzyme coded by FGSG_03667.

4.1 Conclusion

In conclusion, my thesis contributes to the understanding of the role of some SA-induced genes toward the degradation of SA in *F. graminearum*. In this study three candidate genes, FGSG_09063, FGSG_03657, and FGSG_09061, for the initial step of SA degradation and three candidate genes, FGSG_03667, FGSG_08358, and FGSG_08037, for the second step of the SA degradation pathway were inactivated and the mutant strains tested for their ability to use SA. In our experimental conditions, two genes for the first step, FGSG_03657 and FGSG_09061 had a partial role in degradation of SA when individually inactivated, indicating that those two genes collaborate with each other in order to initiate the conversion of SA to catechol. In contrast, only one candidate gene for the step 2, FGSG_03667, was an essential gene in the degradation of SA. Deletion of the genes FGSG_09063, FGSG_08358 and FGSG_08037 had no effect on SA degradation. This study suggested that catechol was an intermediate in the catabolic pathway, even though a predicted 1,2-hydroxyquinol dioxygenase, FGSG_03667, was responsible for the second catalytic step. Biochemistry experiments will be needed to investigate the substrate used by the enzyme coded by FGSG_03667 in *F. graminearum*.

4.2 Future work:

To confirm our results showing the involvement of FGSG_03657 in the initial step of SA degradation, additional deletion mutant and ectopic insertion strains produced for this gene will need to be tested in our liquid media procedure. In addition, the creation of double mutant strains for FGSG_03657 and FGSG_09061 would allow us to confirm if those two genes are the only ones contributing to the initial step of SA degradation in *F. graminearum*.

To understand the relationship at the expression level between the six genes studied, RNA would have to be extracted from the wild type and mutant strains. Testing the expression of all six genes in mycelial samples from different time points in our liquid medium procedure would help to determine why there was a delay between inoculation in SA-containing medium and use of SA. It will also help to determine if the genes shown to have no contribution to SA degradation were expressed under our liquid medium conditions. Finally, a comparison between wild type and deletion mutant strains would show if the expression or absence of it, of some of the genes influences the expression of others. RNA extractions could also be done using wild type *F. graminearum*-inoculated plants tissues, to determine if the same genes were expressed in our liquid medium conditions and in planta. Results of those experiments would also provide some insight into the highest expression conditions for the genes studied.

Biochemical experiments aiming at determining which substrate(s) are being used by the enzyme coded by FGSG_03667 would clarify the incertitude in the degradation pathway used by *F. graminearum* for SA. To achieve this goal, protein extracts containing the product of FGSG_03667 will be purified from *F. graminearum* grown in presence of SA, based on the best expression condition determined by the RNA expression profile. Cell-free extracts will be tested for their ability to use catechol (determined at 280 nm by HPLC) and hydroxyquinol (measured at 245 nm). The finding that FGSG_03667 is an essential gene for SA degradation by *F. graminearum* will provide an opportunity to test whether or not this gene, and the ability to degrade SA, is contributing to *F. graminearum* pathogenicity. Inoculation of FHB-susceptible wheat plants with deletion mutant and ectopic insertion strains of FGSG_03667, and comparison of the disease symptoms observed for the different strains would provide insight into this question.

References

Anand, A., Zhou, T., Trick, H. N., Gill, B. S., Bockus, W. W., & Muthukrishnan, S. (2003). Greenhouse and field testing of transgenic wheat plants stably expressing genes for thaumatin-like protein, chitinase and glucanase against *Fusarium graminearum*. *Journal of Experimental Botany*, *54*(384), 1101-1111.

Anderson, J. J., & Dagley, Stanley (1980). Catabolism of aromatic acids in *Trichosporon cutaneum*. *Journal of Bacteriology*, *141*(2), 534-543.

Antoniw, J. F., & White, R. F. (1980). The effects of aspirin and polyacrylic acid on soluble leaf proteins and resistance to virus infection in five cultivars of tobacco. *Journal of Phytopathology*, *98*(4), 331-341.

Bushnell, W. R., Hazen, B. E., Pritsch, C., & Leonard, K. J. (2003). Histology and physiology of Fusarium head blight. *Fusarium head blight of wheat and barley*, 44-83.

Cappellini, R. A., & Peterson, J. L. (1965). Macroconidium formation in submerged cultures by a non-sporulating strain of *Gibberella zeae*. *Mycologia*, 962-966.

Cuomo, C. A., Güldener, U., Xu, J. R., Trail, F., Turgeon, B. G., Di Pietro, A., ... & Kistler, H. C. (2007). The *Fusarium graminearum* genome reveals a link between localized polymorphism and pathogen specialization. *Science*, *317*(5843), 1400-1402.

Deacon, J. W. (2013). *Fungal biology*. John Wiley & Sons.

Delaney, T. P., Friedrich, L., & Ryals, J. A. (1995). *Arabidopsis* signal transduction mutant defective in chemically and biologically induced disease resistance. *Proceedings of the National Academy of Sciences*, *92*(14), 6602-6606.

De Vos, M., Van Oosten, V. R., Van Poecke, R. M., Van Pelt, J. A., Pozo, M. J., Mueller, M. J., ... & Pieterse, C. M. (2005). Signal signature and transcriptome changes of *Arabidopsis* during pathogen and insect attack. *Molecular plant-microbe interactions*, *18*(9), 923-937.

Dodge, A. G., & Wackett, L. P. (2005). Metabolism of bismuth subsalicylate and intracellular accumulation of bismuth by *Fusarium sp*. strain BI. *Applied and Environmental Microbiology*, *71*(2), 876-882.

Durham, D. R. (1984). Initial reactions involved in the dissimilation of mandelate by Rhodotorula graminis. *Journal of Bacteriology*, *160*(2), 778-780.

Durrant, W. E., & Dong, X. (2004). Systemic acquired resistance. *Annu. Rev. Phytopathol.*, *42*, 185-209.

Fernández-Cañón, J. M., & Peñalva, M. A. (1995). Molecular characterization of a gene encoding a homogentisate dioxygenase from *Aspergillus nidulans* and identification of its human and plant homologues. *Journal of Biological Chemistry*, *270*(36), 21199-21205.

Ferraroni, M., Seifert, J., Travkin, V. M., Thiel, M., Kaschabek, S., Scozzafava, A., ... & Briganti, F. (2005). Crystal structure of the hydroxyquinol 1, 2-dioxygenase from *Nocardioides simplex* 3E, a key enzyme involved in polychlorinated aromatics biodegradation. *Journal of Biological Chemistry*, *280*(22), 21144-21154.

Frandsen, R. J., Andersson, J. A., Kristensen, M. B., & Giese, H. (2008). Efficient four fragment cloning for the construction of vectors for targeted gene replacement in filamentous fungi. *BMC Molecular Biology*, *9*(1), 70.

Gaffney, T., Friedrich, L., Vernooij, B., Negrotto, D., Nye, G., Uknes, S., ... & Ryals, J. (1993). Requirement of salicylic acid for the induction of systemic acquired resistance. *Science*, *261*(5122), 754-756.

Goswami, R. S., & Kistler, H. C. (2004). Heading for disaster: *Fusarium graminearum* on cereal crops. *Molecular Plant Pathology*, *5*(6), 515-525.

Government of Canada, Health Canada, Health Products and Food Branch, Food Directorate, Bureau of Chemical Safety. 2005. "Canadian Standards (Maximum Limits) for Various Chemical Contaminants in Foods." http://www.hc-sc.gc.ca/fn-an/securit/chem-chim/contaminants-guidelines-directives-eng.php.

Güldener, U., Seong, K. Y., Boddu, J., Cho, S., Trail, F., Xu, J. R., ... & Kistler, H. C. (2006). Development of a *Fusarium graminearum* Affymetrix GeneChip for profiling fungal gene expression in vitro and in planta. *Fungal Genetics and Biology*, *43*(5), 316-325.

Hayat, S., Ali, B., & Ahmad, A. (2007). *Salicylic acid: biosynthesis, metabolism and physiological role in plants* (pp. 1-14). Springer Netherlands.

Iwasaki, Y., Gunji, H., Kino, K., Hattori, T., Ishii, Y., & Kirimura, K. (2010). Novel metabolic pathway for salicylate biodegradation via phenol in yeast *Trichosporon moniliiforme*. *Biodegradation*, *21*(4), 557-564.

Leslie, J. F., & Summerell, B. A. (2008). *The Fusarium laboratory manual*. John Wiley & Sons.

Li, G., & Yen, Y. (2008). Jasmonate and ethylene signaling pathway may mediate Fusarium head blight resistance in wheat. *Crop Science*, *48*(5), 1888-1896.

Makandar, R., Essig, J. S., Schapaugh, M. A., Trick, H. N., & Shah, J. (2006). Genetically engineered resistance to Fusarium head blight in wheat by expression of Arabidopsis NPR1. *Molecular Plant-Microbe Interactions*, *19*(2), 123-129.

Makandar, R., Nalam, V., Chaturvedi, R., Jeannotte, R., Sparks, A. A., & Shah, J. (2010). Involvement of salicylate and jasmonate signaling pathways in *Arabidopsis* interaction with *Fusarium graminearum*. *Molecular Plant-Microbe Interactions*, *23*(7), 861-870.

Makandar, R., Nalam, V. J., Lee, H., Trick, H. N., Dong, Y., & Shah, J. (2012). Salicylic acid regulates basal resistance to Fusarium head blight in wheat. *Molecular Plant-Microbe Interactions*, *25*(3), 431-439.

Malamy, J., Carr, J. P., Klessig, D. F., & Raskin, I. (1990). Salicylic acid: a likely endogenous signal in the resistance response of tobacco to viral infection. *Science*, *250*(4983), 1002-1004.

Métraux, J. P., Signer, H., Ryals, J., Ward, E., Wyss-Benz, M., Gaudin, J., ... & Inverardi, B. (1990). Increase in salicylic acid at the onset of systemic acquired resistance in cucumber. *Science*, *250*(4983), 1004-1006.

Miller, J. D., & Blackwell, B. A. (1986). Biosynthesis of 3-acetyldeoxynivalenol and other metabolites by Fusarium culmorum HLX 1503 in a stirred jar fermentor. *Canadian journal of botany*, *64*(1), 1-5.

Murakami, S., Okuno, T., Matsumura, E., Takenaka, S., Shinke, R., & Aoki, K. (1999). Cloning of a gene encoding hydroxyquinol 1, 2-dioxygenase that catalyzes both intradiol and extradiol ring cleavage of catechol. *Bioscience, Biotechnology, and Biochemistry*, *63*(5), 859-865.

Pieterse, C. M., Leon-Reyes, A., Van der Ent, S., & Van Wees, S. C. (2009). Networking by small-molecule hormones in plant immunity. *Nature Chemical Biology*, *5*(5), 308-316.

Qi, P. F., Johnston, A., Balcerzak, M., Rocheleau, H., Harris, L. J., Long, X. Y., ... & Ouellet, T. (2012). Effect of salicylic acid on *Fusarium graminearum*, the major causal agent of fusarium head blight in wheat. *Fungal Biology*, *116*(3), 413-426.

Rasband, W.S., ImageJ, U. S. National Institutes of Health, Bethesda, Maryland, USA, http://imagej.nih.gov/ij/, 1997-2014.

Rieble, S., Joshi, D. K., & Gold, M. H. (1994). Purification and characterization of a 1, 2, 4-trihydroxybenzene 1, 2-dioxygenase from the basidiomycete *Phanerochaete chrysosporium*. *Journal of Bacteriology*, *176*(16), 4838-4844.

Saharan, M. S., Kumar, J., Sharma, A. K., & Nagarajan, S. (2004). Fusarium head blight (FHB) or head scab of wheat–a review. *Proceedings of the Indian National Science Academy. Part B, Biological Sciences*, *70*, 255-268.

Santha, R., Savithri, H. S., Appaji Rao, N., & Vaidyanathan, C. S. (1995). 2, 3-Dihydroxybenzoic acid decarboxylase from *Aspergillus niger*: a novel decarboxylase. *European journal of biochemistry*, *230*(1), 104-110.

Stack, R. W. (2000). Return of an old problem: Fusarium head blight of small grains. *APSnet Plant Health Reviews*.

Sze, I. S., & Dagley, Stanley (1984). Properties of salicylate hydroxylase and hydroxyquinol 1, 2-dioxygenase purified from Trichosporon cutaneum. *Journal of bacteriology*, *159*(1), 353-359.

Trail, F. (2009). For blighted waves of grain: *Fusarium graminearum* in the postgenomics era. *Plant physiology*, *149*(1), 103-110.

Trail, F., & Common, R. (2000). Perithecial development by Gibberella zeae: a light microscopy study. *Mycologia*, 130-138.

Uknes, S., Mauch-Mani, B., Moyer, M., Potter, S., Williams, S., Dincher, S., ... & Ryals, J. (1992). Acquired resistance in *Arabidopsis*. *The Plant Cell Online*, *4*(6), 645-656.

Varga, J. M., & Neujahr, H. Y. (1970). Purification and Properties of Catechol 1, 2-Oxygenase from *Trichosporon cutaneum*. *European Journal of Biochemistry*, *12*(3), 427-434.

Ward, E. R., Uknes, S. J., Williams, S. C., Dincher, S. S., Wiederhold, D. L., Alexander, D. C., ... & Ryals, J. A. (1991). Coordinate gene activity in response to agents that induce systemic acquired resistance. *The Plant Cell Online*, *3*(10), 1085-1094.

White, R. F. (1979). Acetylsalicylic acid (aspirin) induces resistance to tobacco mosaic virus in tobacco. *Virology*, *99*(2), 410-412.

Windels, C. E. (2000). Economic and social impacts of Fusarium head blight: changing farms and rural communities in the Northern Great Plains. *Phytopathology*, *90*(1), 17-21.

Wright, J. D. (1993). Fungal degradation of benzoic acid and related compounds. *World Journal of Microbiology and Biotechnology*, *9*(1), 9-16.

You, I. S., Ghosal, D., & Gunsalus, I. C. (1991). Nucleotide sequence analysis of the Pseudomonas putida PpG7 salicylate hydroxylase gene (nahG) and its 3'-flanking region. *Biochemistry*, *30*(6), 1635-1641.

Appendix

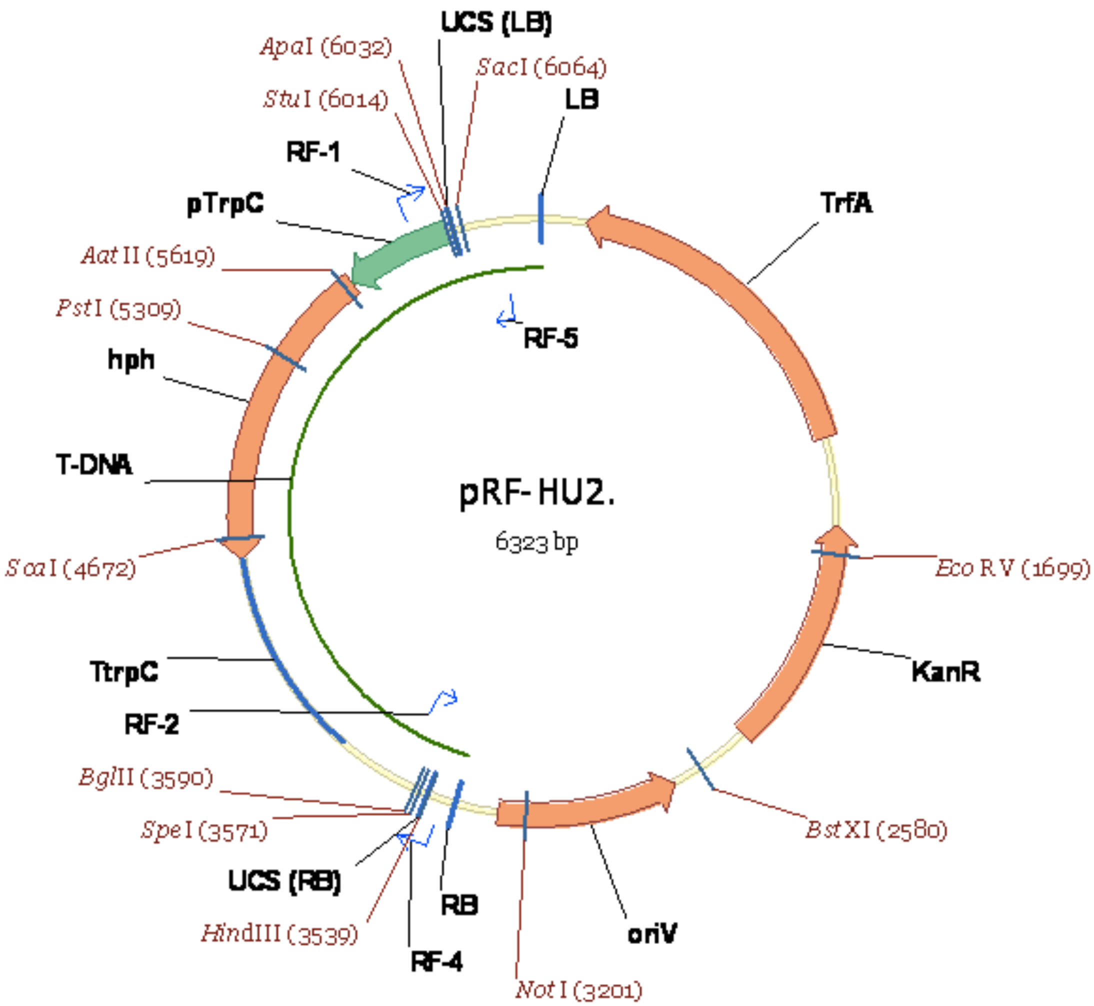

Figure A1: pRF-HU2 gene replacement vector.

(http://www.rasmusfrandsen.dk/prf-hu2.htm)

Table A1: Data of mycelium growth area measurement for all genes.

Growth area (mm2) for gene:		FGSG_09063					
Condition		Δ KO7	Δ KO2	Δ KO14	Δ EC3	Δ EC4	Δ EC10
No SA, No sugar	Replicate #1	16.688	18.694	11.63	8.859	15.644	15.032
	Replicate #2	15.274	15.023	17.013	17.919	11.551	20.112
	Replicate #3	17.927	15.619	14.272	19.202	16.755	17.984
	Means	16.629	16.445	14.305	15.326	14.65	17.709
	Standard deviation	1.3274	1.9700	2.6916	5.6377	2.7406	2.5511
No SA, 0.4g sugar	Replicate #1	19.695	20.351	25.355	15.283	23.53	25.709
	Replicate #2	25.285	24.047	21.546	17.621	23.429	23.115
	Replicate #3	22.963	15.101	19.994	26.592	23.265	22.753
	Means	22.647	19.833	22.2983	19.832	23.408	23.859
	Standard deviation	2.808	4.4954	2.758547	5.969904	0.133742	1.612338
No SA, 2g sugar	Replicate #1	28.741	27.423	26.727	25.702	23.444	22.779
	Replicate #2	24.021	28.191	28.674	25.606	23.845	27.564
	Replicate #3	22.798	23.907	24.382	23.216	18.792	24.053
	Means	25.18	26.507	26.594	24.841	22.027	24.798
	Standard deviation	3.13	2.284	2.14	1.408	2.808	2.478
1.5 mM SA, No sugar	Replicate #1	34.166	32.154	32.129	32.295	32.841	30.322
	Replicate #2	32.328	33.615	32.249	31.219	31.997	33.13
	Replicate #3	32.856	34.694	34.353	31.438	30.557	32.139
	Means	33.116	33.487	32.910	31.650	31.798	31.863
	Standard deviation	0.946	1.274	1.250	0.568	1.154	1.424
6 mM SA, No sugar	Replicate #1	37.062	35.486	38.6	37.236	32.609	35.476
	Replicate #2	41.374	37.261	38.936	35.222	37.763	36.277
	Replicate #3	37.314	37.605	38.939	35.094	34.449	34.821
	Means	38.825	36.784	38.825	35.850	34.940	35.524
	Standard deviation	2.42	1.13	0.19	1.201	2.611	0.729
12 mM SA, No sugar	Replicate #1	37.322	33.237	36.187	34.528	32.78	36.696
	Replicate #2	37.518	37.107	34.827	35.549	34.705	33.883
	Replicate #3	36.32	40.339	35.145	35.359	36.987	35.093
	Means	37.053	36.894	35.386	35.145	34.824	35.224
	Standard deviation	0.642	3.555	0.711	0.543	2.106	1.411

Growth area (mm2) for gene:		FGSG_03657					
Condition		Δ KO12	Δ KO14	Δ KO50	Δ EC6	Δ EC16	Δ EC8
No SA, No sugar	Replicate #1	9.811	10.834	17.187	12.513	17.25	8.327
	Replicate #2	8.937	22.471	13.382	10.32	15.5	15.257
	Replicate #3	7.943	13.29	18.156	8.29	16.04	16.49
	Means	8.897	15.531	16.241	10.374	16.263	13.358
	Standard deviation	0.934	6.133	2.523	2.112	0.896	4.4003
No SA, 0.4g sugar	Replicate #1	26.312	25.567	30.213	20.945	18.732	24.383
	Replicate #2	30.361	27.048	24.766	19.932	23.317	21.729
	Replicate #3	27.253	32.592	27.636	22.932	22.397	20.736
	Means	27.975	28.402	27.538	21.269	21.482	22.282
	Standard deviation	2.118	3.703	2.724	1.526	2.425	1.885
No SA, 2g sugar	Replicate #1	26.784	32.699	26.27	26.576	25.287	25.356
	Replicate #2	26.601	33.428	25.498	25.237	26.576	21.845
	Replicate #3	20.165	29.377	30.732	16.672	25.941	20.646
	Means	24.516	31.834	27.5	22.828	25.934	22.615
	Standard deviation	3.7697	2.159	2.825	5.373	0.644	2.44
1.5 mM SA, No sugar	Replicate #1	34.351	32.907	34.168	31.667	31.959	32.711
	Replicate #2	31.906	35.035	33.381	31.186	31.612	33.342
	Replicate #3		32.811	31.405	34.079	31.126	30.299
	Means	33.123	33.584	32.984	32.310	31.565	32.117
	Standard deviation	1.72	1.25	1.42	1.55	0.41	1.6
6 mM SA, No sugar	Replicate #1	44.201	31.64	34.8	29.241	31.69	32.402
	Replicate #2	38.591	35.369	35.76	30.636	30.587	35.294
	Replicate #3	40.104	35.792	37.546	31.508	30.83	30.562
	Means	40.96	34.26	36.03	30.46	31.03	32.75
	Standard deviation	2.90	2.28	1.39	1.14	0.57	2.38
12 mM SA, No sugar	Replicate #1	36.166	29.68	37	37.108	31.334	34.103
	Replicate #2	36.4	39.232	34.905	31.977	33.868	34.563
	Replicate #3	38.981	37.27	36.956	31.212	30.215	36.257
	Means	37.18	35.39	36.28	33.43	31.80	34.97
	Standard deviation	1.56	5.04	1.19	3.20	1.87	1.13

Growth area (mm2) for gene:		FGSG_09061					
Condition		Δ KO6	Δ KO2	Δ KO7	Δ KO15	Δ EC8	
No SA, No sugar	Replicate #1	39.315	41.366	38.962	38.704	47.584	
	Replicate #2	37.422	40.056	36.897	38.918	49.553	
	Replicate #3	39.144		41.008	39.935	45.465	
	Means	38.627	40.711	38.955	39.18	47.53	
	Standard deviation	1.04	0.926	2.055	0.657	2.044	
No SA, 0.4g sugar	Replicate #1	51.648	49.36	53.066	50.251	51.93	
	Replicate #2	48.705	48.893	52.83	49.108	51.031	
	Replicate #3	48.673	49.798	53.019	49.846	49.039	
	Means	49.675	49.350	52.971	49.735	50.666	
	Standard deviation	1.708	0.452	0.1249	0.579	1.4795	
No SA, 2g sugar	Replicate #1	41.169	43.138	44.041	44.087	42.158	
	Replicate #2	36.506	43.153	45.276	36.768	41.6	
	Replicate #3	41.455	42.604	44.992	44.404	37.096	
	Means	39.71	42.965	44.769	41.753	40.284	
	Standard deviation	2.778	0.312	0.646	4.320	2.775	
1.5 mM SA, No sugar	Replicate #1	43.679	46.345	49.784	43.231	49.736	
	Replicate #2	44.638	47.353	50.847	43.846	49.192	
	Replicate #3	45.353	49.956	45.269	49.973	47.345	
	Means	44.556	47.884	48.633	45.683	48.757	
	Standard deviation	0.839	1.863	2.961	3.727	1.25	
6 mM SA, No sugar	Replicate #1	42.746	45.054	46.711	43.108	44.586	
	Replicate #2	41.248	43.671	48.31	42.813	45.532	
	Replicate #3	43.861	45.994	46.821	41.112	45.356	
	Means	42.618	44.906	47.280	42.344	45.158	
	Standard deviation						
12 mM SA, No sugar	Replicate #1	36.065	34.954	35.14	38.754	40.458	
	Replicate #2	38.253	40.947	36.445	38.907	36.689	
	Replicate #3	37.516	36.94	40.341	33.915	37.194	
	Means	37.278	37.613	37.308	37.192	38.113	
	Standard deviation	2.8389	1.1132	3.0527	2.04589	2.7059	
Growth area (mm2) for gene:		FGSG_03667					
Condition		Δ KO7	Δ KO2	Δ KO3	Δ EC6	Δ EC4	Δ EC1
No SA, No sugar	Replicate #1	34.478	41.415	41.359	41.505	42.011	40.16
	Replicate #2	41.303	42.255	39.326	43.566	40.802	41.16
	Replicate #3	40.831	42.177	42.697	41.248	40.094	41.27
	Means	38.870	41.949	41.127	42.106	40.969	40.86
	Standard deviation	3.8114	0.464	1.697	1.270	0.969	0.608
No SA, 0.4g sugar	Replicate #1	52.238	52.001	55.446	52.853	51.625	52.36
	Replicate #2	53.079	50.909	51.069	55.552	53.095	53.61
	Replicate #3	53.005	52.755	54.925	52.205	50.343	53.31
	Means	52.774	51.888	53.813	53.536	51.687	53.09
	Standard deviation	0.465	0.928	2.390	1.775	1.377	0.655

No SA, 2g sugar	Replicate #1	37.418	34.281	30.51	33.783	35.321	38.378
	Replicate #2	34.223	38.282	29.747	35.655	39.152	43.398
	Replicate #3	42.219	38.146	27.981	35.053	38.382	44.574
	Means	37.953	36.903	29.412	34.830	37.618	42.116
	Standard deviation	4.024	2.271	1.297	0.955	2.026	3.290
1.5 mM SA, No sugar	Replicate #1	41.471	43.418	39.224	52.777	53.042	50.459
	Replicate #2	41.914	40.35	39.108	53.968	51.895	48.99
	Replicate #3	43.947	49.661	40.12	54.306	50.17	46.726
	Means	42.444	44.476	39.484	53.683	51.702	48.725
	Standard deviation	1.320	4.744	0.553	0.803	1.445	1.880
6 mM SA, No sugar	Replicate #1	37.497	34.905	35.522	51.025	42.324	43.717
	Replicate #2	36.279	38.518	35.931	48.993	42.343	40.971
	Replicate #3	43.866	36.522	37.057	50.093	41.906	43.852
	Means	39.214	36.64	36.17	50.037	42.191	42.84
	Standard deviation	4.074	1.809	0.794	1.017	0.247	1.625
12 mM SA, No sugar	Replicate #1	34.003	41.612	38.575	40.045	39.484	37.568
	Replicate #2	30.25	36.612	32.733	45.036	38.079	38.859
	Replicate #3	33.594	32.059	31.897	45.589	38.908	41.256
	Means	32.615	36.761	34.401	43.556	38.823	39.227
	Standard deviation	2.0589	4.7782	3.638	3.053	0.706	1.871

Growth area (mm2) for gene:		FGSG_08358					
Condition		Δ KO9	Δ KO4	Δ KO8	Δ EC3	Δ EC2	Δ EC5
No SA, No sugar	Replicate #1	40.108	46.302	42.699	38.829	35.921	38.198
	Replicate #2	41.367	46.256	41.018	38.476	35.367	34.905
	Replicate #3	39.086	42.074	37.369	39.915	36.971	
	Means	40.187	44.877	40.362	39.073	36.086	36.5515
	Standard deviation	1.1425	2.427	2.724	0.749	0.814	2.328
No SA, 0.4g sugar	Replicate #1	43.655	46.905	45.406	45.014	42.697	34.255
	Replicate #2	43.738	44.925	45.694	41.041	39.764	40.468
	Replicate #3	42.78	46.599	45.293	45.706	42.605	40.621
	Means	43.391	46.143	45.464	43.920	41.688	38.448
	Standard deviation	0.530	1.065	0.206	2.517	1.667	3.632
No SA, 2g sugar	Replicate #1	50.383	53.086	52.953	50.777	48.367	48.355
	Replicate #2	51.024	53.79	50.904	49.293	50.472	49.59
	Replicate #3	50.583	50.303	51.933	49.726	49.946	48.268
	Means	50.663	52.393	51.93	49.932	49.595	48.737
	Standard deviation	0.327	1.843	1.024	0.763	1.095	0.739
1.5 mM SA, No sugar	Replicate #1	43.872	48.029	50.19	49.145	43.567	46.673
	Replicate #2	40.239	47.612	47.389	48	46.139	46.821
	Replicate #3	44.397	49.74	53.109	44.88	46.543	43.697
	Means	42.836	48.460	50.229	47.341	45.416	45.730
	Standard deviation	2.2643	1.127	2.860	2.207	1.614	1.762
6 mM SA, No sugar	Replicate #1	44.843	43.659	46.614	43.001	44.575	44.043
	Replicate #2	47.183	45.866	47.836	44.572	46.145	44.306
	Replicate #3	45.314	51.206	49.944	46.087	44.42	42.489
	Means	45.78	46.910	48.131	44.553	45.046	43.612
	Standard deviation	1.237	3.880	1.684	1.543	0.954	0.981
12 mM SA, No sugar	Replicate #1	38.42	42.47	41.022	34.064	35.655	40.1
	Replicate #2	43.804	43.604	39.819	38.64	37.163	41.372
	Replicate #3	42.738	44.312	40.056	45.779	39.855	40.104
	Means	41.654	43.462	40.299	39.494	37.557	40.525
	Standard deviation	2.850	0.929	0.637	5.904	2.127	0.733

Growth area (mm2) for gene:		FGSG_08037					
Condition		Δ KO16	Δ KO19	Δ KO17	Δ EC18	ΔEC15	Δ EC12
No SA, No sugar	Replicate #1	38.334	38.177	43.25	36.752	39.79	34
	Replicate #2	39.41	37.802	41.704	37.618	37.889	37.153
	Replicate #3	38.125	37.994	42.524	42.081	37.765	40.354
	Means	38.623	37.991	42.492	38.817	38.481	37.169
	Standard deviation	0.689	0.187	0.773	2.859	1.135	3.177
No SA, 0.4g sugar	Replicate #1	50.227	51.077	50.99	51.558	52.146	53.503
	Replicate #2	52.363	53.911	52.428	53.369	50.378	53.333
	Replicate #3	49.705	54.342	49.108	52.594	49.964	52.41
	Means	50.765	53.11	50.842	52.507	50.829	53.082
	Standard deviation	1.408	1.773	1.664	0.908	1.158	0.588
No SA, 2g sugar	Replicate #1	31.359	31.212	33.016	34.006	33.133	42.053
	Replicate #2	26.059	30.329	35.347	32.295	34.173	40.228
	Replicate #3	31.443	30.225	47.401	35.829	35.474	45.163
	Means	29.620	30.588	38.588	34.043	34.26	42.481
	Standard deviation	3.0844	0.542	7.720	1.767	1.172	2.495
1.5 mM SA, No sugar	Replicate #1	47.753	50.437	55.259	47.147	46.385	46.877
	Replicate #2	48.898	48.811	50.655	48.591	44.644	49.46
	Replicate #3	46.339	50.077	52.027	49.739	46.453	47.159
	Means	47.663	49.775	52.647	48.492	45.827	47.832
	Standard deviation	1.281	0.854	2.363	1.298	1.025	1.416
6 mM SA, No sugar	Replicate #1	43.728	46.41	47.461	47.618	45.785	45.019
	Replicate #2	43.48	46.632	48.508	46.485	42.578	43.168
	Replicate #3	42.906	43.649	46.34	47.985	44.837	46.21
	Means	43.371	45.563	47.436	47.362	44.4	44.799
	Standard deviation	0.421	1.661	1.084	0.781	1.645	1.532
12 mM SA, No sugar	Replicate #1	38.402	39.708	42.265	39.821	39.655	35.065
	Replicate #2	38.955	40.328	40.479	36.277	40.646	38.108
	Replicate #3	36.136	41.408	40.785	40.362	38.394	37.143
	Means	37.831	40.481	41.176	38.82	39.565	36.772
	Standard deviation	1.493	0.860	0.955	2.218	1.128	1.555

Table A2: Data of mycelium-integrated density (intensity) for all genes.

Integrated density (pixel) for gene:		FGSG_09063					
Condition		Δ KO7	Δ KO72	Δ KO14	Δ EC3	Δ EC4	Δ EC10
No SA, No sugar	Replicate #1	95.523	114.26	99.13	104.50	112.30	116.48
	Replicate #2	93.831	105.36	117.39	110.44	114.89	103.67
	Replicate #3	95.337	110.38	117.11	114.54	116.71	101.43
	Means	94.897	110.00	111.21	109.8	114.63	107.19
	Standard deviation	0.9278	4.4626	10.467	5.0451	2.2127	8.1184
No SA, 0.4g sugar	Replicate #1	107.99	116.80	129.90	111.82	137.62	126.35
	Replicate #2	110.45	122.44	124.63	119.76	127.80	112.7
	Replicate #3	109.95	113.37	132.38	105.99	129.82	132.38
	Means	109.46	117.54	128.97	112.52	131.75	123.81
	Standard deviation	1.298	4.580	3.95	6.915	5.18	10.084
No SA, 2g sugar	Replicate #1	147.51	151.26	166.57	147.56	163.38	168.82
	Replicate #2	164.66	155.24	159.56	148.34	159.50	160.07
	Replicate #3	157.60	155.82	160.88	154.68	149.49	170.06
	Means	156.59	154.11	162.34	150.19	157.45	166.32
	Standard deviation	8.622	2.48	3.720	3.902	7.168	5.444
1.5 mM SA, No sugar	Replicate #1	112.74	115.82	125.58	124.72	107.85	133.04
	Replicate #2	118.14	124.28	122.40	106.74	106.79	128.12
	Replicate #3	120.79	126.08	120.35	107.76	129.75	134.10
	Means	117.22	122.06	122.77	113.07	114.80	131.75
	Standard deviation	4.104	5.477	2.635	10.09	12.95	3.18
6 mM SA, No sugar	Replicate #1	143.61	119.34	114.77	123.66	117.93	130.11
	Replicate #2	130.93	110.12	120.86	107.75	119.90	141.43
	Replicate #3	134.55	128.64	117.30	109.33	122.45	129.68
	Means	136.36	119.37	117.64	136.36	120.09	133.74
	Standard deviation	6.53	9.26	3.059	8.76	2.26	6.66
12 mM SA, No sugar	Replicate #1	135.41	134.09	119.76	111.78	118.94	142.05
	Replicate #2	130.85	128.6	144.91	111.67	117.27	147.33
	Replicate #3	131.38	127.07	136.10	135.55	117.45	123.59
	Means	132.55	129.93	133.59	119.67	117.89	137.66
	Standard deviation	2.49	3.67	12.7	13.7	0.91	12.46

Integrated density (pixel) for gene:		FGSG_03657					
Condition		Δ KO12	Δ KO14	Δ KO50	Δ EC6	ΔEC16	Δ EC8
No SA, No sugar	Replicate #1	114.198	118.21	103.965	109.46	114.71	110.60
	Replicate #2	116.544	125.745	116.788	111.58	111.97	117.23
	Replicate #3	114.969	121.936	116.963	119.51	116.95	120.02
	Means	115.237	121.963	112.572	113.52	114.54	115.95
	Standard deviation	1.19574	3.767576	7.454394	5.293	2.4916	4.840
No SA, 0.4g sugar	Replicate #1	118.662	134.896	111.956	130.36	126.09	128.01
	Replicate #2	125.287	127.829	107.401	127.77	104.68	126.27
	Replicate #3	133.567	130.25	134.018	135.34	127.47	121.18
	Means	125.838	130.9916	117.7916	131.16	119.42	125.15
	Standard deviation	7.467	3.591	14.23	3.847	12.77	3.549
No SA, 2g sugar	Replicate #1	168.174	169.354	153.303	166.36	163.56	156.92
	Replicate #2	166.805	172.394	146.532	168.68	158.69	165.71
	Replicate #3	166.667	172.235	149.288	169.79	168.77	146.08
	Means	167.2153	171.327	149.707	168.28	163.67	156.23
	Standard deviation	0.83309	1.711	3.404	1.7483	5.041	9.833
1.5 mM SA, No sugar	Replicate #1	103.271	121.335	108.374	128.87	126.49	126.30
	Replicate #2	120.565	124.844	107.076	124.96	109.26	119.07
	Replicate #3	118.314	122.893	124.11	133.44	129.48	127.71
	Means	114.05	123.024	113.1866	129.09	121.74	124.36
	Standard deviation	9.4024	1.7581	9.4821	4.2443	10.913	4.6356
6 mM SA, No sugar	Replicate #1	124.003	122.749	112.117	140.70	137.22	127.98
	Replicate #2	126.587	126.543	108.599	141.36	137.77	131.26
	Replicate #3	93.289	120.379	106.174	139.66	135.18	126.25
	Means	114.62	123.223	108.963	140.57	136.72	128.49
	Standard deviation	18.5237	3.109293	2.98820	0.8585	1.3672	2.543
12 mM SA, No sugar	Replicate #1	122.346	98.798	104.823	124.68	105.36	120.49
	Replicate #2	122.265	119.885	127.216	130.58	121.55	136.20
	Replicate #3	126.542	119.374	107.235	131.99	119.30	119.24
	Means	123.71	112.685	113.091	129.08	115.40	125.31
	Standard deviation	2.44627	12.0297	12.2916	3.8768	8.7693	9.4503

Integrated density (pixel) for gene:		FGSG_09061					
Condition	Δ KO6	Δ KO6	Δ KO2	Δ KO7	Δ KO15	Δ EC8	
No SA, No sugar	Replicate #1	86.149	81.417	82.699	84.902	88.83	
	Replicate #2	80.587	88.672	84.636	82.89	93.005	
	Replicate #3	77.874		86.715	85.037	91.446	
	Means	81.536	85.044	84.683	84.27	91.09	
	Standard deviation	4.218	5.130	2.008	1.202	2.109	
No SA, 0.4g sugar	Replicate #1	92.114	96.143	86.063	92.387	95.907	
	Replicate #2	91.212	96.412	89.761	90.667	91.74	
	Replicate #3	88.143	86.51	95.455	93.027	91.933	
	Means	90.489	93.021	90.426	92.027	93.193	
	Standard deviation	2.081	5.640	4.731	1.220	2.352	
No SA, 2g sugar	Replicate #1	113.99	120.79	107.52	112.65	119.72	
	Replicate #2	120.17	119.58	122.12	115.44	117.03	
	Replicate #3	112.54	110.28	118.43	111.80	110.18	
	Means	115.57	116.89	116.02	113.30	115.64	
	Standard deviation	4.049	5.7514	7.5923	1.9059	4.9200	
1.5 mM SA, No sugar	Replicate #1	87.536	88.219	81.671	78.583	88.223	
	Replicate #2	88.383	87.831	85.962	83.53	87.439	
	Replicate #3	90.38	91.221	92.823	78.669	90.202	
	Means	88.766	89.090	86.818	80.260	88.621	
	Standard deviation	1.460	1.855	5.625	2.831	1.423	
6 mM SA, No sugar	Replicate #1	91.699	90.047	91.506	89.985	85.713	
	Replicate #2	89.92	87.786	93.03	88.547	82.848	
	Replicate #3	91.483	88.742	96.012	90.325	89.069	
	Means	91.034	88.858	93.516	89.619	85.876	
	Standard deviation	0.970	1.134	2.291	0.943	3.113	
12 mM SA, No sugar	Replicate #1	92.313	91.043	91.919	87.941	93.775	
	Replicate #2	91.752	91.039	91.244	88.115	92.634	
	Replicate #3	89.917	92.236	83.373	87.462	93.961	
	Means	91.327	91.439	88.845	87.839	93.456	
	Standard deviation	1.253	0.689	4.751	0.338	0.718	

Integrated density (pixel) for gene:		FGSG_03667					
Condition	Δ KO7	Δ KO7	Δ KO2	Δ KO3	Δ EC6	Δ EC4	Δ EC1
No SA, No sugar	Replicate #1	86.672	80.857	85.631	79.271	80.579	87.72
	Replicate #2	82.162	82.71	88.689	82.313	82.213	86.006
	Replicate #3	81.994	81.002	87.631	81.402	77.744	86.435
	Means	83.609	81.523	87.317	80.995	80.178	86.720
	Standard deviation	2.653	1.030	1.552	1.561	2.261	0.891
No SA, 0.4g sugar	Replicate #1	93.44	90.351	98.901	93.217	98.767	89.667
	Replicate #2	96.179	85.089	93.771	94.305	90.268	88.901
	Replicate #3	93.681	89.375	85.488	96.227	97.995	97.119
	Means	94.433	88.271	92.72	94.583	95.676	91.895
	Standard deviation	1.516	2.799	6.767	1.524	4.699	4.539
No SA, 2g sugar	Replicate #1	113.407	108.315	118.724	113.769	120.56	122.58
	Replicate #2	114.592	111.199	115.069	111.952	118.37	115.33
	Replicate #3	104.208	103.69	107.688	113.803	108.53	114.51
	Means	110.735	107.734	113.827	113.174	115.82	117.47
	Standard deviation	5.684	3.787	5.621	1.058	6.407	4.441
1.5 mM SA, No sugar	Replicate #1	91.334	75.609	81.957	100.105	99.662	89.203
	Replicate #2	86.243	80.717	85.363	89.418	87.131	96.94
	Replicate #3	85.549	103.348	85.139	89.332	92.008	91.897
	Means	87.708	86.558	84.153	92.951	92.933	92.68
	Standard deviation	3.158	14.763	1.905	6.195	6.316	3.927
6 mM SA, No sugar	Replicate #1	78.113	79.554	72.645	85.356	81.536	88.622
	Replicate #2	80.16	83.459	80.616	91.472	87.368	85.011
	Replicate #3	88.361	76.854	77.955	91.273	89.794	93.161
	Means	82.211	79.955	77.072	89.367	86.232	88.931
	Standard deviation	5.423	3.320	4.058	3.475	4.244	4.083
12 mM SA, No sugar	Replicate #1	76.686	82.809	82.558	93.813	96.445	95.238
	Replicate #2	82.464	83.261	83.662	90.168	92.842	94.502
	Replicate #3	77.39	80.3	84.111	89.694	90.227	84.826
	Means	78.846	82.123	83.443	91.225	93.171	91.522
	Standard deviation	3.152	1.595	0.799	2.253	3.122	5.810

Integrated density (pixel) for gene:		FGSG_08358					
Condition	Δ KO9	Δ KO9	Δ KO4	Δ KO8	Δ EC3	Δ EC2	Δ EC5
No SA, No sugar	Replicate #1	99.887	98.702		100.921	101.43	106.57
	Replicate #2	95.637	109.263	100.197	101.723	96.995	102.42
	Replicate #3	100.792	102.82	102.135	101.248	101.91	97.788
	Means	98.772	103.595	101.166	101.297	100.11	102.26
	Standard deviation	2.752	5.322	1.370	0.403	2.713	4.394
No SA, 0.4g sugar	Replicate #1	119.743	109.477	113.144	108.482	106.45	107.34
	Replicate #2	109.654	111.681	108.931	110.439	101.85	116.55
	Replicate #3	101.717	104.752	105.078	108.906	110.19	114.45
	Means	110.37	108.636	109.051	109.275	106.16	112.78
	Standard deviation	9.034	3.540	4.034	1.029	4.175	4.825
No SA, 2g sugar	Replicate #1	136.097	138.102	134.235	129.721	124.29	135.22
	Replicate #2	129.376	132.882	137.761	135.626	129.07	130.53
	Replicate #3	132.885	126.208	136.498	133.409	126.50	131.26
	Means	132.786	132.39	136.164	132.918	126.62	132.33
	Standard deviation	3.361	5.961	1.786	2.982	2.396	2.522
1.5 mM SA, No sugar	Replicate #1	102.812	103.048	102.078	109.474	110.57	107.52
	Replicate #2	89.234	99.255	101.184	106.179	112.93	111.86
	Replicate #3	107.36	101.167	105.967	107.671	108.99	102.84
	Means	99.802	101.156	103.076	107.774	110.83	107.41
	Standard deviation	9.430	1.896	2.542	1.649	1.983	4.511
6 mM SA, No sugar	Replicate #1	101.085	103.815	102.276	101.527	108.73	102.65
	Replicate #2	104.072	108.637	107.76	108.777	109.58	108.01
	Replicate #3	101.487	108.767	101.66	108.648	109.48	99.256
	Means	102.214	107.073	103.898	106.317	109.26	103.30
	Standard deviation	1.621	2.822	3.358	4.149	0.463	4.417
12 mM SA, No sugar	Replicate #1	112.098	115.124	105.679	112.502	102.70	102.73
	Replicate #2	109.043	114.411	106.119	111.464	103.42	101.36
	Replicate #3	110.291	113.656	103.003	102.665	100.99	103.15
	Means	110.477	114.397	104.933	108.877	102.37	102.41
	Standard deviation	1.536	0.734	1.686	5.404	1.249	0.935

Integrated density (pixel) for gene:		FGSG_08037					
Condition	Δ KO16	Δ KO16	Δ KO19	Δ KO17	Δ EC18	Δ EC15	ΔEC12
No SA, No sugar	Replicate #1	94.8	98.4	99.6	95.3	94.667	101.6
	Replicate #2	88.2	102.56	104.39	99.702	101.01	98.422
	Replicate #3	105.46	103.53	99.601	99.556	102.41	100.62
	Means	96.2	101.5	101.2	98.2	99.4	100.2
	Standard deviation	8.704	2.717	2.766	2.503	4.128	1.642
No SA, 0.4g sugar	Replicate #1	101.3	100.7	114.0	109.1	107.31	107.7
	Replicate #2	105.0	108.71	106.52	111.77	105.37	109.26
	Replicate #3	110.93	102.68	115.93	109.59	107.5	105.28
	Means	105.8	104.0	112.2	110.1	106.7	107.4
	Standard deviation	4.8407	4.176	4.970	1.438	1.175	2.007
No SA, 2g sugar	Replicate #1	109.0	127.3	129.9	125.5	127.81	126.0
	Replicate #2	119.2	131.11	130.12	126.89	130.09	131.20
	Replicate #3	125.57	129.14	130.45	128.52	129.68	130.32
	Means	117.9	129.2	130.2	127.0	129.2	129.2
	Standard deviation	8.382	1.912	0.265	1.517	1.215	2.801
1.5 mM SA, No sugar	Replicate #1	94.5	107.7	109.6	104.7	107.20	107.56
	Replicate #2	96.4	102.33	111.07	105.47	103.95	95.31
	Replicate #3	103.02	104.68	106.95	102.66	106.26	
	Means	98.0	104.9	109.2	104.3	105.8	101.4
	Standard deviation	4.464	2.669	2.088	1.457	1.668	8.667
6 mM SA, No sugar	Replicate #1	95.9	106.5	104.0	106.8	105.5	108.4
	Replicate #2	102.5	109.33	107.26	110.71	104.01	102.73
	Replicate #3	98.834	108.57	107.48	109.00	107.77	104.44
	Means	99.1	108.1	106.2	108.8	105.8	105.2
	Standard deviation	3.346	1.481	1.953	1.979	1.895	2.887
12 mM SA, No sugar	Replicate #1	106.3	108.4	114.5	107.1	108.19	108.7
	Replicate #2	105.7	104.70	112.2	114.25	112.30	106.36
	Replicate #3	107.62	106.84	110.54	109.23	108.78	107.36
	Means	106.5	106.7	112.4	110.2	109.8	107.5
	Standard deviation	0.992	1.867	1.976	3.694	2.220	1.189

Table A3:

Statistical analysis:

Integrated density of FGSG_09063 mutant strains in No SA, 0.4g sugar

Groups	fg 09063 Δ	− fg 09063 Δ
Count	3	3
Sum	355.983	368.092
Average	118.66	122.697
Variance	96.074	93.307
SS Between Groups	24.436	
Ss Within Groups	378.764	
Ss Total	403.201	
df Between Groups	1	
df Within Groups	4	
Df Total	5	
MS Between Groups	24.436	
MS Within Groups	94.691	
F	0.258	
P-value	0.638	
F crit	7.708	

Integrated density of FGSG_09063 mutant strains in 12mM SA

Groups	fg 09063 Δ	− fg 09063 Δ
Count	3	3
Sum	396.0843	375.227
Average	132.0281	125.075
Variance	3.5462	119.624
SS Between Groups	72.504	
Ss Within Groups	246.340	
Ss Total	318.845	
Df Between Groups	1	
Df Within Groups	4	
Df Total	5	
MS Between Groups	72.504	
MS Within Groups	61.585	
F	1.177	
P-value	0.338	
F crit	7.708	

Integrated density of FGSG_03657 mutant strains in No SA, 0.4g sugar

Groups	fg 03657 Δ	− fg 03657 Δ
Count	3	3
Sum	374.622	375.742
Average	124.874	125.247
Variance	44.257	34.454
SS Between Groups	0.209	
Ss Within Groups	157.425	
Ss Total	157.634	
Df Between Groups	1	
Df Within Groups	4	
Df Total	5	
MS Between Groups	0.209	
MS Within Groups	39.356	
F	0.005	
P-value	0.945	
F crit	7.708	

Integrated density of FGSG_03657 mutant strains in 12mM SA

Groups	fg 03657 Δ	− fg 03657 Δ
Count	3	3
Sum	349.494	369.811
Average	116.498	123.270
Variance	39.131	49.932
SS Between Groups	68.792	
Ss Within Groups	178.127	
Ss Total	246.919	
Df Between Groups	1	
Df Within Groups	4	
Df Total	5	
MS Between Groups	68.792	
MS Within Groups	44.531	
F	1.544	
P-value	0.281	
F crit	7.708	

Integrated density of FGSG_09061 in mutant strains No SA, 0.4g sugar

Groups	fg 09061 Δ	− fg 09061 Δ
Count	4	1
Sum	359.451	93.456
Average	89.862	93.456
Variance	3.253	
SS Between Groups	10.33	
Ss Within Groups	9.759	
Ss Total	20.092	
Df Between Groups	1	
Df Within Groups	3	
Df Total	4	
MS Between Groups	10.332	
MS Within Groups	3.253	
F	3.175	
P-value	0.172	
F crit	10.127	

Integrated density of FGSG_09061 mutant strains in 12mM SA

Groups	fg 09061 Δ	− fg 09061 Δ
Count	4	4
Sum	359.451	373.826
Average	89.862	93.456
Variance	3.253	0
SS Between Groups	25.831	
Ss Within Groups	9.759	
Ss Total	35.591	
Df Between Groups	1	
Df Within Groups	6	
Df Total	7	
MS Between Groups	25.831	
MS Within Groups	1.626	
F	15.879	
P-value	0.007	
F crit	5.987	

Integrated density of FGSG_03667 mutant strains in No SA, 0.4g sugar

Groups	fg 03667 Δ	− fg 03667 Δ
Count	3	3
Sum	274	280
Average	91.33	93.33
Variance	9.33	4.33
SS Between Groups	6	
Ss Within Groups	27.33	
Ss Total	33.33	
Df Between Groups	1	
Df Within Groups	4	
Df Total	5	
MS Between Groups	6	
MS Within Groups	6.83	
F	0.87	
P-value	0.40	
F crit	7.708	

Integrated density of FGSG_03667 mutant strains in 12mM SA

Groups	fg 03667 Δ	− fg 03667 Δ
Count	3	3
Sum	243	275
Average	81	91.666
Variance	7	1.333
SS Between Groups	170.66	
Ss Within Groups	16.66	
Ss Total	187.33	
Df Between Groups	1	
Df Within Groups	4	
Df Total	5	
MS Between Groups	170.66	
MS Within Groups	4.166	
F	40.96	
P-value	0.003	
F crit	7.708	

Integrated density of FGSG_08358 mutant strains in No SA, 0.4g sugar

Groups	fg 08358 Δ	− fg 08358 Δ
Count	3	3
Sum	328.059	328.228
Average	109.353	109.409
Variance	0.820	10.955
SS Between Groups	0.004	
Ss Within Groups	23.551	
Ss Total	23.556	
Df Between Groups	1	
Df Within Groups	4	
Df Total	5	
MS Between Groups	0.004	
MS Within Groups	5.88	
F	0.0008	
P-value	0.97	
F crit	7.708	

Integrated density of FGSG_08358 mutant strains in 12mM SA

Groups	fg 08358 Δ	− fg 08358 Δ
Count	3	3
Sum	329.808	313.669
Average	109.936	104.556
Variance	22.608	14.0001
SS Between Groups	43.407	
Ss Within Groups	73.217	
Ss Total	116.624	
Df Between Groups	1	
Df Within Groups	4	
Df Total	5	
MS Between Groups	43.407	
MS Within Groups	18.304	
F	2.37144	
P-value	0.198	
F crit	7.708	

Integrated density of FGSG_08037 mutant strains in No SA, 0.4g sugar

Groups	fg 08037 Δ	−fg 08037 Δ
Count	3	3
Sum	321.948	324.289
Average	107.316	108.096
Variance	18.331	3.258
SS Between Groups	0.913	
Ss Within Groups	43.180	
Ss Total	44.094	
Df Between Groups	1	
Df Within Groups	4	
Df Total	5	
MS Between Groups	0.913	
MS Within Groups	10.79	
F	0.08	
P-value	0.78	
F crit	7.708	

Integrated density of FGSG_08037 mutant strains in 12mM SA

Groups	fg 08037Δ	− fg 08037 Δ
Count	3	3
Sum	325.597	327.425
Average	108.532	109.141
Variance	11.175	2.104
SS Between Groups	0.557	
Ss Within Groups	26.561	
Ss Total	27.118	
Df Between Groups	1	
Df Within Groups	4	
Df Total	5	
MS Between Groups	0.557	
MS Within Groups	6.640	
F	0.083	
P-value	0.78	
F crit	7.708	

Table A4: **Amount of SA remaining in the supernatant in function of the starting inoculum.**

Amount of spores/4ml		0h	2hr	4hr	6hr
10.4	Replicate #1	217.0594	266.515	4.68251	0
	Replicate #2	328.4958	281	0	0
	Mean	272.7776	273.7575	2.341255	0
	Standard deviation	78.79741	10.24244173	3.311034574	0
10.6	Replicate #1	243.4555	254.535	0	0
	Replicate #2	274.2943	249.5659	0	0
	Mean	258.8749	252.05045	0	0
	Standard deviation	21.8063246	3.513684306	0	0
10.5	Replicate #1	256.8629	228.7609	0	0
	Replicate #2	212.8987	237.5044	0	0
	Mean	234.8808	233.13265	0	0
	Standard deviation	31.08738395	6.182588141	0	0

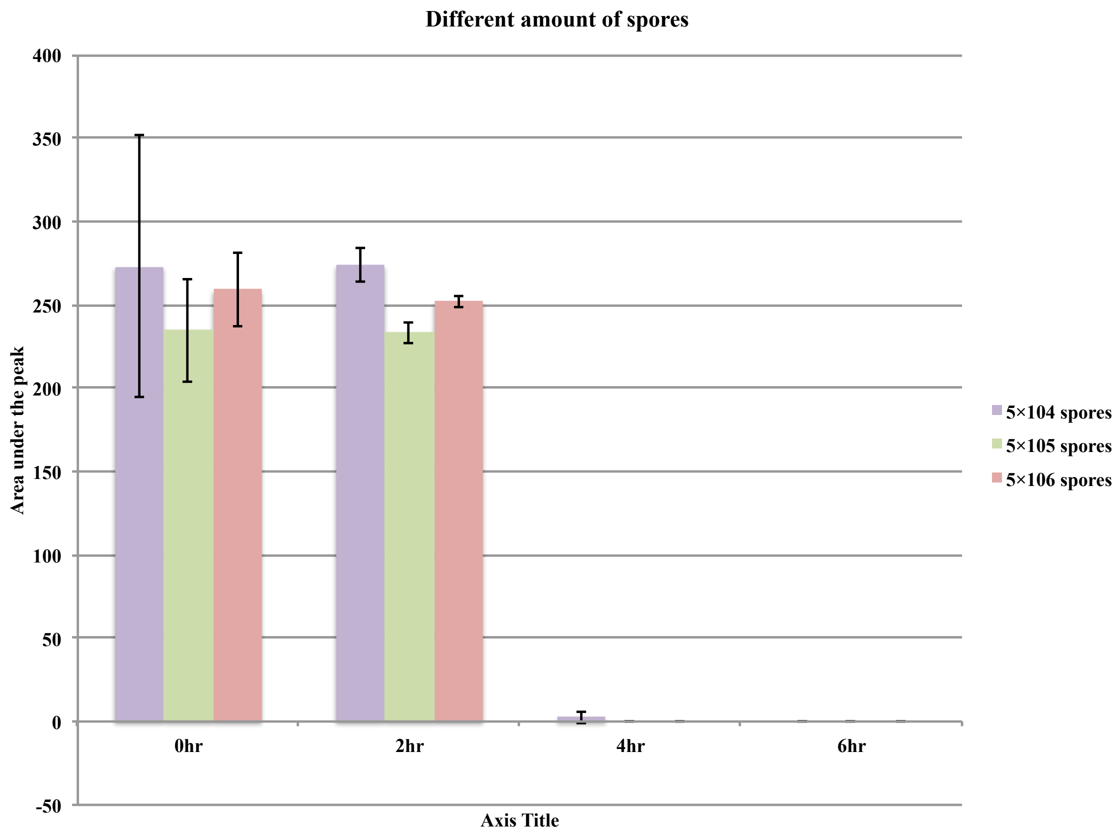

Figure A2: Degradation of SA by different amount of *F. graminearum* in culture media amended with 1mM SA. Error bars represented standard deviation between 2 replicates.

Table A5: Amount of SA remaining in the supernatant when comparing KO strains and WT.

		0hr	2hr	4hr	6hr
FGSG_09063ΔKO2	Replicate #1	109.028	107.881	11.751	0.071
	Replicate #2	97.3478	113.208	32.226	0.055
	Replicate #3	93.6237		36.221	0.058
	Means	100	110.544	26.733	0.061
	Standard deviation	8.037	3.766	13.127	0.008
WT	Replicate #1	94.542	74.038	0.034	0
	Replicate #2	109.420	71.555	0.0493	0
	Replicate #3	96.036	81.678	7.307	0
	Means	100	75.757	2.463	0
	Standard deviation	8.192	5.276	4.194	0

		0hr	2hr	4hr	6hr
FGSG_03657ΔKO14	Replicate #1	118.367	57.197	81.932	62.206
	Replicate #2	81.571	78.302	66.329	76.510
	Replicate #3	100.061	64.529	68.239	69.613
	Means	100	66.676	72.167	69.443
	Standard deviation	18.398	10.715	8.510	7.1536
WT	Replicate #1	106.790	71.499	20.816	0
	Replicate #2	95.197	82.915	1.699	0.038
	Replicate #3	98.012	74.493	0.744	0.328
	Means	100	76.302	7.753	0.122
	Standard deviation	6.046	5.919	11.322	0.179

		0hr	2hr	4hr	6hr
FGSG_09061ΔKO15	Replicate #1	102.894	91.316	105.918	49.918
	Replicate #2	100.450	82.264	67.232	57.327
	Replicate #3	96.655	104.948	94.310	50.428
	Means	100	92.842	89.153	52.558
	Standard deviation	3.143	11.418	19.851	4.138
WT	Replicate #1	101.654	61.451	0	0
	Replicate #2	110.107	86.089	0	0
	Replicate #3	88.237	71.818	0	0
	Means	100	73.119	0	0
	Standard deviation	11.028	12.370	0	0

		0hr	2hr	4hr	6hr
FGSG_03667ΔKO2	Replicate #1	107.238	101.179	111.803	119.399
	Replicate #2	87.663	105.046	108.596	100.024
	Replicate #3	105.097	106.177	119.296	113.594
	Means	100	104.134	113.232	111.006
	Standard deviation	10.737	2.620	5.491	9.943
WT	Replicate #1	120.254	112.037	0.138	0.203
	Replicate #2	118.333	113.072	0	0
	Replicate #3	61.411	115.052	0	0
	Means	100	113.387	0.046	0.067
	Standard deviation	120.254	112.037	0.138	0.203

		0hr	2hr	4hr	6hr
FGSG_08357ΔKO4	Replicate #1	96.246	71.436	57.998	0.114
	Replicate #2	103.753	66.502	56.747	0.028
	Means	100	68.969	57.372	0.071
	Standard deviation	5.308	3.489	0.884	0.061
FGSG_08037ΔKO16	Replicate #1	91.728	91.958	66.153	0.158
	Replicate #2	108.27	89.284	68.890	22.226
	Means	100	90.621	67.521	11.192
	Standard deviation	11.697	1.891	1.935	15.603
WT	Replicate #1	99.957	80.975	72.920	0.160
	Replicate #2	100.042	105.702	60.842	0.140
	Means	100	93.339	66.881	0.150
	Standard deviation	0.060	17.485	8.540	0.014

		0hr	2hr	4hr	6hr
FGSG_09061ΔKO6	Replicate #1	102.324	91.013	103.911	49.856
	Replicate #2	101.880	75.922	93.274	52.896
	Means	95.795	91.752	75.899	57.779
	Standard deviation	100	86.229	91.028	53.510
FGSG_09061ΔKO9	Replicate #1	75.309	144.644	101.406	0
	Replicate #2	98.695	140.485	126.454	85.046
	Means	125.994	148.869	67.807	0
	Standard deviation	100	144.666	98.556	28.348
FGSG_09061ΔEc8	Replicate #1	98.681	73.399	18.802	0
	Replicate #2	100.423	88.907	29.205	0
	Means	100.895	86.663	9.047	0
	Standard deviation	100	82.990	19.018	0

Table A6: All media recipe used in this study.

Name of the medium	Recipe
PDA	**For 1L:** 39 g of PDA powdered medium contains: 4g Potato starch 20g Glucose 15g Agar
SNA	**For 1L:** 1 g KH2PO4 1 g KNO3 0.5 g MgSO4 0.5 g KCl 0.2 g glucose 0.2 g sucrose 20 g agar
Modifieded SNA	**For 1L:** 1 g KH2PO4 1 g KNO3 0.5 g MgSO4 0.5 g KCl 1 g glucose 1 g sucrose 20 g agar
CMC	**For 1L:** 1 gm NH_4NO_3 1 gm KH_2PO_4 0.5 gm $MgSO_4 . 7H_2O$ 1.0 gm Yeast Extract 15 g CMC
1.5% agarose gel in [1X TAE – recipe provided in annex	**For 1L:** 50X TAE stock: 242 g Tris-base 57.1 ml Acetate 100 ml 0.5M sodium EDTA 1X TAE: dilute 20 ml of 50X stock into 980ml of di water.
LB broth	**For 1L:** 40g of LB powdered medium contains:

	10g Tryptone 5g Yeast extract 10g NaCL
IMAS	**For 500 ml:** 200.0 ml 2.5x Salt solution 4.5 ml 20 % (w/v) Glucose 12.5 ml 20 % (v/v) Glycerol 10.0 g Agar 20.0 ml MES-solution 10 ml 10 mM Acetosyringon **10 mM Acetosyringon**: 0.01962 g Acetosyringone 10 ml MilliQ-water Adjust the pH to 8 with 5 M KOH **2.5x Salt solution:** 3.625 g KH_2PO_4 5.125 g K_2HPO_4 0.375 g NaCl 1.250 g $MgSO_4$, $7H_2O$ 0.165 g $CaCl_2$, $2H_2O$ 0.0062 g $FeSO_4$, $7H_2O$ 1.250 g $(NH_4)_2SO_4$ **1 M MES:** 19.52 g MES 80 ml MilliQ-water
DFM	**For 500 ml:** 31.25 ml 20 % Glucose 100.0 ml 50 mM Aspargin 5.0 ml 0.21 M $MgSO_4$ 5.0 ml 1.12 M KH_2PO_4 + 0.7 M KCl (pH 6) 0.5 ml 1000 x Trace elements 10.0 g Agar 348.3 ml MilliQ water **1000 x Trace elements for DFM** 40 mg $Na_2B_4O_7$ * $10H_2O$, 400 mg $CuSO_4$ * $5H_2O$ 1,2 g $FeSO_4$ * $7H_2O$ 700 mg $MnSO_4$ * $1H_2O$ 800 mg $NaMoO_2$ * $2H_2O$ 10 g $ZnSO_4$ * $7H_2O$ to 1000 ml MilliQ water

1st stage media (GYEP)	**For 1L:** 3g NH4C1 0.2 g MgS04*7H20 0.2 g FeS04*7H20 2g KH2PO4: 2g Peptone 2g Yeast Extract 2g Malt Extract 20g Glucose
2nd stage media. modified MYRO	**For 1L:** 1 g (NH4)2HPO4, 3 g KH2PO4, 0.2 g MgSO4$7H2O 5 g NaCl, 40 g sucrose 10 g glycerol adjusted to pH 4.0 with (KOH)

Table A7: Blastn alignment of FGSG_03667 against fungal species.

Description	Max score	Total score	Query cover%	E value	Ident %
Gibberella zeae PH-1 hypothetical protein partial mRNA	632	632	100	0.0	100
Fusarium pseudograminearum CS3096 hypothetical protein partial mRNA	652	652	100	0.0	99
Nectria haematococca mpVI 77-13-4 predicted protein, mRNA	535	535	96	0.0	87
Fusarium graminearum chromosome 2, complete genome	240	910	100	3e-161	88
Pestalotiopsis fici W106-1 hypothetical protein mRNA	447	447	92	7e-155	73
Colletotrichum fioriniae PJ7 dioxygenase mRNA	436	436	97	2e-150	70
Beauveria bassiana ARSEF 2860 intradiol ring-cleavage dioxygenase, core partial mRNA	433	433	92	2e-149	70
Trichoderma reesei QM6a predicted protien (TRIREDRAFT_62165), partial mRNA	429	429	94	7e-148	68
Colletotrichum gloeosporioides Nara gc5 catechol dioxygenase (CGGC5_10400), partial mRNA	428	428	94	2e-147	70
Cordyceps militraris CM01 catechol dioxygenase (CCm_8212), partial mRNA	426	426	92	1e-146	70
Metarhizium anisopliae ARSEF 23 dioxygenase, putative partial mRNA	425	425	92	4e-146	71
Pseudocercospora fijiensis CIRAD86 hypothetical protein mRNA	422	422	95	2e-143	67
Metarhizium acridum CQMa 102 catechol dioxygenase partial mRNA	417	417	92	8e-143	69
Capronia coronate CBS 617.96 hypothetical protein partial mRNA	401	401	95	3e-136	62
Carponia epimyces CBS 606.96 hypothetical protein mRNA	400	400	96	5e-136	62
Exophiala dermatitidis NIH/UT8656 catechol dioxygenase mRNA	400	400	98	1e-132	61
Endocarpon pusillum z07020 hypothetical protein mRNA	387	387	96	1e-130	59
Cladophialophora psammophila CBS 110553 hypothetical protein partial mRNA	386	386	91	1e-130	63
Gaeumannomyces graminis var. tritici R3-111a-1 hydroxyquinol 1,2 dioxygenase	393	393	92	3e-130	65
Cladophialophora carrionii CBS 160.54 hypothetical protein partial mRNA	378	378	91	4e-127	60

Aspergillus nige CBS 513.88 catechol 1,2-dioxygenase, mRNA	376	376	91	7e-127	64
Cyphellophora europaea CBS 101466 hypothetical protein partial mRNA	376	376	91	1e-126	61
Penicillium chrysogenum Wisconsin 54-1255 hypothetical protein (Pc13g01500)mRNA	370	370	91	2e-124	63
Cladophialophora yegresii CBS114405 hypothetical protein partial mRNA	370	370	91	5e-124	59
Aspergillus flavus NRRL3357 catechol dioxygenase, putative, mRNA	368	368	91	9e-124	63
Neosartorya fischeri NRRL 181 dioxygenase, putative (NFIA_035270) partial mRNA	368	368	91	1e-123	63
Botryotinia fuckeliana B05.10 hypothetical protein (BC1G_06739), partial mRNA	368	368	100	1e-123	59
Aspergillus fummigatus AF293 catechol dioxygenase (AFUA_2G02910), partial mRNA	367	367	92	2e-123	63
Aspergillus oryzae RIB40 catecol 1,2dioxygenase, mRNA	368	368	91	1e-122	63
Marssonina brunnea f.sp. 'multigermtubl' MB_m1 hypothetical protein (MBM_02925), mRNA	365	365	92	1e-122	60
Aspergillus oryzae cDNA, contig sequence:AoEST1595	370	370	91	4e-122	63
Magnaporthe oryzae 70-15 hydroxyquinol 1,2-dioxygenase (MGG_03773) mRNA	360	360	91	3e-119	60
Scletrotinia sclerotiorum 1980 hypothetical protein (SS1G_13312) partial mRNA	353	353	92	1e-117	60
Aspergillus nidulans FGSC A4 hypothetical protein AN8998.2 partial mRNA	351	351	91	7e-117	59
Coccidioides posadasii C735 delta SOWgp hydroxyquinol 1,2-dioxygenase, putative, mRNA	346	346	92	5e-155	59
Glarea lozoyensis ATCC 20868 Aromatic compound dioxygenase mRNA	345	345	91	1e-144	59
Coccidioides immitis RS hypothetical protein (CIMG_01300) partial mRNA	344	344	92	2e-144	58
Uncinocarpus reesii 1704 conserved hypothetical protein, mRNA	343	343	91	4e-114	59
Phaeosphaeria nodorum SN15 hypothetical protein partial mRNA	337	337	97	9e-111	54
Bipolaris zeicola 26-R-13 hypothetical protein partial mRNA	334	334	97	3e-110	55
Coniosporium apollinis CBS 100218 hypothetical protein partial mRNA	334	334	99	4e-110	54
Bipolaris oryzae ATCC 44560 hypothetical protein partial mRNA	334	334	99	6e-110	54

Baudoinia compniacensis UAMH 10762 hypothetical protein mRNA	335	335	98	5e-109	52
Neofusicoccum parvum UCRNP2 putative catechol dioxygenase protein mRNA	331	331	97	7e-109	53
Pyrenophora teres f.teres 0-1 hypothetical protein, mRNA	330	330	91	1e-108	55
Cochilobolus sativus ND90Pr hypothetical protein mRNA	332	332	99	1e-107	53
Pyrenophora tritici-repentis Pt-1C-BFP catechol 1,2-dioxygenase 1,mRNA	330	330	91	4e-107	55
Setosphaeria turicica Et28A hypothetical protein partial mRNA	322	322	94	2e-105	54
Colletotrichum gloesporioides Nara gc5 catechol-dioxygenase 1 (CGGC5_6751), partial mRNA	316	316	91	5e-103	52
Sordaria macrospora k-hell hypothetical protein (SMAC_00141),mRNA	315	315	95	1e-102	52
Leptosphaeria maculans JN3 hypothetical protein (LEMA_P018090.1) mRNA	314	314	91	2e-101	84
Chaetomium thermophilum var. thermophilum DSM1495 catechol 1,2-dioxygenase-like protein	311	311	91	3e-101	51
Paracoccidioides brasiliensis Pb18 hypothetical protein partial mRNA	310	310	99	1e-100	53
Trichoderma reesei QM6a predicted protein (TRIREDRAFT_4876), partial mRNA	304	304	91	2e-98	52
Talaromyces stipitatus ATCC 10500 catechol dioxygenase, putative, mRNA	376	376	91	2e-97	63
Paracoccidioides brasiliensis Pb01 conserved hypothetical protein, mRNA	301	301	97	5e-97	51
Chaetomium globosum CBS 148.51 hypothetical protein (CHGG_00655), mRNA	301	301	96	5e-97	49
Exophiala dermatitidis NIH/UT8656 catechol dioxygenase partial mRNA	301	301	91	8e-97	52
Glarea lozoyensis ATCC 20868 Aromatic compound dioxygenase mRNA	300	300	94	8e-97	51
Cladophialophora yegresii CBS 114405 hypothetical protein partial mRNA	300	300	91	1e-96	52
Sordaria macrospora k-hell hypothetical protein (SMAC_00655), mRNA	298	298	91	2e-96	51
Ajellomyces dermatitidis SLH14081 catechol dioxygenase, mRNA	299	299	91	2e-96	54
Neurospora crassa OR74A hypothetical protein NCU00055 partial mRNA	305	305	93	6e-96	52
Aspergillus terreus NIH2624 conserved hypothetical protein (ATEG_05004) partial	298	298	92	6e-96	51

mRNA					
TPA: Aspergillus nidulans FGSC A4 chromosome VII	324	324	91	6e-96	49
Neurospora tetrasperma FGSC2508 hypothetical protein partial mRNA	298	298	93	7e-96	50
Aspergillus nidulans FGSC A4 hypothetical protein AN8566.2 partial mRNA	297	297	92	1e-95	51
Aspergillus niger CBS 513.88 catechol 1,2-dioxygenase, mRNA	297	297	92	1e-95	50
Metarhizium anisopliae ARSEF 23 chlorocatechol 1,2-dioxygenase partial mRNA	296	296	96	4e-95	49
Thielavia terrestris NRRL8126 hypothetical protein (THITE_2126411)mRNA,	295	295	91	5e-95	51
Eutypa lata UCREL1 putative catechol dioxygenase protein mRNA	295	295	99	5e-95	48
Podospora aneserina S mat+hypothetival ptotein (PODANSg5350) partial mRNA	296	296	99	6e-95	48
Penicillium marneffei ATCC 18224 catechol dioxygenase, putative, mRNA	296	296	92	7e-95	49
Talaromyces stipitatus ATCC 10500 catechol dioxygenase, putative, mRNA	298	298	92	7e-95	51
Neurospora tetrasperma FGSC 2508 hypothetical protein partial mRNA	295	295	91	8e-95	50
Neosartorya fischeri NRRL 181 catechol dioxygenase, putative (NFIA_004860) partial mRNA	294	294	91	3e-94	50
Aspergillus fumigatus Af293 catechol dioxygenase (AFUA_3G003030), partial mRNA	293	293	92	3e-94	50
Ajellomyces capsulatus Nam1 conserved hypothetical protein (HCAG_03386) partial mRNA	293	293	96	5e-94	52
Aspergillus clavatus NRRL 1 catchol dioxygenase, putative (ACLA_-59500), partial mRNA	292	292	92	1e-93	50
Cladophialophora psammophila CBS 110553 hypothrtical protein partial mRNA	291	291	91	2e-93	50
Myceliophthora thermophile ATCC42464 intradiol ring-cleavage dioxygenase-like protein	291	291	91	3e-93	50
Coniosporium apollinis CBS 100218 hypothetical protein partial mRNA	290	290	91	4e-93	52
Penicillium chrysogenum Wisconsin 54-1255 hypothetical protein (Pc15g01190) mRNA	290	290	92	1e-92	49